

UNIVERSITÀ DEGLI STUDI DI NAPOLI FEDERICO II



**DIPARTIMENTO DI INGEGNERIA CHIMICA, DEI MATERIALI E
DELLA PRODUZIONE INDUSTRIALE**

XXXII PhD PROGRAMME IN

INDUSTRIAL PRODUCT AND PROCESS ENGINEERING

PHD COORDINATOR: PROF. ING. GIUSEPPE MENSITIERI

*Manufacturing and design of low weight structures and
hybrid composites using hemp fibres*

PHD Project Supervisor

Prof. Ing. Massimo Durante

PHD Candidate

Dario De Fazio

PHD Project Co-Supervisor

PhD Dr. Luca Boccarusso



Unione Europea



La tua
Campania
cresce in
Europa



DI
C
Ma
PI

Dipartimento
di Ingegneria Chimica,
dei Materiali e della
Produzione Industriale
Università degli Studi
di Napoli Federico II

DOTTORATO IN INGEGNERIA DEI PRODOTTI E DEI PROCESSI INDUSTRIALI

PIAZZALE TECCHIO 80—80125 NAPOLI—ITALIA
TEL. (39 81) 7682512/7682552

XXXII PHD PROGRAMME IN

INDUSTRIAL PRODUCT AND PROCESS ENGINEERING

PHD COORDINATOR: PROF. ING. GIUSEPPE MENSITIERI

***Manufacturing and design of low weight structures and hybrid
composites using hemp fibres***

PHD Project Supervisor

Prof. Ing. Massimo Durante

PHD Candidate

Dario De Fazio

PHD Project Co-Supervisor

PhD Dr. Luca Boccarusso

*To my parents,
Constant source of inspiration
and respectful model of life*

Index

<i>Acknowledgments</i>	i
<i>List of figures</i>	ii
<i>List of tables</i>	Vi
<i>Abstract</i>	Viii
<i>1 Chapter 1: Introduction and State of Art</i>	1
<i>1.1 Introduction</i>	1
<i>1.2 Literature Review</i>	2
<i>1.3 Sandwich composite structures</i>	4
<i>1.3.1 Skin failure</i>	7
<i>1.3.2 Indentation</i>	7
<i>1.3.3 Core Shear</i>	8
<i>1.4 Wear behaviour of composite materials</i>	10
<i>1.4.1 Testing procedure</i>	12
<i>1.5 Aim of the thesis</i>	14
<i>2 Chapter 2: Bio-composite materials</i>	21
<i>2.1 Bio-composite characteristics</i>	21
<i>2.2 Historical application of natural fibres composites</i>	24
<i>2.3 Natural fibres sources</i>	28
<i>2.4 Natural fibres comparison</i>	29
<i>2.5 Advantages and disadvantages of natural fibres</i>	31
<i>2.5.1 Advantages</i>	32
<i>2.5.2 Disadvantages</i>	33
<i>2.6 Natural fibre composites matrices</i>	35
<i>2.6.1 Thermoplastic matrices from bio sources</i>	36
<i>2.6.2 Thermoplastic matrices</i>	37
<i>2.6.3 Thermoset matrices</i>	37
<i>2.7 Production technologies</i>	38
<i>3 Chapter 3: Materials and Methods</i>	46
<i>3.1 Materials employed</i>	46
<i>3.2 Historical hemp applications</i>	47
<i>3.3 Hemp for industrial applications</i>	49
<i>3.4 Hemp diffusion around the World</i>	50
<i>3.5 Hemp diffusion in Italy</i>	50

3.6 Hemp plant structure.....	51
3.7 Hemp fibre elements.....	53
3.7.1 Cellulose.....	54
3.7.2 Hemicellulose.....	55
3.7.3 Lignin.....	56
3.7.4 Pectin.....	56
3.8 Influence of the mechanical properties of hemp fibres.....	57
3.8.1 Hemp growing conditions.....	58
3.8.2 Harvesting.....	59
3.9 Hemp fibres as reinforcement.....	60
3.10 Carbon fibres as reinforcement.....	61
3.11 Composite matrix.....	62
3.11.1 Epoxy resin.....	62
3.12 Used epoxy resin.....	64
3.13 Experimental campaign.....	66
3.13.1 Part 1: Continuous production of innovative core for sandwiches structures.....	68
3.13.2 Part 2: Hybrid sandwich structures with bio-based cores.....	70
3.13.3 Part3: Thin hybrid sandwich structures with bio-based cores.....	74
3.13.4 Part 4: Bio-hybrid composite laminates with improved mechanical properties.....	76
3.13.5 Part 5: Tribological behaviour of hemp fibres.....	78
4 Chapter 4: Results and Discussions.....	83
4.1 Part 2: Hybrid sandwich structures with bio-based cores.....	83
4.1.1 Impact tests.....	83
4.1.2 Indentation tests.....	88
4.2 Part 3: Thin hybrid sandwich structures with bio-based cores.....	91
4.2.1 Tensile tests.....	91
4.2.2 Three-point bending tests.....	92
4.3 Part 4: Bio-hybrid composite laminates with improved mechanical properties.....	99
4.3.1 Three-point bending tests.....	99
4.3.2 ILSS tests.....	108
4.3.3 Damping tests.....	111
4.3.4 Impact tests and internal damage detection.....	114
4.4 Part 5: Tribological behaviour of hemp fibres.....	126
4.4.1 Indentation tests.....	126
4.4.2 Tribological tests.....	128

4.4.3 Microgeometrical measurements.....	137
5 Chapter 5: Conclusions.....	143

Acknowledgments

Today, 6th of April 2020, I'm going to discuss my PhD thesis and then I would like to say thank to all people who come with me during this period of my life. First of all, I would like to express my gratitude to my parents, because they surround me every day, are source of inspiration and respectful model of life.

Then, I want to express to my supervisors Prof. Massimo Durante, Prof. Antonio Langella and Luca Boccarusso all my sincere gratitude because this PhD thesis has been possible thanks to their inspirations, precious suggestions and knowledge.

I would like to say thank to the University of Bath, especially to Prof. Michele Meo and Fulvio Pinto because they gave me the opportunity to spend some months here as visiting researcher. Additional thanks must go to the research staff Gian Piero Fierro, Christos Andreades, Stefano Cuomo, Francesco Flora, Francesco Rizzo, Marco Boccaccio and Fabrizio Bucciarelli because all of them have contributed to my professional growing. These guys are part of a larger group that I consider as friends and proceed to make this experience unforgettable.

I would also express my gratitude to the technicians Andrea Barone and Salvatore Varlese because they contributed with their suggestions and knowledge to my professional growing.

Then, finally I would like to say thank to all the research group I worked with during these years because I consider all of them friends and because they have made happy every day spent together.

List of figures

Fig.1: Schematisation of a sandwich structure: disassembled (a) and assembled (b).....	p.5
Fig.2: Sandwich beam subjected to a four-point bending (a) and three-point bending (b).....	p.5
Fig.3: Sandwich structure indentation failure in case of three-point bending test.....	p.7
Fig.4: Sandwich structure core shear failure: curvature of the middle span mode (a), double curvature mode (b).....	p.8
Fig.5: Failure map for sandwich structures.....	p.9
Fig.6: sandwich core structures classification.....	p.10
Fig.7: two-body wear mechanism (a), three body wear mechanism (b).....	p.11
Fig.8: Schematisation of the Block-on-ring testing machine apparatus.....	p.12
Fig.9: Schematisation of the Pin-on-disk testing machine apparatus.....	p.13
Fig.10: Schematisation of the main natural fibres.....	p.22
Fig.11: Henry Ford with the famous Hemp Body Car.....	p.25
Fig.12: Hemp dashboard of the Alfa Romeo Giulia.....	p.26
Fig.13: Some application fields of natural fibre composites: interiors in automotive field (a); dishes (b); mobile phone cover (c); baggage (d).....	p.26
Fig.14: Application of natural fibres as roof in automotive field.....	p.27
Fig.15: Natural fibres Lotus Elise Eco (a); Natural fibres Tesla P100DL race car (b).....	p.47
Fig.16: some natural fibres applications: “Le Ventolux” bike (a); natural fibre speakers (b); natural fibre guitar (c).....	p.48
Fig.17: hemp chairs: Werner Aissinger (a); Canvas Mariposa (b).....	p.49
Fig.18: Hemp plants (a) and parts (b).....	p.51
Fig.19: Cross section of industrial hemp stalk.....	p.52
Fig.20: Structure of hemp stem.....	p.53
Fig.21: Inner structure of hemp fibre.....	p.54
Fig.22: Cellulose structure of natural fibres.....	p.55
Fig.23: Hemp tissues: Maeko fabric (a); Fidia fabric (b).....	p.60
Fig.24: Epoxy group.....	p.63
Fig.25: Chemical structure of epoxy resin.....	p.63
Fig.26: Schematisation of the production system of a new lightweight hemp core geometry.....	p.68
Fig.27: Core configurations: peak to peak assembly (a); peak to valley assembly (b).....	p.69

Fig.28: Not enlarged (a) and Enlarged hemp fabric (b).....	p.70
Fig.28: Not enlarged hemp fabric before the impregnation phase.....	p.71
Fig.29: Polymerised hemp cores: not enlarged (a); enlarged (b).....	p.71
Fig.30: Sandwich skins production phases.....	p.73
Fig.31: Hybrid hemp core sandwich assembling phases.....	p.74
Fig.32: Thin hybrid natural/carbon fibres sandwich structures production phases.....	p.75
Fig.31: Hybrid hemp/carbon laminates production phases.....	p.77
Fig.32: Hemp tow surface before (a) and after (b) the chemical treatment.....	p.79
Fig.33: Hemp, glass and carbon specimen used for the experimental campaign.....	p.80
Fig.34: Experimental set up (a) and schematisation (b) of the impact test.....	p.84
Fig.35: Impact test carried out at 45J on NSF_2P sample (a) and SF_2P sample (b).....	p.85
Fig.36: Impact test carried out at 45J on NSF_4P sample (a) and SF_4P sample (b).....	p.86
Fig.37: Impact test carried out at 45J on NSF_6P sample (a) and SF_6P sample (b).....	p.87
Fig.38: Mean value of the absorbed energy for each sample typology at the end of the 45J impact test.....	p.88
Fig.39: Indentation test 33% of the failure at penetration: indentation force displacement graph (a), NSF sample bottom surface (b), SF sample bottom surface (c).....	p.89
Fig.40: Indentation test at penetration: indentation force displacement graph (a), NSF sample bottom surface (b), SF sample bottom surface (c).....	p.90
Fig.41: Typical force-displacement curves of each sample typology.....	p.92
Fig.42: Typical bending force-displacement curves of each sample typology, case of comparison with the same mechanical properties.....	p.94
Fig.43: Mean value of the flexural stress of each sample typology (a), specific flexural stress of each family (b) in case of comparison with the same mechanical properties.....	p.95
Fig.44: Specific flexural stresses of each sample typology, case of comparison with the same mechanical properties.....	p.96
Fig.45: Typical bending force-displacement curves of each sample typology, case of comparison with the same mechanical properties under the same load conditions.....	p.97
Fig.46: Mean values of the specific flexural force of each sample typology, case of comparison with the same mechanical properties under the same load conditions.....	p.98
Fig.47: Mean values of the specific flexural force of each sample typology, case of comparison with the same weight under the same load conditions.....	p.98
Fig.48: Instron universal testing machine.....	p.99
Fig.49: Flexural test on C configuration: flexural curves (a); failure zone microscope image (b).....	p.101
Fig.50: Flexural test on H configuration: flexural curves (a); failure zone microscope image (b).....	p.101
Fig.51: Flexural test on S configuration: flexural curves (a); failure zone microscope image (b).....	p.103

Fig.52: Flexural test on A-CH configuration: flexural curves (a); failure zone during the bending test (b); failure zone microscope image (c).....	p.104
Fig.53: Flexural test on A-HC configuration: flexural curves (a); failure zone during the bending test (b); failure zone microscope image (c); thickness of bundles of carbon and hemp layers (d).....	p.106
Fig.54: Flexural test on S-U configuration: flexural curves (a); failure zone microscope image (b).....	p.108
Fig.55: ILSS test on H configuration. Microscope image of the failure zone.....	p.109
Fig.56: ILSS test on all configuration: Interlaminar shear stress curves (a); mean value of the shear strength (b).....	p.110
Fig.57: ILSS test A-HC configuration: interlaminar shear stress curves (a); microscope image of the tested specimen (b).....	p.110
Fig.58: Damping test apparatus (a); schematisation of the experimental set-up (b).....	p.112
Fig.59: Logarithmic decrement curves (a); damping ratio chart (b).....	p.113
Fig.60: Non-destructive test, Phased array apparatus.....	p.114
Fig.61: Impact test on C configuration: force-displacement curves (a); B-Scan and C-Scan 5J (b); B-Scan and C-Scan 10J (c); B-Scan and C-Scan 20J (d).....	p.116
Fig.62: Impact test on H configuration: force-displacement curves (a); B-Scan and C-Scan 5J (b); B-Scan and C-Scan 10J (c); B-Scan and C-Scan 20J (d); impacted H configuration specimen (e).....	p.118
Fig.63: Impact test on S configuration: force-displacement curves (a); B-Scan and C-Scan 5J (b); B-Scan and C-Scan 10J (c); B-Scan and C-Scan 20J (d).....	p.120
Fig.64: Impact test on A-CH configuration: force-displacement curves (a); B-Scan and C-Scan 5J (b); B-Scan and C-Scan 10J (c); B-Scan and C-Scan 20J (d).....	p.122
Fig.65: Impact test on A-HC configuration: force-displacement curves (a); B-Scan and C-Scan 5J (b); B-Scan and C-Scan 10J (c); B-Scan and C-Scan 20J (d).....	p.123
Fig.66: Impact test on S-U configuration: force-displacement curves (a); B-Scan and C-Scan 5J (b); B-Scan and C-Scan 10J (c); B-Scan and C-Scan 20J (d).....	p.125
Fig.67: Typical indentation load versus displacement curves of each sample type.....	p.127
Fig.68: Ducom TR20-LE machine (a) tribological test schematisation (b).....	p.128
Fig.69: Wear depth (a) and friction coefficient (b) vs number of revolutions under a normal load of 10 N.....	p.130
Fig.70: Wear depth (a) and friction coefficient (b) vs number of revolutions under a normal load of 20 N.....	p.131
Fig.71: Wear depth (a) and friction coefficient (b) vs number of revolutions under a normal load of 50 N.....	p.132
Fig.72: Wear depth (a) and friction coefficient (b) vs number of revolutions under a normal load of 70 N.....	p.132
Fig.73: Wear track details of hemp (a), carbon (b) and glass (c) composite specimens.....	p.134
Fig.74: Values of coefficient of friction versus the applied normal load for each composite type.....	p.135
Fig.75: Dimensionless wear depth curves versus the sliding time for each un-impregnated fabric type.....	p.136
Fig.76: Un-impregnated samples at the end of the test: glass (a), carbon (b) and hemp (c) fabric.....	p.137

Fig.77: Diametric sample areas on the wear tracks acquired via confocal microscope (a) and an example of one of their 3D representation (b) from which single profiles are extracted (c)..... p.138

Fig.78: Volume variation for each load conditions..... p.140

List of tables

Table 1: Overview on natural fibres.....	p.28
Table 2: Overview on natural fibres as reinforcement in composite materials.....	p.29
Table 3: Available fibre typologies and their production amount.....	p.30
Table 4: Geometrical characteristics of the widely used natural fibres.....	p.30
Table 5: Natural fibres and their principal constituents.....	p.31
Table 6: Comparison between natural and glass fibre.....	p.33
Table 7: Chemical composition of hemp fibres.....	p.53
Table 8: Main properties of hemp fibres.....	p.57
Table 9: Mean tensile properties of hemp fibres.....	p.58
Table 10: Maeko fibres properties.....	p.61
Table 11: Fidia fibres properties.....	p.61
Table 12: Main properties of Toray carbon fabric.....	p.62
Table 13: Mechanical and technical data of the Epoxy resin.....	p.64
Table 14: Main properties of the new hemp core configurations.....	p.69
Table 15: Main properties of Not enlarged and Enlarged hemp cores.....	p.72
Table 16: Carbon fibre prepreg mechanical properties.....	p.72
Table 17: Classification and main properties of thin hybrid sandwich structures.....	p.76
Table 18: Classification and main properties of thin hybrid sandwich structures.....	p.78
Table 19: Main characteristics of all samples under inspection.....	p.79
Table 20: Impact results of the test carried out at 45J on 2 layers hemp core.....	p.85
Table 21: Impact results of the test carried out at 45J on 4 layers hemp core.....	p.86
Table 22: Impact results of the test carried out at 45J on 6 layers hemp core.....	p.87
Table 23: Main results of the quasi-static characterisation on the hybrid laminates.....	p.111
Table 24: Impact results of configuration C at the end of the test.....	p.116
Table 25: Impact results of configuration H at the end of the test.....	p.118
Table 26: Impact results of configuration S at the end of the test.....	p.121
Table 27: Impact results of configuration A-CH at the end of the test.....	p.121
Table 28: Impact results of configuration A-HC at the end of the test.....	p.124
Table 29: Impact results of configuration S-U at the end of the test.....	p.126

Table 30: Indenter Properties.....	p.127
Table 31: Pin-on-disk test conditions.....	p.129
Table 32: Depth and width of the wear tracks for each sample type of the specimen n°1.....	p.139
Table 33: Depth and width of the wear tracks for each sample type of the specimen n°2.....	p.139
Table 34: Depth and width of the wear tracks for each sample type of the specimen n°3.....	p.139

Abstract

On the basis of the environmental sensitivity and the waste materials problems, the new industrial products must reduce the environmental impact. If the attention is focused on composite materials, the environmental issue is relevant due to the large use of synthetic and petroleum fibres. In this context, it is possible to consider the use of natural fibres as reinforcement of composite materials but, even if they show good specific properties, natural fibre laminates are not able to offer mechanical performances comparable with traditional composite materials.

In order to overcome the employing limit of natural fibres composites related to their mechanical performances, there is need to investigate the possible use of hemp fibre in hybrid composite laminates and in sandwich structures as core solution in primary structural applications.

Therefore, on the basis of these issues, this PhD thesis has been focused on the manufacturing technologies of lightweight bio-based composite materials, and on the quasi-static and dynamic characterisation of hybrid carbon/hemp-based composite structures. Moreover, in all application in which these hybrid composite structures are subjected to tribological loads, additional wear tests are required on bio-based composite structures.

The thesis work is then organised in five chapters.

In the first, after a brief overview on the historical use of bio-based composite materials, the state of art of bio-based hybrid composite structures and the wear behaviour of natural fibre laminates is analysed. Therefore, on the basis of this overview, is expressed the need to investigate on the possible use of hemp fibres in hybrid composite laminates and sandwich structures. Moreover, in case of hybrid bio-based composite with hemp fibres on the external ply subjected to tribological loads, a wear characterisation of these materials is required.

In the second chapter are reported a detailed overview on natural fibre concerning their classifications, their advantage compared to traditional fibres and their disadvantages, thermoplastic and thermoset matrix usually used and then the traditional production technologies.

The third chapter is focused on the materials and methods employed in the research topics, in detail: the production of a new geometry of lightweight hemp core for sandwich structures; a quasi-static and dynamic behaviour of bio-based hybrid laminates and sandwich structures; a study on the wear behaviour of hemp fibres. After a detailed overview on reinforcements and matrix employed in the experimental campaign, a detailed description of the research topics and of the production techniques are presented. Moreover, in order to make the structure of the thesis better arranged, the experimental campaign sections were divided in five parts each one of these is dedicated to a specific research topic.

As well as the third chapter, in order to make more fluent the reading, the fourth chapter is divided in four parts (from part 2 to part 5) in which is described the experimental set-up and are discussed the relative results.

The fifth chapter close the thesis work in which the main results of each research topic are discussed.

Chapter 1: Introduction and State of Art

1.1 Introduction

Because of the environmental sensitivity, waste material problems, reduction of petroleum resources and the introduction of new orders by the legislative authorities, the new industrial products must reduce the environmental impact. The environmental protection concept is connected with an efficient waste management, an intelligent use of energy resources and materials, with the use of production technologies and materials with less environmental impact. If the attention is focused on composite manufacturing field, the environmental issue is relevant because petroleum and synthetic fibres are still widely used. Nowadays numerous industrial fields such as automotive and aeronautic industry, but in general the transportation industries in which the drive for weight and costs saving is greatest, are focusing their research on lightweight composite structures. The materials required from these fields should be as light as possible as well as cheap, and must be characterised by high mechanical properties. In this contest, is possible to take into account the use of bio-based materials in order to increase their engineering application fields, their usage matches with the environmental issue, costs and lightweight requirements. These aspects, in addition with the advantage and opportunities related with low costs, high specific properties and their availability as renewable resource, have attracted more and more interests [1–3], so numerous research works are focused on the study of recyclable composite materials reinforced by natural fibres such as jute, oil palm, coconut, flax, hemp and kenaf [4–13]. Between a large number of natural fibres, hemp is one of the most interesting plant because it can grow easily around the world, moreover it is characterised by low cost, low density, high specific strength if compared to glass or aramid fibres. Hemp plant is also characterised by the ability of extracting heavy metals from the soil, but the most important aspect is that it is available as renewable source.

Looking at the historical use of hemp fibre, it was widely used in applications in which a high tensile strength was required i.e. the use for roping, but its employ declined due to legislative rules related with the drug production [14]. After a few decades of oblivion, thanks to the availability of new variety of plants with low tetrahydro-cannabinoids (THCs) content, the hemp production resumed [15].

The bio-based fibres are employed in composite structures coupling both with thermoplastic and thermoset matrix, but its selection is restricted by the glass transition temperature that

deteriorate the natural fibres properties. A large part of natural fibres used as reinforcement in composite materials, are thermally instable around 200 °C, but in some conditions it is possible to operate them at higher temperature for a brief period [3]. For these reasons, only thermoplastic matrix with a glass transition temperature below this limit and thermoset polymers can be used as matrix [16]. The great potential obtained by coupling natural fibres with thermoplastic matrix is the recycling process, this composite material could be continuously softened by heat application, formed and then hardened by cooling. A better emphasis of the fibres mechanical properties is obtained by using thermoset polymers as matrix because they are characterised by reactive functional groups that make them compatible with the hydrophilic fibre surface [17].

However, even though synthetic fibres composite materials are characterised by very interesting in plane mechanical properties, justified by their wide use in different industrial applications, the out of plane brittle behaviour limits their use in all applications in which the impact resistance is required. For these reasons, a new challenge is the hybridisation of synthetic fibres with natural fibres both in laminate and sandwiches structures, combining the ductility of bio-based fibres with the strength of synthetic ones, in order to design a hybrid system characterised by improved flexural properties and impact resistance.

1.2 Literature review

The use of natural fibre in some industrial fields such as buildings and automotive is growing, this because in these application fields, the challenge is the cost reduction and the decrease of the total energy consumption during the manufacturing process [18–22].

Referring to the automotive field, during the last years, the natural fibres has begun to employ in the production of both external and internal parts in order to reduce the total weight of vehicles, to optimise the fuel consumption and increase the sustainability [23]. Numerous car manufacturers such as Mercedes Benz, Volkswagen group, Fiat group, Toyota and Honda have introduced composite materials reinforced by flax, sisal and hemp fibres in door cladding, seatbacks, underbody panels and dashboards [24]. Other car industries, like Jaguar and Land Rover, have experimented new thermoplastic composite car door [25]. The results at the end of the experimental campaign showed the same performances compared to the current part, but a weight reduction around the 60% compared to the steel part in case of Land Rover, while a

weight reduction around 35% compared to a glass reinforced polypropylene in case of Jaguar. This is just an example of study carried out on natural fibre reinforced composites. During the last years, numerous research works have been focused on bio-based composite materials concluding that, if correctly designed, these materials offer analogous mechanical properties compared to the conventional composite materials. Mallaiah et al. [26] studied sandwich structures by comparing the mechanical properties of bio-based and synthetic based fibre composites. The results showed that the hybridisation of bamboo and glass fibres presents higher values of core shear stress and face bending stress than that of sandwiches produced with pure glass and pure bamboo fibres.

As above mentioned, lightweight composite materials are largely used as interiors in automotive, aeronautic and building sectors. In these applications, a possible damage of the manufactured surface or wear load conditions could represent a risk for the human health causing the synthetic fibre exposition, and then irritant contact dermatitis due to the penetration into the skin of fragmented fibres. In this circumstance, could be interesting the synthetic fibres replacing with natural ones, and then a study on the wear behaviour of bio-based composite materials. Chin and Yousif [27] used kenaf fibres as reinforcement for bearing application and concluded that the bio-based composites showed a better wear behaviour when the fibre orientation is normal to the sliding direction. Xsin et al. [28] studied the sisal fibre reinforced composite with different fibre content for brake application. At the end of the experimental campaign, they concluded that the sisal fibre could be a good substitute of asbestos fibres in brake pads applications.

On the basis of these conclusions, is clear that there is need to investigate on the wear behaviour of natural fibres in order to extend their use in all applications where a wear load acts on the composite surface.

Recently, composite materials have seen a crucial rising use in aerospace and aeronautic fields as structural parts, where the guideline are high mechanical properties and weight saving. Moreover, the high level of tailorability of composite materials permits to incorporate in the same system, two or more fibre typologies in order to combine their characteristics and obtain a final composite structure with unique properties. The materials resulting from this hybridisation are known as fibre-hybrid composites (FHCs), they are characterised by a synergic effect that leads to properties that neither of the constituents possess [29–33]. Several works are focused on the hybridisation effects of composite materials, Kretsis [34] proved that the tensile module is generally in agreement with the rule of mixture. Zhang et al. [35]

concluded that the stacking sequence didn't influence the tensile properties of the laminate, but influenced significantly the flexural and compressive properties. However, due to the environmental sensitivity, a very interesting approach is the use of new materials that minimise the environmental impact and the design freedom of composite materials, then the substitution of synthetic fibres with natural ones both in laminate and in sandwich structures. Many research works are focused on composite materials hybridised with natural fibres, i.e. Sarasini et al. [36] proved that flax/carbon hybrid composites show improved mechanical properties and enhanced impact absorption performance if compared with traditional carbon fibres laminates. They also studied the post-impact performances, observing that the hybridisation process can lead to an improvement of damage tolerance if compared to the configuration with carbon fibres maintaining satisfactory residual flexural strength and stiffness. Le Guen et al. [37] pointed out that the damping coefficient of carbon/flax hybrid composites, was 4 times higher than composites reinforced with carbon fibres when natural fibres are localised on the external part of the laminate. Other researcher focalised their attention on sandwich structures, it is known that these structures are composed by a thick core which is characterised by a low strength and two stiffer and stronger skins. Zuhri et al. [23] studied different geometry of core honeycomb constituted by polypropylene and polylactide polymers reinforced by flax fibres. Rao et al. [38] studied the energy absorption capability and the core-skin bond strength of sandwich structures made from polypropylene reinforced by chopped sisal fibres and pine sawdust.

On the basis of this overview, it is clear that a large part of research work is concentrated on the study of flax fibres and their application, whilst few articles are focused on hemp fibres. Then, to fill this gap and further extend the use of natural fibres in primary structural applications, there is need to investigate the possible use of hemp fibres in hybrid composite laminates and in sandwich structures as core solution.

1.3 Sandwich composite structures

It is known that a sandwich structure is characterised by a lightweight core that separates the skins and transfers loads from one skin to the other, two thin strong skins and an adhesive film in order to transmit the shear stress and the axial loads to and from the core. In fig.1 is reported a schematic representation of the sandwich structure.

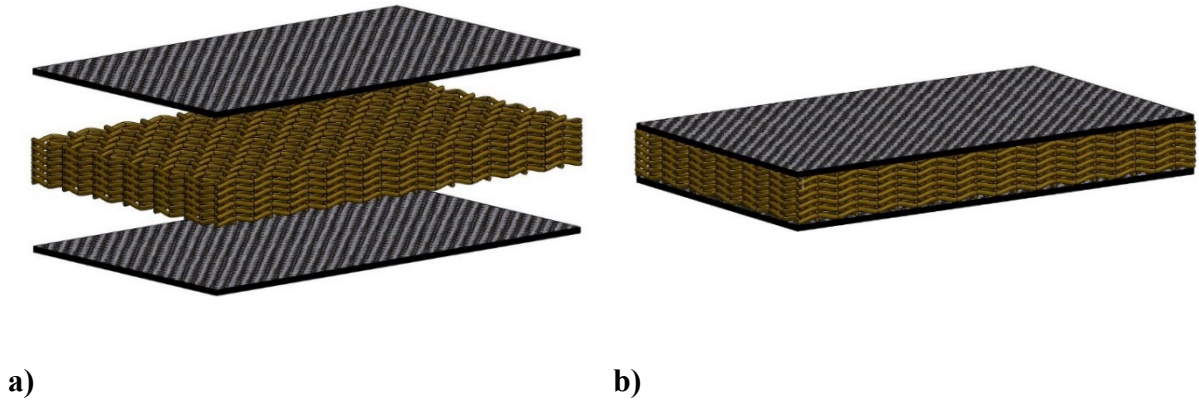


Fig.1: Schematisation of a sandwich structure: disassembled (a) and assembled (b).

The separation of the two skins from the neutral plane of the laminate, increases the moment of inertia of the sandwich material with a little improvement of the total weight. This skins separation produces an improvement of the bending and buckling loads resistance of the composite material.

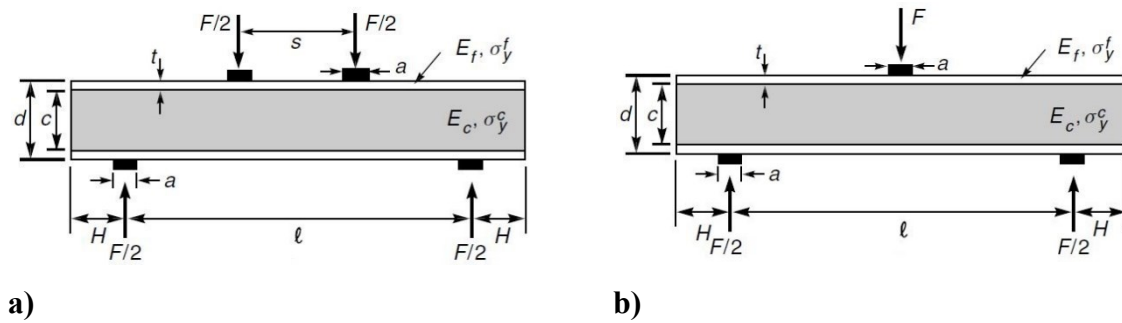


Fig.2: Sandwich beam subjected to a four-point bending (a) and three-point bending (b).

Figs.2a and 2b, show a sandwich beam subjected to a four-point and three-point bending. The sandwich structure is characterised by a uniform width b , skins of thickness t perfectly bonded to a core of thickness c . In both loading cases, l is the span between the supports and H is the overhang distance beyond the inner supports. In both cases it is possible to evaluate the maximum flexural moment acting on the structure, the longitudinal bending stress and the elastic deflection of the top support on the top skin. Taking into account the maximum moment acting on the sandwich structures, it is given by the following equations.

$$M = \frac{F l}{4} \quad \text{eq.1}$$

In case of the three-point bending solicitation.

$$M = \frac{F (l-s)}{4} \quad \text{eq.2}$$

In case of the four-point bending solicitation, s represents the distance between the loading supports.

The longitudinal bending stresses of the skin and the core in case of three-point and four-point bending are given by the following equations.

$$\sigma^s = \frac{M E_s}{(EI)_s} y \quad \text{eq.3}$$

$$\sigma^c = \frac{M E_c}{(EI)_c} y \quad \text{eq.4}$$

Where M is the flexural moment at the distance y from the neutral axis, E_s and E_c are the elastic modulus of the skin and core respectively and EI_s and EI_c are the moment of inertia of the skin and core respectively.

The elastic deflection δ of the top support on the upper skin both in case of three-point and four-point bending, is the sum of the flexural and shear deflection and it is given by the following equations [39].

$$\delta = \frac{F l^3}{48(EI)_{eq}} + \frac{F l}{4(AG)_{eq}} \quad \text{eq.5}$$

$$\delta = \frac{F (l-s)^2 (l-2s)}{48(EI)_{eq}} + \frac{F (l-s)}{4(AG)_{eq}} \quad \text{eq.6}$$

Where EI_{eq} is the equivalent flexural rigidity and AG_{eq} is the equivalent shear rigidity of the sandwich material.

It is known that there are different failure mechanisms of sandwich structures that involve skins failure, core failure or both of them. In the next paragraph, each failure mechanism will be investigated in detail.

1.3.1 Skin failure

The skin failure takes place when the face sheets are made with a material characterised by a low strength, with more detail the skin failure starts when the maximum tensile or compressive stress caused by bending, reaches the maximum yield strength. The failure load is determined by the following equation in case of three-point bending conditions.

$$F = \frac{4bt(c+t)}{l} \sigma_y^s + \frac{bc^2}{l} \sigma_y^c \tag{eq.7}$$

Where b is the width of the sandwich material, t is the thickness of the skin, c is the thickness of the core, l is the span between the lower supports, σ_y^s and σ_y^c are the flexural stresses of the skin and core respectively.

1.3.2 Indentation

The indentation failure mechanism showed in fig.3, involves the collapse of the upper skin under the loading support, at the same time causes the compressive yielding of the core [40].

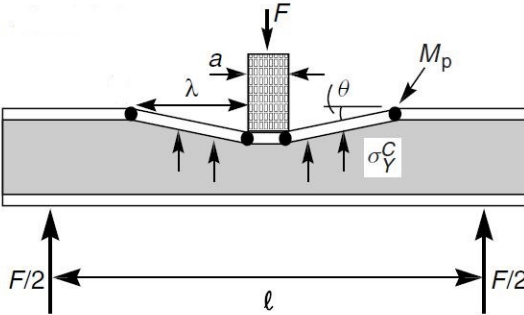


Fig.3: Sandwich structure indentation failure in case of three-point bending test.

Considering two segments on the damaged skin region with a length λ rotated through a small angle θ by the indentation, the failure force can be evaluated by using the following equation.

$$F = \frac{4M}{\lambda} + (a + \lambda)b\sigma_y^c \quad \text{eq.8}$$

Where M is the maximum moment on the face sheet section, λ is the length of the two segments, b is the width of the sandwich structure, a is the section of the loading support and σ_y^c is the compressive strength of the core.

1.3.3 Core shear

The core shear is a failure mechanism that occurs when a sandwich structure is subjected to a shear force. This solicitation is carried by the core that collapse when the maximum stress is reached. Two main core shear mechanism can be identified in case of three-point bending solicitation.

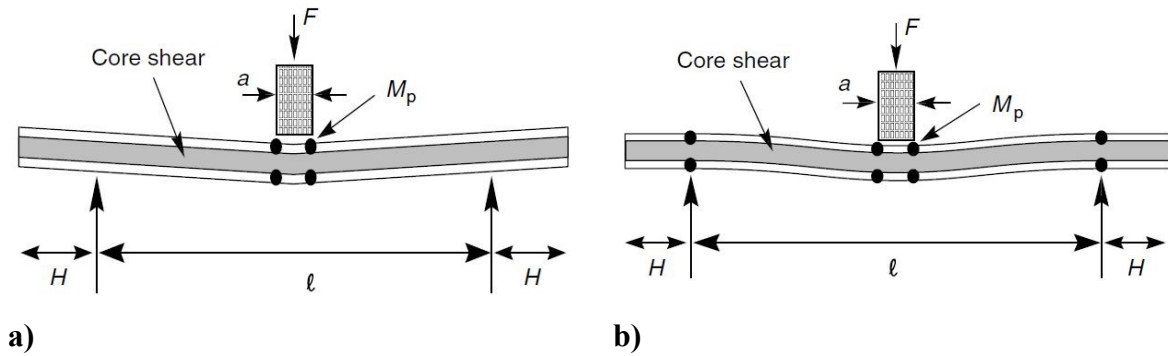


Fig.4: Sandwich structure core shear failure: curvature of the middle span mode (a), double curvature mode (b).

The first one (fig.4a), comprises a curvature in the mid-span of the sandwich panel, whilst the second one (fig.4b) causes a double curvature localised both in the mid-span of the sandwich and at the outer supports. Considering the first mechanism, the failure force is given by the eq. 9.

$$F = \frac{2bt^2}{l}\sigma_y^s + 2bc\tau_y^c \left(1 + \frac{2H}{l}\right) \quad \text{eq.9}$$

Where b is the width of the sandwich plate, l is the span between the supports, c is the thickness of the core, H is the overhang length, σ_y^s is the stress of the skin and τ_y^c is the shear strength of the core. The failure force referred to the second collapse mechanism is evaluated by the eq.10.

$$F = \frac{4bt^2}{l}\sigma_y^s + 2bc\tau_y^c \tag{eq.10}$$

In this case, the core undergoes simple shear over the span length, with more detail on the overhang region. Therefore, it is possible to conclude that the first or the second core shear failure mechanism depends on the overhang dimension. The first one is activated by a small length of the overhang and is characterised by a higher value of the failure force, whilst the second one is activated by a large length of the overhang and characterised by a lower value of the failure force.

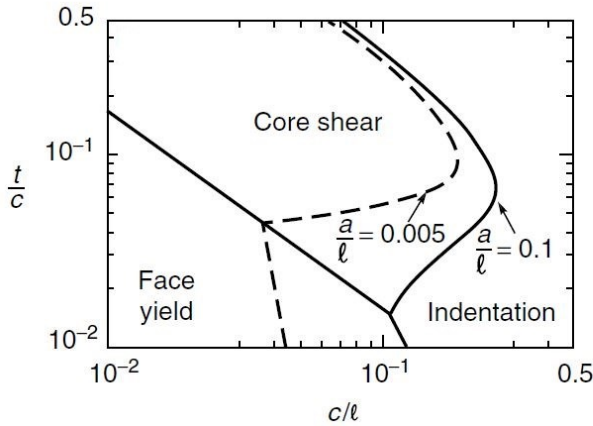


Fig.5: Failure map for sandwich structures.

All these failure mechanisms can be shown in failure maps (fig.5) by plotting a non-dimensional value of the failure force. These charts are characterised by a-dimensional axes obtained by the ratio between the core thickness and the support span c/l for the x-axis and between the skin and core thickness t/c for the y-axis. In this way it is possible to predict the failure mechanism that occur, knowing the geometry of the composite material and the loading conditions.

Usually, a sandwich panel cores are made of balsa-wood, foamed polymers, glue bonded aluminium honeycomb or Nomex honeycomb are characterised by various dimensions and shapes (fig.6).

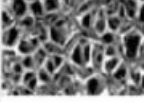





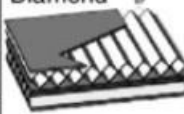





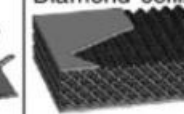

Cellular materials					
Stochastic		Periodic			
Open cell	Closed cell	2D		3D (lattice)	
		Honeycombs	Prismatic	Truss	Textile
		Hexagonal  Square  Triangular 	Triangular  Diamond  Navtruss 	Tetrahedral  Pyramidal  3D kagome 	Diamond textile  Diamond collinear  Square textile 

Fig.6: sandwich core structures classification.

Some of these widely used core materials such as polymer foams, even if are characterised by a low density, possess low shear strength and low out of plane compression properties. Moreover, they are expensive due to the production technology complexity, especially when the design requires curved panels. These drawbacks could be improved by using natural fibres as core in sandwich structures. Since bio-based fabrics are characterised by a large mesh, they can be used as core in sandwich panels in order to produce porous structures. The drapeability that characterises bio-based fabrics with a large mesh, allows to a major level of design, this aspect permits the production of more complex geometries. Moreover, the lower cost of natural fibres and the simplicity of the production systems, allow to a reduction of the total cost of the composite material.

1.4 Wear behaviour of composite materials

Composite structures are employed in numerous application fields, often these materials are involved in contacts with components that cause abrasive wear [41–43]. Then, the improvement of their application in practical situation requires a study of their wear behaviour.

During an abrasive wear in which two bodies are in contact each other, a progressive loss of material is involved due to the relative movement between the surfaces. There are different typologies of wear, i.e. abrasive, adhesive, fretting, fatigue and erosion wear, but the most important mechanism is the abrasive one because it is responsible of almost the 60% of the total cost of wear [41,44]. This process can be distinguished in two main mechanism (fig.7): a three-body and a two-body wear.

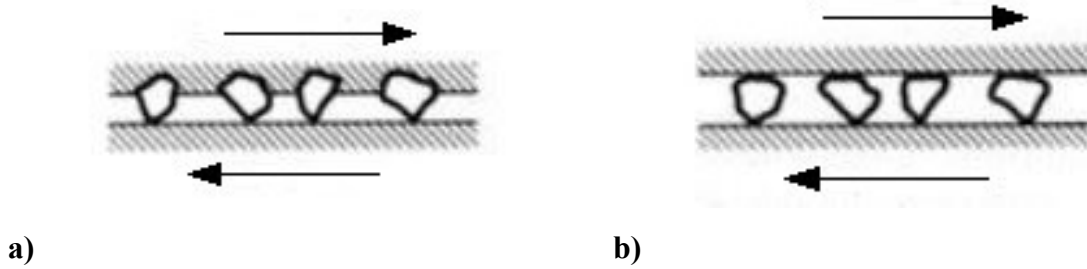


Fig.7: two-body wear mechanism (a), three body wear mechanism (b).

Both cases are characterised by a relative motion between the two surfaces in contact, but in a three-body wear mechanism, some particles are trapped between the surfaces and are free to roll and slide. Usually, the wear mechanism of composite materials is influenced by the load condition, and the three or two body wear process take place if the reinforcement is damaged or not. The two-body wear track (fig.7a) appearance is smooth, and it is characterised by small cracks that are perpendicular to the sliding direction. These cracks derive from patches of matrix teared from the surface and redeposited along the wear track, indeed sometimes the reinforcement is covered with a resin film deriving from the resin regions. When the failure of the reinforcement occurs, a three-body wear mechanism (fig.7b) takes place. In that case, the broken fibres are the third body and improve the wear rate of the composite material, this aspect is demonstrated by the following equation [41,43].

$$W_{s,c} = W_{s,s}(V_f) + W_{s,fc}(V_f) \quad \text{eq.11}$$

Where $W_{s,c}$ and $W_{s,s}$ are the wear rate of the composite structure and of the sliding process respectively, $W_{s,fc}$ is the additional wear rate that depends by a combination of fibre breakage and pull-out mechanism, V_f is the fibre volume fraction.

1.4.1 Testing procedure

The wear test can be carried out by using a block-on-ring or pin-on-disk tribo test machines. The first one is characterised by a pin pressed with a defined normal load against a rotating cylinder, the machine schematisation is visible in fig.8 [41,43].

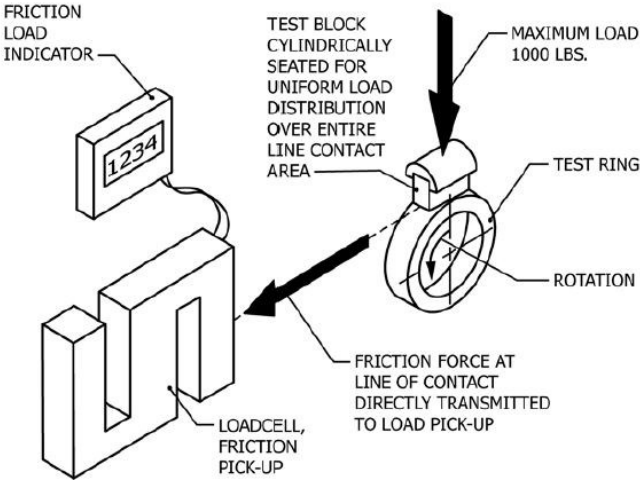


Fig.8: Schematisation of the Block-on-ring testing machine apparatus.

Initially, the contact between the pin and the ring is a line but as the test proceeds, the contact line becomes an area that increases with the test time. In that case, in order to evaluate the friction force and then the coefficient of friction, it is important to take into account the contact area variation [41,43].

The other testing machine is the pin-on-disk and its schematisation is shown in fig.9.

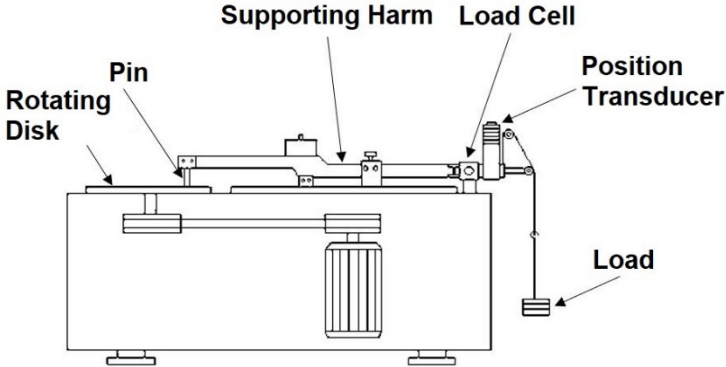


Fig.9: Schematisation of the Pin-on-disk testing machine apparatus.

In this case, a 10 x 10 mm² square specimen is pressed against a rotating disk by means of a specimen holder arm with a defined normal load [45]. For both the testing machines, wear is measured by means of a position transducer and the friction force by using a piezoelectric load cell connected to the specimen holding apparatus.

At the end of the test, the wear behaviour is characterised by the a-dimensional wear rate ratio defined in the following equation [41,43].

$$W = \frac{\Delta V}{AL} \quad \text{eq.12}$$

Where ΔV is the volume loss during the tribological test, A is the apparent contact area and L is the sliding distance. As said before, the contact area is a critical parameter to take into account during a tribological test, especially when the pin-on-ring machine is used, this because the contact area evolves during the tribological test, then the wear conditions evolve continuously during the test. Sometimes the wear rate is evaluated using the mass loss of the sample, in these cases the specimen weight is measured before and after the tribological test, then, knowing the material density, the volume loss is evaluated as:

$$\Delta V = \frac{\Delta m}{\rho} \quad \text{eq.13}$$

Moreover, the sliding distance can be expressed by the product between the velocity and the test duration:

$$L = vt \quad \text{eq.14}$$

With these simplifications, the wear rate can be expressed in terms of parameters experimentally measured by the following equation.

$$\Delta V = \frac{\Delta m}{\rho Avt} \quad \text{eq.15}$$

The tribological behaviour is not represented only by the wear rate, often the coefficient of friction is measured because it gives a good interpretation of the friction level between the two surfaces in contact each other. This a-dimensional parameter is evaluated by the ratio between the tangential friction force in Newton and the applied load:

$$\mu = \frac{F_t}{g P} \quad \text{eq.16}$$

Where μ is the coefficient of friction, F_t is the tangential friction force measured by the piezoelectric load cell, g is the acceleration of gravity and P is the normal load applied. The contact area is not considered in eq.16 because, in case of the pin-on-disk machine, it is the same for all the tribological test duration and then neglected.

1.5 Aim of the thesis

After an overview on the state of art of bio-based composite materials in this chapter, it has been demonstrated that there is the necessity of a more detailed study on these materials in order to extend their application fields. With more detail, a study on a more eco-friendly composite materials and on cheaper manufacturing processes easily to introduce in an industrial reality to produce low-density natural composite materials, are required. A study on the wear behaviour of natural fibre composite materials, is mandatory in all applications in which traditional synthetic reinforced composite materials are subjected to tribological loads, and the fibre exposition could be dangerous for the human health.

Therefore, the thesis work has been focused on the manufacturing process used to produce a new geometry of lightweight hemp/epoxy core for their use in sandwich structures in application as interiors in automotive, aeronautic and transportation fields. Moreover, some manufacturing technologies were used in order to produce lightweight hemp/epoxy core with different densities and thin core for sandwich structures, then the mechanical properties of these composite materials were widely investigated. Therefore, in case of application of composite materials as structural part, a quasi-static and dynamic mechanical properties of hybrid bio-based composite laminates were investigated. Finally, in case of tribological load on structural composite laminates, the idea was to replace the external layers of synthetic fibres with natural ones especially in case of human contact. For these reasons, the tribological behaviour of hemp

fibre reinforced composite was studied and was compared with the wear behaviour of the widely used synthetic reinforced polymer materials.

Reference

- [1] K. Rohit, S. Dixit, A Review - Future Aspect of Natural Fiber Reinforced Composite, *Polym. from Renew. Resour.* 7 (2016) 43–59. doi:10.1177/204124791600700202.
- [2] M. García, I. Garmendia, J. García, Influence of natural fiber type in eco-composites, *J. Appl. Polym. Sci.* 107 (2008) 2994–3004. doi:10.1002/app.27519.
- [3] K.L. Pickering, M.G.A. Efendy, T.M. Le, A review of recent developments in natural fibre composites and their mechanical performance, *Compos. Part A Appl. Sci. Manuf.* 83 (2016) 98–112. doi:10.1016/j.compositesa.2015.08.038.
- [4] L. Zhang, M. Miao, Commingled natural fibre / polypropylene wrap spun yarns for structured thermoplastic composites, *Compos. Sci. Technol.* 70 (2010) 130–135. doi:10.1016/j.compscitech.2009.09.016.
- [5] B. Baghaei, M. Skrifvars, L. Berglin, Composites : Part A Manufacture and characterisation of thermoplastic composites made from PLA / hemp co-wrapped hybrid yarn prepregs, *Compos. PART A.* 50 (2013) 93–101. doi:10.1016/j.compositesa.2013.03.012.
- [6] S. Phillips, J. Baets, L. Lessard, P. Hubert, I. Verpoest, Characterization of flax / epoxy prepregs before and after cure, (2012). doi:10.1177/0731684412473359.
- [7] N. Graupner, J. Müssig, Composites : Part A A comparison of the mechanical characteristics of kenaf and lyocell fibre reinforced poly (lactic acid) (PLA) and poly (3-hydroxybutyrate) (PHB) composites, *Compos. Part A.* 42 (2019) 2010–2019. doi:10.1016/j.compositesa.2011.09.007.
- [8] A.K. Rana, A. Mandal, B.C. Mitra, R. Jacobson, R. Rowell, A.N. Banerjee, Short Jute Fiber-Reinforced Polypropylene Composites : Effect of Compatibilizer, (1997) 329–338.
- [9] I. Modification, C. Products, *Journal of Reinforced Plastics and*, (2005). doi:10.1177/0731684405041717.
- [10] B.F. Yousif, S.T.W. Lau, S. McWilliam, Polyester composite based on betelnut fibre for tribological applications, *Tribol. Int.* 43 (2010) 503–511. doi:10.1016/j.triboint.2009.08.006.
- [11] P. Taylor, W.L. Lai, M. Mariatti, M.J. S, *Polymer-Plastics Technology and Engineering The Properties of Woven Kenaf and Betel Palm (Areca catechu) Reinforced Unsaturated Polyester Composites The Properties of Woven Kenaf and*

- Betel Palm (*Areca catechu*) Reinforced Unsaturated Polyester Composites, (2008) 37–41. doi:10.1080/03602550802392035.
- [12] B.F. YOUSIF, N.S.M. EL-TAYEB, THE EFFECT OF OIL PALM FIBERS AS REINFORCEMENT ON TRIBOLOGICAL PERFORMANCE OF POLYESTER COMPOSITE, *Surf. Rev. Lett.* 14 (2007) 1095–1102. doi:10.1142/S0218625X07010561.
- [13] D. Rouison, M. Sain, M. Couturier, SCIENCE AND Resin transfer molding of hemp fiber composites : optimization of the process and mechanical properties of the materials, 66 (2006) 895–906. doi:10.1016/j.compscitech.2005.07.040.
- [14] C. Hill, M. Hughes, Natural Fibre Reinforced Composites Opportunities and Challenges, *J. Biobased Mater. Bioenergy.* 4 (2010) 148–158. doi:10.1166/jbmb.2010.1079.
- [15] D.W. Lachenmeier, L. Kroener, F. Musshoff, B. Madea, Determination of cannabinoids in hemp food products by use of headspace solid-phase microextraction and gas chromatography?mass spectrometry, *Anal. Bioanal. Chem.* 378 (2004) 183–189. doi:10.1007/s00216-003-2268-4.
- [16] G. Aparecido dos Santos, Paulo / Giriolli, Joao Carlos / Amarasekera, Jay / Moraes, Natural fibers plastic composites for automotive applications, in: SPE Automotive & Composites Division, 2008.
- [17] M.S. Islam, K.L. Pickering, N.J. Foreman, Influence of Alkali Fiber Treatment and Fiber Processing on the Mechanical Properties of Hemp / Epoxy Composites, (2010). doi:10.1002/app.
- [18] E. Sassoni, S. Manzi, A. Motori, M. Montecchi, M. Canti, Experimental study on the physical–mechanical durability of innovative hemp-based composites for the building industry, *Energy Build.* 104 (2015) 316–322. doi:10.1016/j.enbuild.2015.07.022.
- [19] A.J. Marszal, P. Heiselberg, J.S. Bourrelle, E. Musall, K. Voss, I. Sartori, A. Napolitano, Zero Energy Building – A review of definitions and calculation methodologies, *Energy Build.* 43 (2011) 971–979. doi:10.1016/j.enbuild.2010.12.022.
- [20] E. Franzoni, *Procedia Engineering Materials selection for green buildings : which tools for engineers and architects ?*, (2011). doi:10.1016/j.proeng.2011.11.2090.
- [21] A. Korjenic, V. Petránek, Development and performance evaluation of natural thermal-insulation materials composed of renewable resources, 43 (2011) 2518–2523. doi:10.1016/j.enbuild.2011.06.012.

- [22] E. Sassoni, S. Manzi, A. Motori, M. Montecchi, M. Canti, Novel sustainable hemp-based composites for application in the building industry: Physical, thermal and mechanical characterization, *Energy Build.* 77 (2014) 219–226. doi:10.1016/j.enbuild.2014.03.033.
- [23] M.Y.M. Zuhri, Z.W. Guan, W.J. Cantwell, Composites : Part B The mechanical properties of natural fibre based honeycomb core materials, *Compos. PART B.* 58 (2014) 1–9. doi:10.1016/j.compositesb.2013.10.016.
- [24] J. Holbery, D. Houston, Natural-fiber-reinforced polymer composites in automotive applications, *JOM.* 58 (2006) 80–86. doi:10.1007/s11837-006-0234-2.
- [25] B. WEAGER, High-performance biocomposites: novel aligned natural fibre reinforcements, *JEC Compos.* (2010) 31–32.
- [26] S. Mallalah, K.V. Sharma, M. Krishna, Development and Comparative Studies of Bio-based and Synthetic Fiber Based Sandwich Structures, (2012) 332–335.
- [27] A.A. El-Sayed, M.G. El-Sherbiny, A.S. Abo-El-Ezz, G.A. Aggag, Friction and wear properties of polymeric composite materials for bearing applications, *Wear.* 184 (1995) 45–53. doi:10.1016/0043-1648(94)06546-2.
- [28] H.H. Parikh, P.P. Gohil, Experimental investigation and prediction of wear behavior of cotton fiber polyester composites, *Friction.* 5 (2017) 183–193. doi:10.1007/s40544-017-0145-y.
- [29] Y. Swolfs, L. Gorbatikh, I. Verpoest, Fibre hybridisation in polymer composites: A review, *Compos. Part A Appl. Sci. Manuf.* 67 (2014) 181–200. doi:10.1016/j.compositesa.2014.08.027.
- [30] F. Rizzo, F. Pinto, M. Meo, Development of multifunctional hybrid metal/carbon composite structures, *Compos. Struct.* 222 (2019) 110907. doi:10.1016/j.compstruct.2019.110907.
- [31] S.B. Visweswaraiyah, L. Lessard, P. Hubert, Interlaminar shear behaviour of hybrid fibre architectures of randomly oriented strands combined with laminate groups, *Compos. Struct.* 176 (2017) 823–832. doi:10.1016/j.compstruct.2017.06.002.
- [32] C. Bellini, G. Parodo, W. Polini, L. Sorrentino, Experimental investigation of hydrothermal ageing on single lap bonded CFRP joints, *Procedia Struct. Integr.* 9 (2018) 101–107. doi:10.1016/j.prostr.2018.06.017.
- [33] C. Bellini, V. Di Cocco, F. Iacoviello, L. Sorrentino, Performance evaluation of CFRP / Al fibre metal laminates with different structural characteristics, *Compos. Struct.*

- 225 (2019) 111117. doi:10.1016/j.compstruct.2019.111117.
- [34] G. Kretsis, A review of the tensile, compressive, flexural and shear properties of hybrid fibre-reinforced plastics, *Composites*. 18 (1987) 13–23. doi:10.1016/0010-4361(87)90003-6.
- [35] J. Zhang, K. Chaisombat, S. He, C.H. Wang, Hybrid composite laminates reinforced with glass/carbon woven fabrics for lightweight load bearing structures, *Mater. Des.* 36 (2012) 75–80. doi:10.1016/j.matdes.2011.11.006.
- [36] F. Sarasini, J. Tirillò, S. D’Altilia, T. Valente, C. Santulli, F. Touchard, L. Chocinski-Arnault, D. Mellier, L. Lampani, P. Gaudenzi, Damage tolerance of carbon/flax hybrid composites subjected to low velocity impact, *Compos. Part B Eng.* 91 (2016) 144–153. doi:10.1016/j.compositesb.2016.01.050.
- [37] M.J. Le Guen, R.H. Newman, A. Fernyhough, G.W. Emms, M.P. Staiger, The damping–modulus relationship in flax–carbon fibre hybrid composites, *Compos. Part B Eng.* 89 (2016) 27–33. doi:10.1016/j.compositesb.2015.10.046.
- [38] S. Rao, K. Jayaraman, D. Bhattacharyya, *Composites : Part B Micro and macro analysis of sisal fibre composites hollow core sandwich panels*, *Compos. Part B.* 43 (2012) 2738–2745. doi:10.1016/j.compositesb.2012.04.033.
- [39] H.G. Allen, *Analysis and design of structural sandwich panels: the commonwealth and international library: structures and solid body mechanics division*, Elsevier, 2013.
- [40] E.W. Andrews, G. Gioux, P. Onck, L.J. Gibson, The role of specimen size, specimen shape and surface preparation in mechanical testing of aluminium foams, *Mater. Sci. Eng. A.* (2000).
- [41] A.P. Harsha, U.S. Tewari, Two-body and three-body abrasive wear behaviour of polyaryletherketone composites, *Polym. Test.* 22 (2003) 403–418. doi:10.1016/S0142-9418(02)00121-6.
- [42] I.M. Hutchings, M. Science, P. Street, C.B. Uk, *Mechanisms of wear in powder technology : a review*, 76 (1993) 3–13.
- [43] M.C.R. No, K. Friedrich, R.B. Pipes, Evaluation of polymer composites for sliding and abrasive wear applications, 19 (1988).
- [44] Michael Neale Mark Gee, *A Guide to Wear Problems and Testing for Industry*, William Andrew, New York, 2001.
- [45] H. Benabdallah, D. Olender, Finite element simulation of the wear of polyoxymethylene in pin-on-disc configuration, 261 (2006) 1213–1224.

doi:10.1016/j.wear.2006.03.040.

Chapter 2: Bio-composite materials

2.1 Bio-composite characteristics

Fibre reinforced polymer (FRP) composite industry was born in the middle of the 20th century, when glass fibres were coupled with polyester polymers for the first time [1], it started to grow because the demand for composite materials increased as a consequence of the extension of the application fields. These materials were attractive due to their tailorable design and their capacity to combine the mechanical properties of various materials in order to produce a composite material characterised by high performance. Up to now, glass fibres are the most common reinforcement in polymer composite materials, this because these fibres are relatively easy to produce and are characterised by a lower price if compared with the other common synthetic reinforcements such as carbon fibres. Other advantages of this fibre typology are the high tensile strength, the high chemical stability and chemical resistance. However, on the other hand, glass fibres are characterised by some weakness. They have low yield modulus if i.e. they are compared with carbon fibres, high specific weight among the other synthetic fibres, are characterised by a low fatigue resistance, are sensitivity to abrasion and their high hardness is responsible of wear phenomenon on moulding dies and machining tools [2]. The biggest problem that characterises glass and the other common fibres is related to the non-biodegradable nature, their recycling process and disposal issue [3,4].

During the last years, governative laws such as Energy Policy Act of 2005, Biomass Research and Development Act of 2000, the Farm Security and Rural Investment Act of 2002 were established due to the growing attention on the depletion of petroleum resources and an increased sensitivity on the environmental pollution caused by the production, use and disposing of synthetic materials [1]. These regulations incentive an investigation on bio-composites or other renewable materials as good alternatives to synthetic composites. The use of natural fibres as reinforcement in polymer matrix composites, is currently receiving an improving attention due to the above mentioned issues. These annual agriculture crops are characterised by higher mechanical strength if compared with the most commonly wood based fibres i.e. wood flour and wood fibres. Some research works on annual crop, conclude that these materials could be potentially employed as reinforcement for both thermoset and thermoplastic matrix. Among the bio-based fibres, even if hemp and flax show higher mechanical properties if compared to the other natural fibres, are the least used due to many problems associated with

the fibre incorporation into the matrix. The first issue is related to the poor compatibility between the hydrophilic fibre nature and the hydrophobic matrix nature that is traduced into a poor fibre-matrix interface, and then into poor mechanical properties of composite materials [5]. Poor thermal stability and a high moisture absorption of bio-based fibres that results in a dimensional composite instability and a reduction of mechanical properties.

Considering the polymer typology used, these natural fibres can be coupled with bio-based matrix in order to obtain a totally biodegradable composite material, this class of bio-materials are affected by an issue related to a long term durability and then further studies are still required on this subject. However, natural fibres are widely coupled with thermoset and thermoplastic matrix still considering these composite as Bio-composite materials, indeed it is so defined a composite material when one or more phases derive from renewable sources [6]. So, Bio-composite are characterised by a widely range of environmental friendliness, depending from the materials employed for their production and their ability to biodegrade. A schematisation of these class of materials is shown in fig.10.

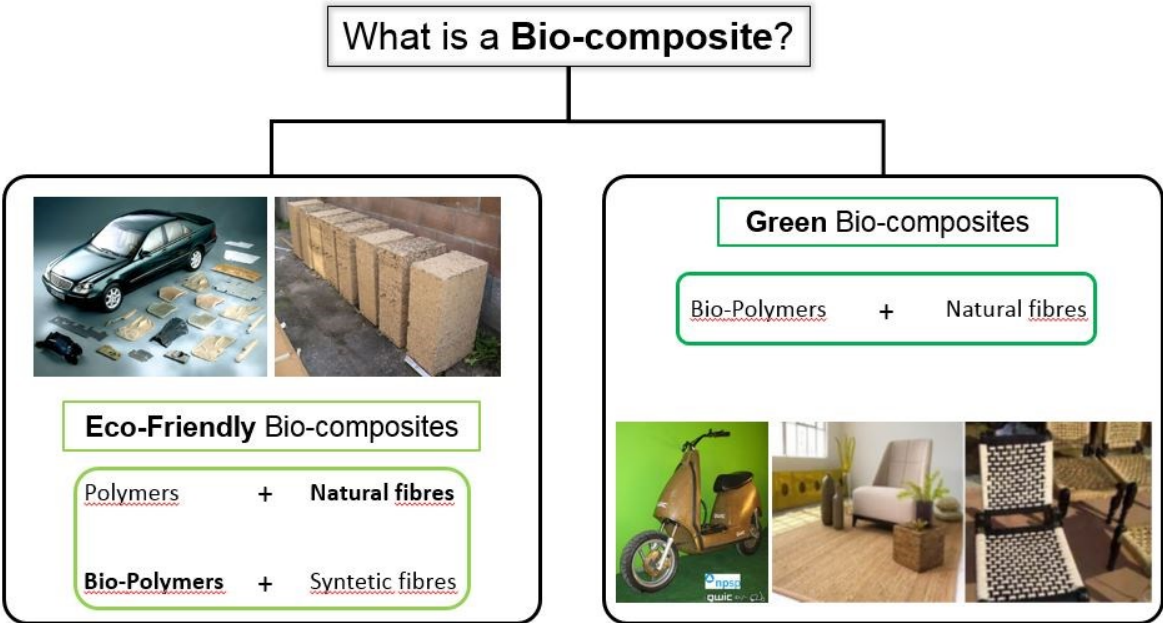


Fig.10: Schematisation of the main natural fibres.

As above discussed, natural fibres are usually coupled with thermoplastic and thermoset resins. Numerous research works are focused on polymers that derive from natural resource of plant origin, from natural monomers like PLA or polymers that derive from microbial monomers like

PHB in order to use these materials as matrix in thermoplastic composite materials [7,8]. In this way it is possible to obtain an eco-friendly material that is recyclable, characterised by low processing cost and have the ability to be remoulded into complex part.

Studies on reinforced natural fibres PLA are very limited [9,10], but Bodros et al. [11] studied the tensile strength of PLA/flax composite material, this study demonstrates that their mechanical properties are higher than PP/flax composite materials and that the specific properties of PLA/flax are very close to that of glass/ polyester composite. Then, in order to make natural fibre able to compete with synthetic ones, an improvement of the mechanical properties is required, this goal can be reached by obtaining a better adhesion between fibre and matrix. For this motivation, up to now, natural fibres are coupled with thermoset resin in all applications in which higher mechanical properties are required. Thermoset matrices are characterised by cross functional groups that permit a development of a better interface between fibre and matrix, this because when an epoxy resin is employed, the functional groups form covalent bonds with the plant cell walls through -OH groups [12]. It is also known that thermoset composites are characterised by a higher thermal stability and a moisture absorption that is lower than thermoplastic composite materials. Moreover, thermoset resin can be cured at room temperature and this aspect does not reduce the mechanical properties of natural fibres. Focusing the attention on the total cost of composite materials, it is known that synthetic fibres are expensive, but the manufacturing process is well developed, and this aspect reduces the total cost of composite material. If the attention is focused on bio-based composite, is possible to assess that some materials are more expensive than petroleum-based polymers, but it is expected that the low cost of the natural reinforcement with a technological development and the increasing of the demand, can help to reduce the total composite material cost. This cost reduction is given in part from the reduced energy required for the natural fibre production. Many researchers demonstrate that the energy consumption required to produce a natural fibre is almost 9,7 MJ/kg and includes cultivation, harvesting and fibre production. This value is around the 18% of the total energy required for the glass fibre production that is around 55 MJ/kg [13]. Moreover, a large part of natural fibres is characterised by a density that is around the 40% lower than that of glass fibre, this aspect allows to additional cost reduction when these bio-based composites are employed in application fields such as automotive or transportation. This because they permit a better efficiency in fuel consumption. Taking into account these aspects it is clear that bio-composites can offer many potential advantages if compared to the traditional composite materials.

2.2 Historical application of natural fibres composites

The production and use of composite materials can be founded in the early human existence, these materials were employed in order to produce refuges, generic tools, clothes and weapons. Traces of composite materials reinforced by natural fibres in building application have been found almost 3000 years ago during the Egyptian period. Straw was used as reinforcement of clay bricks for buildings application.

Successively, the introduction of new materials such as ceramics or stainless steel for structural application led natural fibres in a period of oblivion. It was during the first middle of the 1900 that composite materials began to be widely used when a salesman of the Owens Corning Fibreglass Company started to sell glass fibres in the United States. However, it was during the second World War that composite materials assumed a growing attention. The United States government became to be worried about the availability of metal replacement parts for aircraft, so the engineers were invited to redesign and produce these parts with composite materials by using the current best production practices. However, it was in the early 1960 that composite materials became a large scale products with the introduction of carbon and boron fibres. These materials were employed as reinforcement both in thermoplastic and thermoset matrix in some application such as automotive or aeronautic fields [14].

However, it is during the last years that bio-based composite materials have attracted the attention as replacement of synthetic fibres, this happens due to the increasing of the environmental sensitivity and sustainability. Moreover, natural fibres are characterised by a lower cost than the synthetic ones and are also easily renewable. They are characterised by a lower density, and then by specific mechanical properties that are comparable with the most commonly employed synthetic materials like glass fibres.

Initially, natural fibres were used only in textile and building application, successively there was an extension of the bio-based composite materials in automotive application field as interior components [15–17]. This because of their low density, mechanical properties that are appropriate in these applications and the low processing costs.

It was in the 1941 that natural fibres composite materials were massive used in automotive application with Henry Ford. In this year was presented the famous Hemp Body Car, known also as Ford Cannabis. This car was characterised by a steel body frame and panels produced with soybeans and hemp fibres, the reasons of this choice must be founded in the low metal

availability during the second World War. Henry Ford justified the use of this typology of fibre with these words:



Fig.11: Henry Ford with the famous Hemp Body Car.

“why use up the forest which were centuries in the making and the mines which required ages to lay down, if we can get the equivalent of forest and mineral products in the annual growth of the hemp fields?”

This car was lighter but also stronger than the other car used in that period, moreover, its lightness leads to a more efficient fuel consumption than a normal steel body car. The Hemp Body Car was also designed to run with biofuel, so this car was a real eco-friendly product of the car history. From this moment natural fibres composites failed in a new period of oblivion, especially hemp fibres due to the anti-drug laws.

However, during the last years of the 1900, natural fibres were widely employed in automotive application by Mercedes-Benz in non-structural parts as interiors and door panels. From this moment, numerous car production companies began to use these materials leading to a growing of the market of natural fibres [18]. It is demonstrated that German car industries improved the use of bio-composite materials starting from an use of around 4000 tons in 1996, to 18000 tons in 2003 with an almost linear increasing rate of 10 to 20% from 1996 to 2002 [19].

Mercedes-Benz was a pioneer car industry in the use of bio-based composite materials, nowadays, numerous companies such as Audi group, BMW, Volkswagen group, Ford, Opel and FCA group use natural fibres composites in some application as interior components such as door panels or dashboard. For example, the door panels of the Audi A2 model derives from

a hybrid polyurethane matrix reinforced by flax/sisal and the Alfa Romeo Giulia dashboard (fig.12) derives from bio-based composite material.



Fig.12: Hemp dashboard of the Alfa Romeo Giulia.

All these components provide to a global vehicle weight reduction, and then to an improved fuel consumption saving that is proportional to the total weight lost [20].

Furthermore, as it is possible to see in fig.13, bio-based composites are employed in several applications such as in buildings and construction as door frame, wall or windows. These materials can be used also in packaging, for example boxes production and food trays, electronic device such as external cover for mobile phones, inner fenders and bumper in railroad and automotive applications, toys and generally in all applications in which are not required very high mechanical properties but a cost reduction [21–24].



a)



b)



c)



d)

Fig.13: Some application fields of natural fibre composites: interiors in automotive field (a); dishes (b); mobile phone cover (c); baggage (d).

Bio-based composite materials have been employed also in car roof structures (fig.14). However, studies were carried out on roof production in building application, these bio-based materials were manufactured from soy oil-based resin reinforced by cellulose fibres in paper sheets form made from recycled cardboard boxes [25].



Fig.14: Application of natural fibres as roof in automotive field.

Other research works are oriented on the substitution of asbestos fibres in roof employing with pulp of sisal and coco fibres and from eucalyptus recycled fibres [26].

Remaining in building theme, particular attention must be dedicated to the temporary house. These housing are usually made of wood plastic composites and are installed when a

catastrophe occurs. This context could be an interesting application field for bio-based recyclable materials. Usually, these temporary houses are dismissed at the end of their usage and are put into landfills, then, in order to reduce this waste problem, bio-composite materials can be used because they can be composed or recycled at the end of their service life [24].

2.3 Natural fibres sources

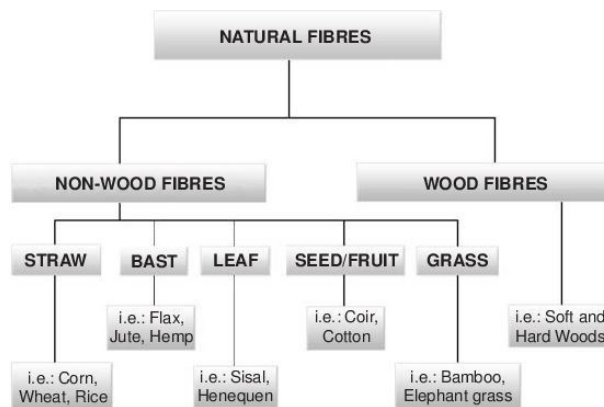
The table 1, shows an overview on natural fibres, these can be obtained by mineral, plants and animal origins.

Table 1: Overview on natural fibres



Plant fibres are a renewable source and are characterised by the ability to be recycled, these fibres are usually employed as reinforcement of polymeric matrices. A schematic classification of natural fibres is showed in table 2 [27].

Table 2: Overview on natural fibres as reinforcement in composite materials



The guideline to the substitution of glass fibres with natural ones is that these fibres are renewable and eco-friendly, but if they are burned for disposal, natural fibres come back to the atmosphere less carbon dioxide than that absorbed during the plant growing. Another motivation is given by the lower price that characterises natural fibres if compared for example to glass fibres. These ones are more expensive than natural fibres, their price is around 1,96 €/kg whilst the price of bio-based fibres varies from 0,2 to 0,5 €/kg. Furthermore, if the mechanical properties of natural fibres are compared with that of glass ones, these are characterised by lower values of the tensile stress and Young modulus. However, if the specific properties are considered, natural fibre shows a specific Young modulus that is comparable or higher than glass fibre. This because natural fibres have a density that varies between 1,2 and 1,5 g/cm³ while glass fibre has a higher density that is equal to 2,5 g/cm³. These aspects, with the possibility of material cost saving and the advantage of being non-abrasive on the moulding dies, make these fibre typologies an existing alternative to conventional fibres in many application fields.

2.4 Natural fibres comparison

There are several factors that can be used to classify natural fibres and choose for their use as reinforcement in polymer matrix. These factors are identified in chemical composition, possible structural defects, surface characteristics, strength, stiffness and cost. This last parameter depends by the above mentioned properties of natural fibres, but also supply, quality and demand of natural fibres [27]. It is clear that wood fibres are the cheapest natural fibres because

of their availability and extended use in pulp and paper industries [28]. However, other natural fibres such as hemp, flax, jute and kenaf are improving their status in composite production due to their better strength and stiffness among the other natural fibres. In table 3 are listed the commercially available cellulose fibres [29].

Table 3: Available fibre typologies and their production amount

Source	Species	World production (10 ³ tonnes)	Origin
Wood	(>10'000 species)	1'750'000	Stem
Bamboo	(>1'250 species)	10'000	Stem
Cotton Lint	Gossypium sp.	18'450	Fruit
Jute	Corchorus sp.	2'300	Stem
Kenaf	Hibiscus cannabinus	970	Stem
Flax	Linum usitatissimum	830	Stem
Sisal	Agave sisilana	378	Leaf
Roselle	Hibiscus sabdariffa	250	Stem
Hemp	Cannabis sativa	214	Stem
Coir	Cocos nucifera	100	Fruit
Ramie	Boehmeria nivea	100	Stem
Abaca	Musa textiles	70	Leaf
Sunn Hemp	Crorolaria juncea	70	Stem

Hemp, jute, flax and kenaf fibres are often recognised as bast fibres because they derived from the inner bark of the stem of dicotyledonous plants, some geometrical characteristics of these materials are listed in table 4 [30].

Table 4: Geometrical characteristics of the widely used natural fibres

Fibre typology	Length of the textile fibre (mm)	length of the ultimate fibre (mm)	Diameter (µm)	Weight per length	Density (g/cm ³)
Hemp	1300 – 3000	5 – 55	16 – 50	3,20	1,40
Flax	300 – 900	13 – 60	12 – 30	1,70 – 17,80	1,40
Jute	150 – 360	0,80 – 6	5 – 25	13,27	1,40
Sisal	600 – 1000	0,80 – 8	100 – 400	9 – 400	1,20 – 1,45
Ramie	1500	40 – 250	16 – 125	4,60 – 6,40	1,40
Kenaf	900 – 1800	1,50 – 11	14 - 33	50	-

All these fibre typologies are characterised by a similar morphology, with more detail, cellulose, hemicellulose and lignin are the principal fibre constituents and are responsible of the mechanical and geometrical properties of these reinforcements. Gassan and Bledzki [28] concluded that these three constituents and pectin cell walls vary in composition and in their structure as function of the age of the plants and the climatic conditions. In the following table 5, are reported the natural fibres as function of their principal constituents and water absorption [29].

Table 5: Natural fibres and their principal constituents

Fibre type	Cellulose	Hemicellulose	Lignin	Pectin	Water solubles	Fat and wax	moisture
Hemp	67,00	16,10	3,30	0,80	2,10	0,70	10,00
Flax	64,10	16,70	2,00	1,80	3,90	1,50	10,00
Jute	64,40	12,00	11,90	0,20	1,10	0,50	10,00
Sisal	65,80	12,00	9,90	0,80	1,20	0,30	10,00
Ramie	68,60	13,10	0,60	1,90	5,50	0,30	10,00
Sunn	67,80	16,60	3,50	0,30	1,40	0,40	10,00
Abaca	63,20	19,60	5,10	0,50	1,40	0,20	10,00

From this table is possible to assert that the chemical constituents of these fibres are very important, this because their composition influences their choice and then their utilisation, Robson [29] confirmed that the chemical constituent have a specific function in the cell wall. Indeed, cellulosic microfibrils form crystalline parts that give high stress and stiffness to the fibres, hemicellulose and cellulose form semi-crystalline structure that gives flexibility and the amorphous lignin part contributes to the rigidity and causes the hydrophilic behaviour of these categories of fibres [30].

2.5 Advantages and disadvantages of natural fibres

It is known that natural fibres have been widely used in many application fields, the high strength of these fibre typology was utilised to produce ropes, textiles products and tools. Another application of natural fibres is in building field, but these are just some of the past and present application of natural fibres over other materials typology. But, even if bio-based

materials are characterised by advantages that allow to their use over traditional materials, there are some disadvantages that characterise these materials.

2.5.1 Advantages

Some research works demonstrated that bio-based materials possess interesting mechanical properties, but there are other interesting qualities that make natural fibre very interesting. These fibres are typically obtained from annual and renewable plants, these aspects make natural fibres cheaper and much less sensitively subjected to economic fluctuation. Furthermore, their cultivation reduces the environmental awareness linked to the depletion of natural resources. In addition, these fibres are characterised by a density that is lower than synthetic fibre such as carbon and around a half of the most commonly used fibres like glass [31]. This aspect makes the resulting bio-based composite material lighter than the traditional ones allowing to reduced costs when employed in transportation field. Natural fibres are also characterised by a non-toxicity and this feature allows to a safe utilisation [32–34]. On the other hand, synthetic fibres reinforced polymers such as fibre glass composites, produces particles during the processing phase or during the life cycle, that can cause allergic reaction, skin irritation or irritation to the respiratory system if these fibre particles are inhaled [35,36].

Natural fibre composites are also characterised by an upgraded life cycle assessment, this because natural reinforcement requires less energy for growing and production phases, these aspects reduce the carbon footprint if compared with carbon or glass fibre production. The improved life cycle assessment can be attributed to the fact that when natural fibres are dismissed and then burned or subjected to degradation, give back the same amount of carbon dioxide that absorbed during their growing phase defining these plants as a carbon neutral material. Moreover, the energy used for the production of natural fibres is estimate around 9,7 MJ/kg. This amount of energy includes cultivation, harvesting and fibre maceration and it is demonstrated that is less than a quarter of the total energy spent for the production of glass fibre that is almost 56 MJ/kg [13]. Sustainable et al. [37] performed life cycle assessments (LCAs) for some bio-based materials, they concluded that these materials possess an interesting potential for the environmental benefits and can be a valid contribution to a more environmentally friendly and sustainable world. Joshi et al. [17] carried out a study referred to guidelines for improved environmental performance of natural fibres composites compared with glass fibres composites in automotive application. These guidelines established a lower

environmental impact for natural fibres production, substitution of based polymer parts with a higher volume of natural fibres and credits for carbon emission or energy production deriving from the incineration at the end of the life cycle. At the end of this research work, they concluded that natural fibre composites are environmentally friendly more than glass fibre composites.

In the following table 6 [33] all the aspects treated in this section are resumed and a comparison between natural fibres and glass fibres is made.

Table 6: Comparison between natural and glass fibre

	Natural fibres	Glass fibres
Density	low	Twice than NF
Cost	Low	Low, but higher than NF
Energy consumption	Low	High
CO ₂ neutral	Yes	No
Health risk when inhaled	No	Yes
Renewability	Yes	No
Disposal	Biodegradable	Not biodegradable
Recyclability	Yes	No

2.5.2 Disadvantages

Even if natural fibres have many advantages on synthetic materials, some weakness inhibit their application as substitution of traditional composite materials. In this section some disadvantages are presented and analysed in detail.

The first issue that characterises the bio-based fibres is the mechanical properties variation. It is known that the production process of these plant fibres differs from that of traditional ones. Conventional fibres can be produced in a defined range of properties with particular accuracy, conversely natural fibres are subjected to a wide range of variation of properties when produced. Indeed, a large variation of mechanical properties of natural fibres is found. This aspect is a complication for the widespread natural fibre employ improvement.

The mechanical properties of natural fibres are influenced by numerous aspects such as the moisture content, the type of fibres and their form i.e. mat, fabric and type of fabric, yarn or chopped. Moreover, these properties are affected by environmental factors such as the place

where the fibres are grown, cultivation conditions, the growing and harvesting period, the production process and the part of the plant that is used for their production. Furthermore, the mechanical properties are influenced by the fibre orientation, and these categories of materials are particularly affected by this aspect. Usually natural fibre composites are produced with random and oriented fibres. It is clear that there is a large variation of the mechanical properties when oriented or random fibres are employed, but it was found that the tensile strength of these composites decreased about four times when the angle between the fibre orientation and the test direction increases to around 26°. It was found that the Young modulus is less affected by the fibre orientation and decreases by around two times.

An important issue related to natural fibre is the fibre-matrix interfacial bonding. An inefficient wetting of the reinforcement causes a poor adhesion and then an ineffective interface between fibre and matrix. This is an important issue that characterises bio-based composite materials, because a good adhesion between matrix and fibres permits an efficient stress transmission from matrix to the reinforcement and then good mechanical properties. Most thermoplastic polymers such as polypropylene and polyethylene are hydrophobic (non-polar), this aspect makes these polymers incompatible with the reinforcement and leads to a poor interface with natural fibres that are hydrophilic (polar). Conversely, thermoset matrix such as epoxy or phenolic are characterised by polymeric chain on which there are active groups that are able to form covalent cross-links with the -OH groups of the fibre cell walls. However, natural fibre composites are performed below their capability due to the presence of unstable hemicellulose and lignin components. Then, in order to increase the long-term stability of these composites, and in order to improve the wettability of the reinforcement, some chemical treatments are carried out on untreated fibres. Some of these treatments are alkalisation, acetylation and silane treatment. Usually, the alkalisation is the most widely used process in which natural fibres are wet with sodium hydroxide (NaOH), this because it has a good efficiency and is a cheap process [38,39].

Natural fibres are also characterised by a low thermal stability, with more detail with the temperature increasing, there is a cellulosic degradation and the production of volatile substances that affect the mechanical properties. For these reasons, the processing temperatures are limited around to 200 °C, even if natural fibres can be processed at higher temperature for a brief period and under defined production conditions [40]. This weakness limits the thermoplastic matrix typologies that can be used with bio-based fibres, and then reduces the application fields of these categories of composite materials to low temperature work conditions.

Natural fibres are also affected by the moisture. This is an important aspect to take into account when these composite materials are produced, indeed if there is water on the external surface of the fibre, it can be as a separation film between fibre and matrix during the matrix-fibre interface formation. Then, in order to avoid this issue, natural fibres are often dried before the composite production. In this way it is possible to prevent the evaporation of water particles during composite production over 100 °C, and then the most undesirable defect of composite material is reduced such as the presence of voids that reduce the mechanical properties of the laminate. Bledzki et al. [41] studied the effect of the drying process of natural fibres on the mechanical properties. They concluded that this process leads to an increase of the tensile strength and of the Young modulus about 10% and 20% respectively. But bio-based composites are also affected by the moisture absorption during their service life. This issue causes the fibre swelling and then micro cracks that affect the mechanical properties of the composite material. Joseph et al. [5] carried out a study on the moisture absorption, and concluded that this phenomenon can be reduced by improving the interfacial adhesion through chemical treatments of the reinforcement. The water absorption with environmental agents can cause the natural fibres degradation. This aspect could be a good feature that justify the sustainability of these composite materials typology and the sensitivity to the environmental awareness, but it can be an important aspect to consider when bio-based materials are employed in outdoor applications and are subjected to environmental agents. Then, in order to improve the life cycle for several years, some chemical treatments are executed in order to modify the cell walls chemistry and then reduces the natural degradation. These chemical treatments act on the -OH groups limiting the overall capability of water absorption and then reducing the fibre swelling and the biological degradation.

2.6 Natural fibre composites matrices

The matrix phase is fundamentally significant in a composite structure. This because it is responsible of the load transferring to the fibres, it is a sort of barrier against the environmental agents and protects the fibres from mechanical abrasion. Usually, both thermoplastic and thermoset matrices are used with natural fibres, but the use of the first one is limited from the production temperature at which natural fibres degrade [42]. As mentioned above, natural fibres are unstable at 200 °C and this aspect limits the thermoplastic matrix choice [43].

2.6.1 Thermoplastic matrices from bio sources

Natural fibres are widely coupled with conventional thermoplastic polymers such as Polypropylene and Polyethylene because of the availability at low cost of these materials [40]. It is about the last two decades that the bio-based matrices are growing their attention due to the environmental concerns and the awareness that petroleum resources are limited [44]. Globally, polymers that derive from renewable sources can be distinguished by natural polymers such as protein and cellulose, synthetic polymers that derive from natural monomers such as PLA and polymers from biological fermentation such as polyhydroxy butyrate (PHB). The development of synthetic polymers that derive from natural monomers like PLA, has been a driving force for the progress of bio-based polymers from renewable sources. Up to now, PLA matrix is the most interesting polymer between the bio-derivable polymers [45]. This because its mechanical properties are better than the widely employed polymers such as Polypropylene [46]. If the degradation process is considered, it can be assessed that when PLA degrades, it does not emit carbon dioxide in the atmosphere like other biodegradable materials. The degradation of PLA occurs by a hydrolysis process to lactic acid that is metabolised by micro-organisms in water and carbon dioxide. Then, the degradation of PLA material can occur in a pair of weeks and its wastes can disappear in a month. The PLA polymer consists of a linear aliphatic polyester of lactic acid that can be obtained from renewable agricultural materials fermentation, these materials are corn, sugarcane and sugar beets [45]. To date, the major applications of PLA polymer is in household objects, such as waste bags, barrier for sanitary products, cups and plates. However, the driving force is the production of a totally bio composite material by using biodegradable polymers coupled with natural fibres [44,46]. Keller et al. [47] studied a composite material produced with PLA matrix reinforced by natural fibres, they concluded that these composite materials can be used as light weight construction materials. Oskman et al. [46] studied a bio-composite material obtained by coupling PLA matrix with flax fibres. They concluded that the bio-composites shows a strength that was about 50% higher than polypropylene matrix reinforced by flax fibres. Then, the increasing interest for natural fibre reinforced composites in automotive or building fields combined with the increasing interest of environmentally friendly materials, can be an interesting research area for fully biodegradable composites.

2.6.2 Thermoplastic matrices

Even if the guideline is the implementation of the application fields for totally bio-composite, to date natural fibres are widely coupled with traditional thermoplastic polymers. But, as above mentioned, the choice of these materials is limited by the thermal instability of natural fibres[48]. Due to this limitation, only thermoplastic polymers with a low glass transition temperature can be used such as polyethylene, polypropylene, polyvinylchloride and polystyrene as matrix [40]. Moreover, it was found that, due to the different natures of these matrices (hydrophobic) and natural fibres (hydrophilic), a poor interface adhesion established between the two phases, and then the composite material is characterised by low mechanical properties. For these reasons, to date natural fibres are mostly coupled with thermoset matrices, but an important aspect is that thermoset polymers are capable of being repeatedly softened by heat application and then hardened by cooling, then these polymers have the potential to be easily recycled [49].

2.6.3 Thermoset matrices

During the last years, there has been a growing interest in using natural fibres in automotive application. But, in order to obtain good mechanical properties, a good adhesion between fibre and matrix is required. Epoxy and phenolic resin are able to form an interfacial adhesion that is stronger than that of thermoplastic matrices with natural fibres, this because thermoset matrices are able to form covalent cross links with fibres -OH groups [12,50]. These resins have the peculiarity to polymerise at room temperature and not produce volatile products, then their use avoid the thermal instability that characterise the bio-based fibres and reduce the possibility to have voids into the laminate. Both these aspects reduce the mechanical properties of the composite material.

2.7 Production technologies

Usually, bio-based composite materials are produced by using the same production techniques customised for traditional composite materials. These production technologies include production systems both in case of thermoplastic and thermoset matrices composites and can be distinguished in resin transfer moulding (RTM), vacuum bag infusion process, extrusion, compression moulding and injection moulding. These technologies are well experienced with the production of traditional composite materials and permit the production of laminate with a controllable quality [51]. However, there are still some issues related to the production of natural fibres composites due to the materials employed, with more detail because of their thermal instability, their geometry and structural properties. Indeed, in order to improve the adhesion between fibre and matrix, some chemical treatments are required because of the hydrophilic nature of the natural fibres and the hydrophobic nature of matrix phase.

Then, in order to select the most appropriate production technology of bio-based composites, design and manufacturing engineers focused their attention on some selection criteria. These selection criteria are the size and shape of the product, desired mechanical properties, speed and manufacturing costs and so on.

If the size and shape is considered, in case of small or medium dimension of the laminate, injection and compression moulding are chosen due to the simplicity of the production process and velocity. However, in case of large size composites, are preferred open moulding and autoclave process techniques.

If the performance of composites is considered, some aspects must be taken into account such as the length and the diameter of the fibres, their orientation and the volumetric content of fibre. The interface adhesion plays an important role on the composite material performance, but it does not depend from the production technology used. Indeed, to ensure a good interfacial bonding some chemical treatments are performed on the natural fibres before the production phase in order to remove surface coatings in case of silk or coir fibres and prepare the surface of the fibre in case of hemp fibres.

Some production technologies such as Resin Transfer Moulding, Injection Moulding, Compression Moulding, Extrusion and Pultrusion are the most used production technologies. Some of these, in detail Compression Moulding and Pultrusion have been used with good results to produce flax fibres weaved with polypropylene yarns coupled with thermoset matrix [52,53]. The Extrusion technique is used for thermoplastic composite materials, the matrix

usually in form of pellets is heated and mixed with the fibres into a chamber, then by means of one or two rotating screws, the composite material is forced out from the chamber at a steady rate through a die. Usually, when this production technology is used, attention must be placed on the extrusion velocity. A fasted production process means a higher temperature for the matrix softening, moreover it causes air entrapment and possible fibre breakage [40]. Conversely, low production velocity can cause low mixing process and insufficient fibre wetting. It has been shown that the extrusion by means of two screws leads to a better chopped fibre dispersion into the matrix, and then better mechanical properties [54]. Usually this production technique is used to produce precursors for the Injection Moulding process. Moreover, the Extrusion process is characterised by a fibre orientation variation through the cross section of the composite material. With more detail, close to the die walls it is possible to observe a fibre alignment along the composite filament axis due to a shear flow caused by the friction along the walls of the die, whilst fibres transverse aligned to the material flow direction at the centre of the composite material [49,55]. Another process technique is the Injection Moulding, but due to the fibre friction with the die and the viscosity of the material, the fibre volume percentage is almost 40%.

Compression Moulding process is commonly used for thermoplastic polymers. Usually, fibre and matrix layers are stacked alternating plies of fibres with layer of matrix in form of sheet. For a good quality laminate, it is important to control the matrix viscosity, holding time, pressure and temperature [55]. A critical parameter is the matrix viscosity linked to the moulding temperature, this parameter must be controlled with attention, especially in case of thick laminates in order to ensure that the matrix fully penetrate the fibre structure.

Temperature must be carefully controlled during the Compression Moulding especially when there is a little difference between the melting point temperature of the matrix and that of fibre degradation. It was found in literature that, in case of compression moulding with natural fibres, a strength reduction occurs at temperatures both at 150 °C and 200 °C [49]. However, a study carried out on flax reinforced polyester amide polymer demonstrates that there is a compromise between a good fibre wetting and the fibre degradation avoiding. The optimum was found for a temperature of 150 °C, flexural properties of these composites below this threshold temperature were not influenced, whilst reduce for higher temperature [56]. Another study carried out on jute yarn and bacterial copolyester bipolar, individualised an optimum for the compression temperature at 180 °C [49]. The highest strength was found at 200 °C in case of polypropylene matrix reinforced with natural fibre mat [56].

With the Resin Transfer Moulding process, a liquid thermoset resin is injected through a fibre preform placed in a mould. Some parameters must be controlled during a RTM process, with more detail the resin and mould temperature, the resin viscosity, injection pressure and the preform architecture. The most important advantage obtained by using this production technique, is the lower production temperature that avoid the fibre degradation [57]. Conversely, the use of natural fibres in the RTM allows to a fibre volume percentage that is lower than the glass fibre composites due to the geometry of natural fibres. Moreover, a lower degree of fibre alignment is obtained with this technique due to the resin flow through the reinforcement, but on the other hand, good component strength can be obtained with this process.

Reference

- [1] L.T.D. Amar K. Mohanty, Manjusri Misra, *Natural Fibers, Biopolymers, and Biocomposites*, CRC Press - Taylor & Francis Group, 2005.
<https://www.crcpress.com/Natural-Fibers-Biopolymers-and-Biocomposites/Mohanty-Misra-Drzal/p/book/9780849317415>.
- [2] P.K. Mallick, *Fiber-reinforced composites : materials, manufacturing, and design*, Marcel Dekker, New York, 1993.
- [3] F.M. AL-Oqla, S.M. Sapuan, M.R. Ishak, A.A. Nuraini, Predicting the potential of agro waste fibers for sustainable automotive industry using a decision making model, *Comput. Electron. Agric.* 113 (2015) 116–127. doi:10.1016/j.compag.2015.01.011.
- [4] A.K. Ilanko, S. Vijayaraghavan, Wear behavior of asbestos-free eco-friendly composites for automobile brake materials, *Friction.* 4 (2016) 144–152.
doi:10.1007/s40544-016-0111-0.
- [5] P. V Joseph, M.S. Rabello, L.H.C. Mattoso, K. Joseph, S. Thomas, Environmental effects on the degradation behaviour of sisal fibre reinforced polypropylene composites, 62 (2002) 1357–1372.
- [6] P.A. Fowler, J.M. Hughes, R.M. Elias, *Biocomposites : technology , environmental credentials and market forces*, 1789 (2006) 1781–1789. doi:10.1002/jsfa.
- [7] A.P. Mathew, K. Oksman, M. Sain, *Mechanical Properties of Biodegradable Composites from Poly Lactic Acid (PLA) and Microcrystalline Cellulose (MCC)*, (2004). doi:10.1002/app.21779.
- [8] L.Y. Mwaikambo, M.P. Ansell, A. Dufresne, M. Hughes, C. Hill, P.M. Wild, Current international research into cellulosic fibres and composites, 6 (2001) 2107–2131.
- [9] T. Kasuga, Y. Ota, M. Nogami, Y. Abe, Preparation and mechanical properties of polylactic acid composites containing hydroxyapatite " bers, 22 (2001) 19–23.
- [10] J. Hoon, T. Gwan, H. Sik, D. Sung, Y. Kwan, S. Chul, J. Nam, Thermal and mechanical characteristics of poly (l -lactic acid) nanocomposite scaffold, 24 (2003) 2773–2778. doi:10.1016/S0142-9612(03)00080-2.
- [11] E. Bodros, I. Pillin, N. Montrelay, C. Baley, *SCIENCE AND Could biopolymers reinforced by randomly scattered flax fibre be used in structural applications ?*, 67 (2007) 462–470. doi:10.1016/j.compscitech.2006.08.024.
- [12] L. Prasannakumari, *INFLUENCE OF INTERFACIAL ADHESION ON THE MECHANICAL PROPERTIES AND FRACTURE BEHAVIOUR OF SHORT SISAL*

FIBRE REINFORCED, 32 (1996) 1243–1250.

- [13] N.W. FT Wallenberger, *Natural Fibers, Plastics and Composites*, Springer, 2003.
- [14] N.E. Zafeiropoulos, D.R. Williams, C.A. Baillie, F.L. Matthews, *Engineering and characterisation of the interface in flax fibre / polypropylene composite materials . Part I . Development and investigation of surface treatments*, 33 (2002) 1083–1093.
- [15] G. Sèbe, N.S. Cetin, C.A.S. Hill, M. Hughes, *RTM Hemp Fibre-Reinforced Polyester Composites*, *Appl. Compos. Mater.* 7 (2000) 341–349. doi:10.1023/A:1026538107200.
- [16] T. Corbière-Nicollier, B. Gfeller Laban, L. Lundquist, Y. Leterrier, J.-A.. Månson, O. Jolliet, *Life cycle assessment of biofibres replacing glass fibres as reinforcement in plastics*, *Resour. Conserv. Recycl.* 33 (2001) 267–287. doi:10.1016/S0921-3449(01)00089-1.
- [17] S.. Joshi, L.. Drzal, A.. Mohanty, S. Arora, *Are natural fiber composites environmentally superior to glass fiber reinforced composites?*, *Compos. Part A Appl. Sci. Manuf.* 35 (2004) 371–376. doi:10.1016/j.compositesa.2003.09.016.
- [18] A. Bledzki, V. Sperber, O. Faruk, *Natural and Wood Fibre Reinforcement in Polymers*, 2002.
- [19] M. García, I. Garmendia, J. García, *Influence of natural fiber type in eco-composites*, *J. Appl. Polym. Sci.* 107 (2008) 2994–3004. doi:10.1002/app.27519.
- [20] A.K. Mohanty, M. Misra, L.T. Drzal, *Sustainable Bio-Composites from Renewable Resources: Opportunities and Challenges in the Green Materials World*, *J. Polym. Environ.* 10 (2002) 19–26. doi:10.1023/A:1021013921916.
- [21] J. Rout, S.S. Tripathy, M. Misra, A.K. Mohanty, S.K. Nayak, *The influence of fiber surface modification on the mechanical properties of coir-polyester composites*, *Polym. Compos.* 22 (2001) 468–476.
- [22] K. Rohit, S. Dixit, *A Review - Future Aspect of Natural Fiber Reinforced Composite*, *Polym. from Renew. Resour.* 7 (2016) 43–59. doi:10.1177/204124791600700202.
- [23] Y. Cao, S. Shibata, I. Fukumoto, *Mechanical properties of biodegradable composites reinforced with bagasse fibre before and after alkali treatments*, 37 (2006) 423–429. doi:10.1016/j.compositesa.2005.05.045.
- [24] Srikanth Pilla, *Handbook of Bioplastics and Biocomposites Engineering Applications*, Scrivener Publishing LLC, 2011.
- [25] M.A. Dweib, B. Hu, H.W.S. Iii, R.P. Wool, *Bio-based composite roof structure : Manufacturing and processing issues*, 74 (2006) 379–388. doi:10.1016/j.compstruct.2005.04.018.

- [26] V. Agopyan, Developments on vegetable fibre – cement based materials in Sa ~ o Paulo , Brazil : an overview, 27 (2005) 527–536. doi:10.1016/j.cemconcomp.2004.09.004.
- [27] D. Robson and J. A. Hague, Comparison of wood and plant fibre properties, in: Third International Conference on Woodfibre-plastic composites, Madison, Wisconsin, USA:, 1995.
- [28] A.K. Bledzki, J. Gassan, Composites reinforced with cellulose based fibres, 24 (1999) 221–274.
- [29] D Robson, Survey of natural materials for use in structural composites as reinforcement and matrices, Bangor, Gwynedd : Biocomposites Centre, University of Wales, 1993.
- [30] R R Franck, Bast and Other Plant Fibres 1st Edition, Woodhead Publishing, 2005.
- [31] A.K. Mohanty, M. Misra, G. Hinrichsen, Biofibres , biodegradable polymers and biocomposites : An overview, 24 (2000) 1–24.
- [32] H. Cheung, M. Ho, K. Lau, F. Cardona, D. Hui, Natural fibre-reinforced composites for bioengineering and environmental engineering applications, Compos. Part B Eng. 40 (2009) 655–663. doi:10.1016/j.compositesb.2009.04.014.
- [33] P. Wambua, J. Ivens, I. Verpoest, Natural fibres: can they replace glass in fibre reinforced plastics?, Compos. Sci. Technol. 63 (2003) 1259–1264. doi:10.1016/S0266-3538(03)00096-4.
- [34] A. Shalwan, B.F. Yousif, In State of Art: Mechanical and tribological behaviour of polymeric composites based on natural fibres, Mater. Des. 48 (2013) 14–24. doi:10.1016/j.matdes.2012.07.014.
- [35] K. Inthavong, A.P. Mouritz, J. Dong, J.Y. Tu, Inhalation and deposition of carbon and glass composite fibre in the respiratory airway, J. Aerosol Sci. 65 (2013) 58–68. doi:10.1016/j.jaerosci.2013.07.003.
- [36] J. Company-quirola, S. Alique-garc, E. Esteban-garrido, F.E. Rojas-farias, A.A. Garrido-r, C. Susana, Skin stripping technique : A diagnostic clue for fiberglass dermatitis, (2019) 2018–2019. doi:10.1016/j.jaad.2018.08.023.
- [37] H. Sustainable, A. Biopolymers, B. Products, T. Hope, How Sustainable Are Biopolymers and Biobased Products? The Hope, the Doubts, and the Reality, (n.d.).
- [38] A. Shahzad, Effects of Alkalization on Tensile , Impact , and Fatigue Properties of Hemp Fiber Composites, (2012). doi:10.1002/pc.
- [39] H. Liu, L. You, H. Jin, W. Yu, Influence of alkali treatment on the structure and properties of hemp fibers, Fibers Polym. 14 (2013) 389–395. doi:10.1007/s12221-013-

0389-8.

- [40] K.L. Pickering, M.G.A. Efendy, T.M. Le, *Composites : Part A* A review of recent developments in natural fibre composites and their mechanical performance, 83 (2016) 98–112. doi:10.1016/j.compositesa.2015.08.038.
- [41] J.O.C.H.E.N. Gassan, A.K. Bledzki, *Effect of Moisture Content on the Properties of Silanized Jute-Epoxy Composites*, (1997) 179–184.
- [42] J. Holbery, D. Houston, *Natural-fiber-reinforced polymer composites in automotive applications*, *JOM*. 58 (2006) 80–86. doi:10.1007/s11837-006-0234-2.
- [43] J. Summerscales, N.P.J. Dissanayake, A.S. Virk, W. Hall, *Composites : Part A* A review of bast fibres and their composites . Part 1 – Fibres as reinforcements, *Compos. Part A*. 41 (2010) 1329–1335. doi:10.1016/j.compositesa.2010.06.001.
- [44] B. Bax, *SCIENCE AND Impact and tensile properties of PLA / Cordenka and PLA / flax composites*, 68 (2008) 1601–1607. doi:10.1016/j.compscitech.2008.01.004.
- [45] L. Yu, K. Dean, L. Li, *Polymer blends and composites from renewable resources*, 31 (2006) 576–602. doi:10.1016/j.progpolymsci.2006.03.002.
- [46] K. Oksman, M. Skrifvars, J. Selin, *Natural fibres as reinforcement in polylactic acid (PLA) composites*, 63 (2003) 1317–1324. doi:10.1016/S0266-3538(03)00103-9.
- [47] A. Keller, D. Bruggmann, A. Neff, B. Müller, E. Wintermantel, *Degradation Kinetics of Biodegradable Fiber Composites*, *J. Polym. Environ.* 8 (2000) 91–96. doi:10.1023/A:1011574021257.
- [48] G. Aparecido dos Santos, Paulo / Giriolli, Joao Carlos / Amarasekera, Jay / Moraes, *Natural fibers plastic composites for automotive applications*, in: *SPE Automotive & Composites Division*, 2008.
- [49] K.L. Pickering, M.G.A. Efendy, T.M. Le, *A review of recent developments in natural fibre composites and their mechanical performance*, *Compos. Part A Appl. Sci. Manuf.* 83 (2016) 98–112. doi:10.1016/j.compositesa.2015.08.038.
- [50] M.S. Islam, K.L. Pickering, N.J. Foreman, *Influence of Alkali Fiber Treatment and Fiber Processing on the Mechanical Properties of Hemp / Epoxy Composites*, (2010). doi:10.1002/app.
- [51] U. Riedel, J. Nickel, *Natural fibre-reinforced biopolymers as construction materials– new discoveries*, *Die Angew. Makromol. Chemie.* 272 (1999) 34–40.
- [52] I. Angelov, S. Wiedmer, M. Evstatiev, K. Friedrich, G. Mennig, *Pultrusion of a flax/polypropylene yarn*, *Compos. Part A Appl. Sci. Manuf.* 38 (2007) 1431–1438. doi:https://doi.org/10.1016/j.compositesa.2006.01.024.

- [53] E. Rodríguez, R. Petrucci, D. Puglia, J.M. Kenny, A. Vázquez, *Journal of Composite Materials*, (2005). doi:10.1177/0021998305046450.
- [54] R. Malkapuram, V. Kumar, Y.S. Negi, *Journal of Reinforced Plastics and Recent Development in Natural Fiber*, (2009). doi:10.1177/0731684407087759.
- [55] M. Ho, H. Wang, J. Lee, C. Ho, K. Lau, J. Leng, D. Hui, *Composites : Part B Critical factors on manufacturing processes of natural fibre composites*, *Compos. Part B.* 43 (2012) 3549–3562. doi:10.1016/j.compositesb.2011.10.001.
- [56] L. Jiang, G. Hinrichsen, *Flax and cotton fiber reinforced biodegradable polyester amide composites*, 1, 268 (1999) 13–17.
- [57] E.S. Rodri, *Experimental study of the compaction response of jute fabrics in liquid composite molding processes*, (2011). doi:10.1177/0021998311410484.

Chapter 3: Materials and Methods

3.1 Materials employed

Even if the use of natural fibre composites is increasing due to the environmental awareness, their use is still limited to some application fields due to their low mechanical properties if compared with traditional composite materials. Then, as mentioned in the introduction to composite materials, the aim of this thesis is the production of new geometries of core structure for sandwich composites, new hybrid sandwich structures and hybrid laminates in order to characterise the quasi-static and dynamic properties of these materials. Then an additional tribological characterisation of hybrid materials was executed. This research was carried out in order to have a better interpretation of the properties of bio-based materials in applications such as automotive and aeronautic fields.

Among the cellulosic fibres, hemp was chosen in this study because it is characterised by some aspects that make this fibre typology very interesting. Hemp derives from renewable source, it is obtained from the *Cannabis sativa* annual plant and is highly available thanks to the ability to be easily grown around the World. It has also the ability to extract heavy metals from the soil and is characterised by low cost. Moreover, the hemp fibres show low density and high specific strength if compared to synthetic materials such as glass and aramid fibres.

Hemp fibre had a significant history, thanks to the high stiffness this material was employed as roping in naval application and as reinforcement in building field [1]. Then, due to anti-drug laws, these fibres went through a period of oblivion but the availability of plants with low tetrahydro-cannabinoids (THCs) content, allows to a renewed increase of their usage [2].

As matrix an epoxy resin was chosen because it is the most commonly used matrix for high performance composites. Moreover, it is characterised by high resistance from the environmental agents and low curing temperature. These properties avoid hemp fibre degradation due to environmental agents and moisture absorption and reduce the fibre degradation as consequence of the production temperature.

3.2 Historical hemp applications

The historical use of hemp fibres in the modern era began in the early 1900 as result of the environmental sensitivity and the depletion of the petroleum resources. One of the most interesting application field of this fibre typology was the automotive, indeed in 1941 Henry Ford produced a car prototype, in which a large number of body and interiors part were manufactured with composite materials reinforced by natural fibres. These body parts demonstrated improved impact properties around ten times than the equivalent metal parts. However, this car did not enter in the mass production due to economic limitations.

During the last years of the 1900, German factories were at the vanguard in using composite materials reinforced by natural fibres in the automotive field. A recent investigation demonstrated that natural fibres employing doubled from almost 9000 tons during the 1999 to around 19000 tons in the 2005 [4,5]. At the same manner, the natural fibre used in automotive application doubled from around 15000 to 30000 tons during the same time duration, indeed is estimated that almost 5,5 million cars produced in the 2005 used 4 kg of natural fibres composite per car. Over time, the use of these category of composite material in automotive application increased, indeed the Lotus company presented a green version of Elise named “Elise Eco” (fig.15a) [3]. This car uses natural fibres as hemp, wood and sisal to produce internal parts such as roof, seat cover, door panels and hard top. As well as Lotus, in 2018 the Tesla car producer revealed the race version of the “Tesla P100DL” model (fig.15b) [4].

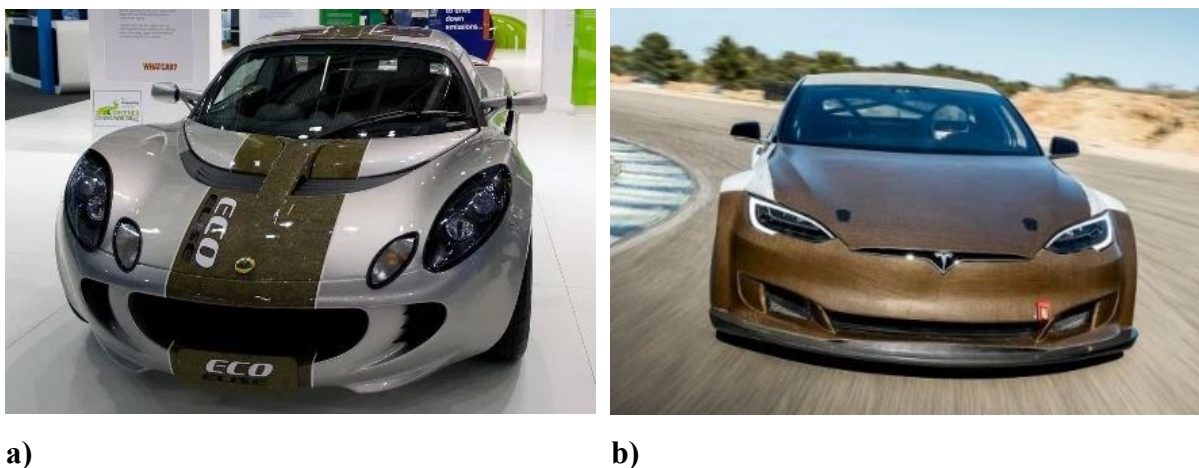


Fig.15: Natural fibres Lotus Elise Eco (a); Natural fibres Tesla P100DL race car (b).

It is 500 kg lighter than the road version thanks to the use of natural fibres reinforced panels both for external body parts as internal ones. The use of these materials combines high performances with low weight and safer crash behaviour. However, hemp fibres are not used only in automotive field, but are also employed in some applications such as sport goods, music industry and home furniture. Examples of sports goods are “Artengo” tennis racket, “ArcWin” arc and “Le Ventolux” bike produced by combining some natural fibres such as flax and hemp ones. All these natural fibres applications are shown in the fig.16 [5].



a)



b)



c)

Fig.16: some natural fibres applications: “Le Ventolux” bike (a); natural fibre speakers (b); natural fibre guitar (c).

Hemp fibres are also used in the sound industry (fig.16b and fig.16c) in order to produce a new product in which the good mechanical properties are combined with the good acoustic insulation that characterises the hemp fibres. Moreover, hybrid flax-glass speaker cone was produced for the automotive sound system, in this way a homogeneous sound is reached in a richer range of frequencies. As above mentioned, hemp fibres are also used for home furniture

i.e. chair production, fig.17 shows some examples of hemp chairs produced by Werner Aisslinger and by Canvas Mariposa [6,7].



a)



b)

Fig.17: hemp chairs: Werner Aisslinger (a); Canvas Mariposa (b).

3.3 Hemp for industrial applications

Hemp plant is one of the oldest annual crops known, there are some evidences of its use that date back to around 600 – 800 before Christ. There are evidences of its use in form of rope, canvas and cordage. Often, these plants are confused with marijuana plants due to their aspect but, although these plants are similar to each other, industrial cannabis sativa is characterised by a low value of THCs content. Hemp plant aspect is like that of flax, kenaf, jute and ramie plant. It is characterised by long and slender primary fibres that compose the plant bast, these fibres are attached to the core fibres with a pectin soluble gelatinous carbohydrate. The primary fibres can be employed for roping and textile and pulp production. The internal fibres with a wood like aspects can be used to produce building materials and biofuel. Moreover, the seeds have an amount of 25 – 35 % of oil in weight that contain essential acids that is demonstrated to be necessary for the human health [8].

3.4 Hemp diffusion around the World

The production of hemp fibre for the commercialisation come from Central Asia but it was planted in all the European continent. Successively, in 1645, hemp fibres were introduced in the United States and in New England as fibre for the house textile employing.

Then, New England exported hemp fibres in the Australian hemisphere at the end of the 18th century, with more detail in Australia and New Zealand because these places were considered as ideal for hemp production and because the scope was the independency from the Russian hemp. However, this fibre typology use starts to fall due to the introduction of cheaper materials such as jute and sisal fibres from India, Bangladesh and China at the beginning of the 19th century. These materials were also more readily available than hemp fibre and this aspect improved the hemp fibre decline. This period of oblivion of hemp fibres continued in the 20th century due to the rise of petrochemical industries that improved the competition with bio-based materials. An additional contribute to the hemp fibre decline was the introduction of anti-drugs laws in the United States in the middle of the 1900. These legislative roles, required the registration and licensing of all hemp producer to the federal government in order to reduce the marijuana production. With the United States many other nations followed these regulations, and this procedure made the hemp production and detention illegal. The cultivation of hemp plants raised up during the second World War, in this period natural fibre composite materials raised up due to the non-availability of metal parts. It was in the 1992 that some countries officially passed the anti-drug laws and began to produce hemp with low THCs content. At the end of the 2001 new legislative laws permitted the cultivation of hemp plants with a THCs content under the 0,3%. Then, in this scenario a new improve of hemp production is required in all countries where it is again legal.

3.5 Hemp diffusion in Italy

The hemp cultivation in Italy goes back in the 1500. Italian hemp (*cannabis sativa*) was considered the best in the World considering the fibre quality, indeed, the Italian hemp production was second after Russia, that was the major hemp producer. For many years the hemp cultivation was the main crop in Italy, and more than hundred thousand hectares were employed for hemp production. But even though Italy was famous for hemp cultivation, during

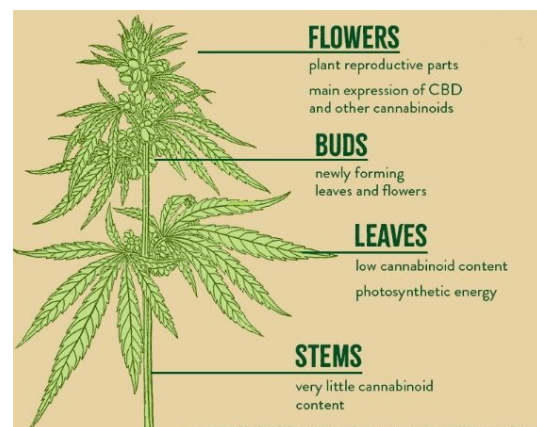
the 20th century there was a regression of the production. The reason of this decline is attributed to economic crisis that affect this country in the middle of 1900. During these years, the hemp crop became less profitable, and farmers were forced to switch on other crops to survive. Moreover, this deflection of the hemp production was unavoidably referred to the cannabinoids content. Unfortunately, this crop restriction, caused the loss of germplasm of some Italian variegations and the stop of the development of new machine for the cultivation and production of hemp fibres [9]. In the last decade of the 1900, some eco-friendly movements promoted the production of hemp plants, but some anti-drug laws by the European Community, established a limit of the THC content of 0,2% lower than 0,3% of the previous regulation. Considering that the lower THC limit to consider a substance as drug is almost 10%, then these new rules seemed to be unnecessary and discouraged hemp producer to cultivate these plants.

3.6 Hemp plant structure

Hemp plants are separated in male and female plants, fig.18 shows an example of this plant typology [10]. Moreover, it is possible to obtain monoecious plant variety by breeding and plant selection. Hemp plant are sensitive to the environmental condition, with more detail they are sensitive to the day length and get the maturation when the days become shorter. Then, for these reasons, it is easy to understand that the growing session of hemp plant is from the middle of April until the middle of September.



a)



b)

Fig.18: Hemp plants (a) and parts (b).

If the cross section of hemp stem is considered, it is orbicular at the bottom of the plant whilst it is angular at the top. The hemp plant is usually 1,5 – 2,5 meters tall, and the stem is almost 4 -10 millimetres thick. The cross section of the stem can be seen in fig. 19 where a hollow inner part is observed, this part is surrounded by a wood core cell called hurd. These fibres are thin and shorter than the outer fibres, usually these fibres are used to make paper or fuel, but are not considered for the composite production. The outer part of the stem is characterised by the presence of long fibres commonly used for the composite production. Hemp seeds are usually 3 – 6 millimetres long and are composed for the 29 – 34% of oil. This oil is beneficial for the human health and it is composed by three different fatty acids like linoleic (54 – 60%), linolenic (15 – 20%) and oleic (11 – 13%).

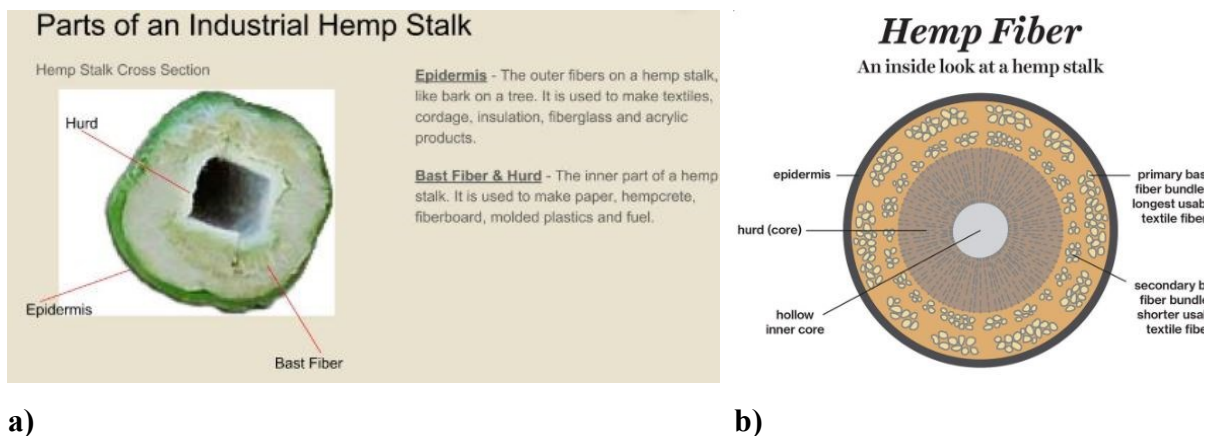


Fig.19: Cross section of industrial hemp stalk.

The main advantage of hemp plant is the capability to grow in a large soil variegation, but it does the best in well drained loam soils with a large amount of organic materials. Hemp plants also require abundant moisture especially during the first six weeks of growing. Hemp illness occur occasionally, and it is caused by fungi that develops on seeds or soil, this issue can be controlled by seed treatments before planting. Usually, under favourable conditions, these treatments are not required because hemp plant is very competitive with unwanted plants.

Taking into account the hemp fibre, it is composed by three main elements, in detail cellulose microfibrils in amorphous materials like hemicellulose and lignin. Generally, the hemp fibre structure is characterised by a primary cell wall that is a thin layer and consist of lignin, pectin and cellulose, the second cell wall is thicker twice or more than the primary cell wall and consists of cellulose microfibrils and amorphous cellulose. Considering the hemp plant stem,

the technical fibre is a part of the bast fibre bundle, and the elementary fibre is a single fibre of the technical one. The fig.20 below shows this fibre distinguish.

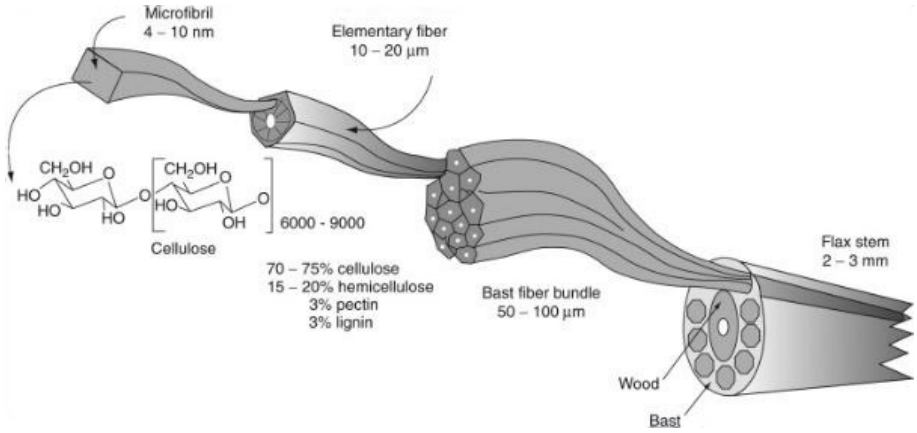


Fig.20: Structure of hemp stem.

3.7 Hemp fibre elements

The main elements that characterise the hemp fibre are cellulose, hemicellulose, lignin and pectin. Their amount depends on some factors such as the place where the plant is grown, the plant variety and the maturity when the plant is harvested. The main constituent variations are reported in the table 7 below [11].

Table 7: Chemical composition of hemp fibres

Cellulose	Hemicellulose	Lignin	Pectin	Residuals
[% W/W]	[% W/W]	[% W/W]	[% W/W]	[% W/W]
64,40	14,40	3,40	7,30	10,50
73,80	11,80	5,00	2,50	6,90
72,40	13,80	4,90	4,00	4,90
78,40	13,00	2,40	1,90	4,30
65,90	14,90	4,60	4,00	10,60
63,70	17,30	4,10	4,20	10,70
73,40	14,60	4,30	2,40	5,30

As above mentioned, the hemp fibres have a cell wall structure. In fig.21 is represented the fibre structure, as it is possible to appreciate from the scheme, there are a primary and a secondary wall, the second wall is composed by three distinct layers: S1, S2 and S3. these layers are composed by cellulose, hemicellulose and lignin with amounts that depend from the microfibrils. Usually, the S2 layer is the thicker one and is responsible of the mechanical properties of the hemp fibre.

In this paragraph each of the main constituent of hemp fibre is treated in detail.

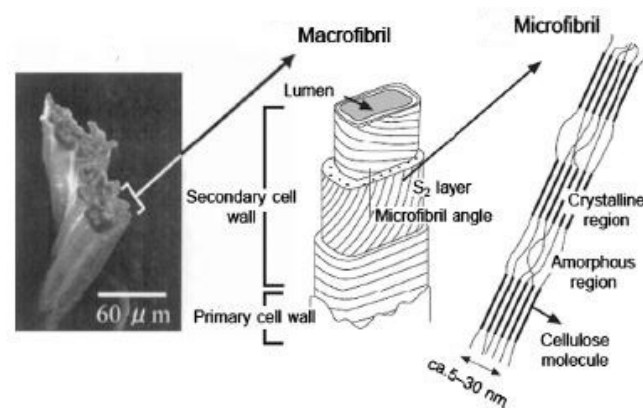


Fig.21: Inner structure of hemp fibre.

3.7.1 Cellulose

The cellulose is the constituent of the long thin crystalline microfibrils of the second wall, this material is the responsible of the mechanical properties of these fibres [12]. This material consists of a linear polymeric chain (fig.22) where monomers are linked each other by β -1,4-glycosidic linkages with the elimination of one water molecule between the -OH groups.

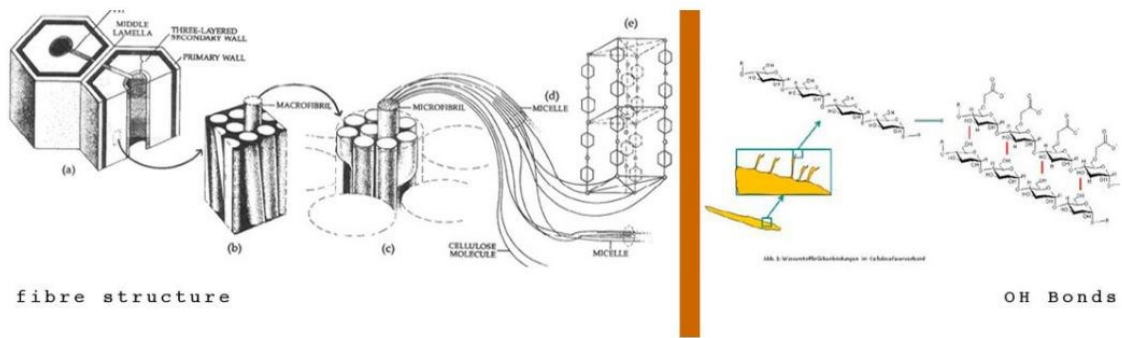


Fig.22: Cellulose structure of natural fibres.

The monomers in the cellulose structure, are able to form hydrogen bonds within the principal chain forming the elementary fibril, but are also able to form intermolecular hydrogen linkage forming microfibrils. Then, these linkage lead to a formation of a linear crystalline structure, that gives high strength to the fibre. In the amorphous region, the -OH groups are not used at all, then these groups are able to form linkage with water molecules and are responsible of the hydrophilic behaviour of hemp fibres. Therefore, there are some free -OH groups in the crystalline region where the cellulose structure of the fibrils is characterised by tightly packed chains. Then, in order to reduce the hydrophilic behaviour of this fibre, only strong acids and alkali solutions can penetrate into the crystalline structure and modify the cellulose surface.

3.7.2 Hemicellulose

This constituent in hemp fibre is composed by polysaccharides linked together in short chains highly branched. Hemicellulose differs from the cellulose by different aspects, first of all unlike cellulose it contains numerous saccharides; it is characterised by short chains but highly branched whilst cellulose is a linear and not to branched chain; finally the degree of polymerisation of cellulose is hundred times higher than that of hemicellulose, moreover, unlikely cellulose the constituents of this material varies plant to plant.

Due to the high chain breaching of hemicellulose and then to its high linking ability, the hemicellulose chain can deteriorate leading to the disintegration of the fibres into cellulosic microfibrils resulting in lower fibre bundles strength [13]. Moreover, the acid residues linked to the hemicellulose structure, make it highly hydrophilic, then increase the water absorption causing a rising of the risk of fibre degradation. Moreover, it has been found that hemicellulose

is characterised by a lower temperature resistance than cellulose, indeed it thermally degrades around 150 – 180 °C whilst cellulose degrades around 200 – 230 °C.

3.7.3 Lignin

The lignin with the cellulose is the most important component of natural fibres. It is responsible for the compression strength of these fibres, this because it links all fibres together in order to obtain a stiffer structure. This is the reason why trees 100 meters tall such as coniferous and heavy trees such as oaks are able to remain upright. Lignin is a disordered and cross-linked polymer deriving from the polymerisation of more monomers structurally related to phenylpropane [14]. Then, it is possible to assess that the lignin matrix is characterised by a structure that is similar to a thermoset matrix in traditional composite materials. It was found that under ultraviolet exposition, lignin suffers the photochemical degradation [15]. Moreover, the treatment of hemp fibres with the p-radiata-cell leads to the degradation of lignin and pectin causing a slight reduction of the fibre bundle tensile strength. Then, as above mentioned, a parallelism can be done between lignin and thermoset matrix in composite materials, because this constituent of natural fibres transfers stress to the microfibrils as well as a matrix transfers the load stresses to the fibres.

3.7.4 Pectin

Pectin is a particularly branched structure composed by acidic polysaccharides found in bast fibres. This component is characterised by linear chains of α -(1-4)-D-galacturonic acid and some backbone of α -(1-2)-L-rhamnose- α -(1-4)-D-galacturonic sections that contains some neutral chains of D-galactose, L-arabinose and D-xylose.

Pectin constituent is the most hydrophilic component of natural fibres due to the presence of carboxylic acid groups, for this reason it is easily deteriorated by fungi attack [12]. Some tests carried out on hemp fibres by using pectinase enzymes, demonstrated that there is a pectin degradation that leads to a slightly reduction of the fibre strength.

3.8 Influence of the mechanical properties of hemp fibres

The mechanical properties of hemp fibres are influenced by some aspects such as the presence of defects localised in the fibre structure, the degree of crystallinity and amorphousness or the orientation of the polymer chains of the fibrils. There are also chemical reasons that influenced the mechanical strength of natural fibres, such as the chemical composition or the presence of imperfections due to the growing condition and the harvesting process. There are also many factors such as the plant maturity, the type of soil and the environmental condition at which a plant grows. Indeed, as largely mentioned, the mechanical strength of natural fibres varies from a plant to another and varies if changes the part of the plant employed. The crystallinity of the natural fibres makes that strong to tensile stresses, but a high degree of crystallinity can causes the presence of internal nodes that affect the mechanical properties of the fibres [16]. In tables 8 and 9 are reported respectively the main properties and tensile properties of hemp fibres reported by different authors [3].

Table 8: Main properties of hemp fibres [3]

Properties	Value
Ultimate length [mm]	8,30 – 14
Ultimate diameter [mm]	17 – 23
Aspect ratio [length/diameter]	549
Specific apparent density	1500
Micro-fibrils angle [°]	6,20
Moisture content [%]	12
Cellulose content [%]	90
Tensile strength [MPa]	310 – 750
Specific tensile strength [MPa/ ρ]	210 – 750
Young's modulus [GPa]	30 – 60
Specific Young's modulus [GPa/ ρ]	20 – 41
Failure strain [%]	2 – 4

Table 9: Mean tensile properties of hemp fibres [3]

Tensile strength [MPa]	Tensile modulus [GPa]	Elongation at break [%]
690	-	1,60
1235	-	4,20
310 – 750	30 – 60	2 – 4
550 – 900	70	1,60
690	-	1,60
895	25	-
500 – 1040	32 – 70	1,60
920	70	-
690 – 1000	50	1,00 – 1,60
920	70	1,70
270 – 900	20 – 70	1,60

From the tables it is possible to observe that these fibres are characterised by high values of tensile properties, these aspects in addition with the low weight and then low density, make hemp fibres suitable for using in composite materials. Therefore, some disadvantages limit their use in composites as well as large part of the other natural fibres, these negative aspects are identified in a variability of the mechanical properties, water absorption and then the fibre deterioration.

3.8.1 Hemp growing conditions

The growing conditions are responsible of the variation of the mechanical properties, but it is an interesting crop because it is easily to cultivate. Generally, this plant grows in a wide range of soils but it matures best in temperate zone, on soils non-acid and well drained characterised by a large amount of organic materials. These plants are distinguished in male and female and flourished from June up to October. Hemp plant is a very resistant culture, indeed it does not require pesticides to protect the plant from parasites, fungi and undesired weeds. An extensive culture of hemp plants leads to further advantages, these plants are able to limit the soil erosion, extract heavy metal from the soil and are also identified as carbon dioxide consumer. During their growing, hemp plants absorb carbon dioxide from the atmosphere and, at the end of their life cycle, these plants give back less carbon dioxide than that absorbed during their growing

phase. Moreover, an intensive crop is possible because these plants grow with a density of 150 plants per square meter and reach a height between two and five meters during the three months of growing.

3.8.2 Harvesting

Hemp harvesting can take place at different time as function of the final product. When the goal is the production of high quality fibres, the stem of hemp plant must be harvested as the plant flourished whilst for the production of seeds and stalks, the harvest must occur four or six weeks after the plant flowering [17]. If the goal is the production of hemp for pulp or textile, the harvest must be done with appropriate equipment as the flowers are produced and before the seed formation. Some research works were carried out on the influence of the harvesting period for the hemp fibre production. Liu et al. [18] concluded that the harvest of hemp plant during the flour formation is beneficial for the production of high strength fibres. This because the fibre bundles are close to the epidermis during this stage and results in a single large fibre. The reduction of mechanical properties attributed to the bast fibre harvested after the plant flowering, then in the plant maturity, is attributed to the reduction of the cellulose amount and to the develop of secondary fibres that cause the deterioration of the primary fibres. It is known that the secondary fibres are totally different from the primary ones both regarding the chemical composition as the morphology. Another important aspect to take into account is the moisture amount. During the harvesting phase it is important that the moisture is around the 54% and during the storage this value must be less than 15% in order to avoid the fibre degradation due to microorganisms.

At the end of the harvest, hemp plants are leaved to macerate on the soil in order to obtain the fibres. During this phase, a large part of the absorbed matters is released on the soil and ready for the new crop.

On the basis of these considerations, highly lignified fibres are not desirable for retting, this because these fibres are characterised by a low value of cellulose and then low mechanical properties. Then hemp harvested at the beginning of the plant flowering is recommended for the production of fibres with high mechanical properties and then the production of strong composite materials.

3.9 Hemp fibres as reinforcement

In order to produce lightweight core for sandwich composite structures, and to characterise the dynamic behaviour of hybrid bio-based laminates, two different hemp fabrics were employed. These two textiles are shown in fig. 23a and fig.23b, they differ each other by the areal density, the thickness and mesh.

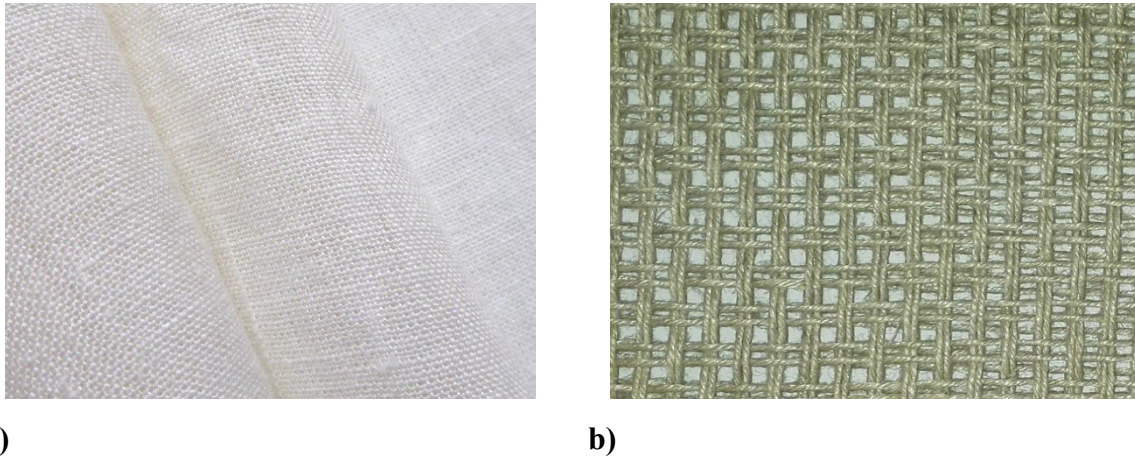


Fig.23: Hemp tissues: Maeko fabric (a); Fidia fabric (b).

To date, long fibres in form of fabric are the most used reinforcement, this because these fibre organisation permits a good fibre orientation along the load direction. This is the reason why in this thesis hemp fibres were employed in form of fabric. Moreover, the choice of a larger mesh fabric is linked to the possibility to take advantage of the large mesh to produce porous core for sandwich structures. These reinforcements are supplied by Maeko S.r.l. [19] and Fidia S.r.l. [20], their properties are reported in tables 10 and 11.

Table 10: Maeko fibres properties [19]

Single un-impregnated yarn	
Tensile strength [MPa]	507
Tensile modulus [GPa]	18,40
Elongation at break [%]	3,27
Density [g/cm ³]	1,50
Fabric	
Tex [g/km]	40
Grams per meter square [g/m ²]	160

Table 11: Fidia fibres properties [20]

Single un-impregnated yarn	
Tensile strength [MPa]	507
Tensile modulus [GPa]	18,40
Elongation at break [%]	3,27
Density [g/cm ³]	1,50
Fabric	
Tex [g/km]	334
Grams per meter square [g/m ²]	320

3.10 Carbon fibres as reinforcement

A carbon fibre was used for the quasi-static and dynamic characterisation of hybrid laminate composites. These carbon fibres in form of fabric are coupled with hemp fibres and are characterised by a similar areal density and thickness. These characteristics have been chosen in order to avoid a geometrical influence on the mechanical behaviour of the laminates. The carbon fibres are supplied by Toray International S.r.l. [21] and their properties are reported in table 12.

Table 12: Main properties of Toray carbon fabric [21]

Single un-impregnated yarn	
Tensile strength [MPa]	3650
Tensile modulus [GPa]	231
Elongation at break [%]	1,40
Density [g/cm ³]	1,80
Fabric	
Tex [g/km]	198
Grams per meter square [g/m ²]	200

3.11 Composite matrix

Epoxy resins are widely used as matrix in composite materials. These thermoset resins are characterised by a low cure shrinkage and no volatile reaction products during the polymerisation phase allowing to a reduced probability of defects internal to the laminate. Moreover, these matrices demonstrate a good adhesion to a large variety of substrate, good chemical and environmental resistance and good insulating properties [22]. All these aspects make these matrix typologies the most used in some applications that go from aeronautic to sports good.

Epoxy resins are also characterised by the possibility to modify their composition to vary the matrix performances and then the application field. Some materials can be mixed with epoxy resin in order to modify the cure rate, the temperature of polymerisation or to improve the temperature resistance.

3.11.1 Epoxy resin

Epoxy resin is characterised by a complex chain structure with the presence of a number of epoxy groups that varies from 2 to 6 per molecule. In this chain there are some ring structures known as epoxide, oxirane and ethoxyline group. The main structure of these groups is shown in fig. 24, these groups are characterised by a high reaction capability with many substances.

For these reasons, the epoxy resin structure is complex and composed by numerous crosslink network between the polymer chains.

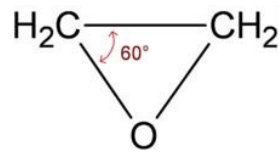


Fig.24: Epoxy group.

Epoxy resin can be characterised by a low or high viscosity caused by their main chain structure and generally, when a low viscosity resin is used, it is possible to obtain a good fibre impregnation without using high impregnation temperature or high pressure. Conversely, if a more viscous resin is used, there is need to increase both temperature and impregnation pressure. There are many epoxy resins in use, the most common is based on reacting epichlorohydrin (ECH) with bisphenol A, the fig. 25 shows a typical chemical structure of this type of epoxy resin.

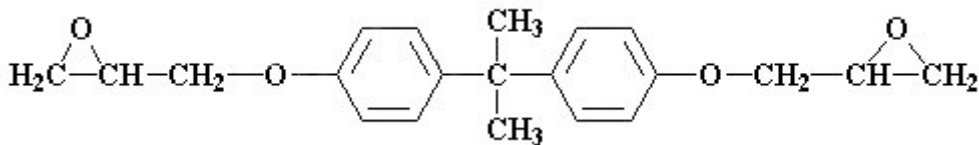


Fig.25: Chemical structure of epoxy resin.

As above mentioned, in order to facilitate the impregnation phase and modify the resin properties, some other substances are added i.e. solvents, plasticisers or curing accelerators. In this last case the curing accelerators are added in order to reduce the weakness of epoxy resins that consist of long curing time.

Moreover, as it is possible to appreciate from the fig. 25, the epoxy resin molecule contains two ring groups that are able to react to thermal and mechanical stresses better than the linear chain of thermoplastic resins. This characteristic gives to the epoxy resin stiffness, toughness and thermal resistance.

Epoxy resin are also characterised by high adhesive strength, this aspect is attributed to the polarity of the aliphatic -OH groups. Whit more detail these external groups promotes links between the epoxy resin and the polar fibres [23].

3.12 Used epoxy resin

In this thesis an epoxy resin SX 10 EVO supplied by Mates Italiana S.r.l. [24] was used to produce all samples. Its mechanical and technical data are reported in the tables below.

Table 13: Mechanical and technical data of the Epoxy resin [24]

1	Low viscosity	SX 10 EVO is an epoxy resin of modified bisphenol with variable reactivity possibility of acceleration it has low viscosity that ensures excellent impregnation of the reinforcements also in the case of multi-axial or high GMS reinforcement.
2	Low toxicity	Its special formulation makes it one of the least toxic epoxy resins on the market, with a significant reduction on the risk of sensitization phenomena for the users. The absence of smell due to the absence of volatile solvents allows its use without requiring expensive facilities of room ventilation.
3	Great versatility	With the ability to accelerate the polymerization and with the possibility of processing both at room temperature and at average temperature, the resin SX10 shows a high flexible in its applicability.
4	High glass transition temperature	With 7 days of hardening cycle at 25 ° C, values of 55-63 °C, are reached for the glass transition temperature while with a cycle of 8 hours at 25 ° C + 24 hours at 60 ° C the mean value of the glass transaction temperature reaches 83-89 °C. The maximum reachable value is 91 °C.
5	Excellent mechanical properties	The mechanical properties in the two above mentioned cases of the curing cycle (7 days at 25 °C or 8 hours at 25 °C + 24 hours at 60 °C) show that the SX 10 is a resin suitable for the manufacture of products for advanced composite for structural applications where high mechanical properties are required.
6	Careful mixing	As all the epoxy resin systems to respect the more precisely as possible mixing proportions of resin and hardener is strictly necessary. An error greater than 5% involves a lowering of the final characteristics of the resin. For this epoxy system, the ratio between the resin and the hardener weigh must be 100:26.
7	Pot-life	This time, variable with the room temperature and with the presence of accelerator, is called pot life. Keep in mind that it is good practice to distribute the mixed product in large and shallow containers that facilitate the dissipation of the heat produced by the exothermic reaction. Smaller the amount of resin in the trays of application and higher will be the time of applicability.
8	Use of fillers	To change the thixotropy and the density of a product can be useful to add inert fillers to the resin, according to the proportions in large and shallow containers that facilitate heat dissipation.

Technical data			
Resin			
Type	Epoxy resin of modified bisphenol		
Physical state	Liquid		
Gardner index	≤ 3		
Viscosity at 25°C [mPas]	1200÷ 250		
Volatile substances at 100%	>0,3		
Density at 20 °C [g/cm ³]	1,1 ÷ 1,15		
Flammability point	>100 °C		
Hardener			
	MEDIUM (M)	SLOW (S)	EXTRA SLOW (ES)
Type	Modified cycloaliphatic polyamine		
Physical state	Liquid		
Gardner index	≤ 4	≤ 8	≤ 3
Viscosity at 25°C [mPas]	30÷ 10	40÷ 10	40÷ 10
Volatile substances at 100%	>0,5	>0,5	>0,5
Density at 20 °C [g/cm ³]	0,95 ÷ 0,05	0,95 ÷ 0,05	0,95 ÷ 0,05
Flammability point	98	104	100

Mechanical properties		
Curing cycles	7 days at 25 °C	8 hours at 25 °C + 24 hours at 60 °C
Tensile strength (UNI 5819) [MPa]	55÷ 65	60÷ 70
Breaking point (UNI 5819) [%]	2,0÷ 3,0	3,5÷ 5,0
Tensile modulus (UNI 5819) [MPa]	2800÷ 3300	2700÷ 3200
Flexural strength (UNI 7219) [MPa]	85÷ 95	105÷ 120
Flexural elongation (UNI 7219) [mm]	7,5÷ 8,5	9,5÷ 10,5

Flexural modulus (UNI 7219) [MPa]	2500÷ 3000	2400÷ 2900
Compression strength (UNI 4279) [MPa]	105÷ 120	100÷ 120
Glass transition temperature [°C]	50÷ 58	75÷ 85
Maximum reachable glass transition temperature [°C]	82÷ 89	91

3.13 Experimental campaign

In this section, is going to be treated in detail the experimental procedure used for the manufacturing of core structures for sandwich composite materials, the production of hybrid laminates for their quasi-static and dynamic characterisation and the production of composite materials for their tribological behaviour characterisation. In order to make the thesis structure better arranged, the experimental campaign will be divided in five parts.

Part 1: Continuous production of innovative core for sandwich structures

This section is focused on the production of an innovative core structure for sandwich composite. A composite material was manufactured by combining hemp natural fibres with the epoxy resin in order to obtain a lightweight core structure. The aim of this new structure geometry is the production of a core, that at the same time demonstrates both a lower density value if compared to the widely used polymeric foams and an improved compression strength. Then, since the potentiality of the final product and the flexibility of the production system, a patent (n. 102018000009972) was edited and up to now it is still under review.

Part 2: Hybrid sandwich structures with bio-based cores

This part is a natural evolution of a previous thesis work focused on the quasi-static characterisation of bio-based core materials. Then, the aim of this part is the production of lightweight hemp core with two different densities and different thickness. A dynamic

characterisation was carried out on the sandwich materials obtained by coupling the bio-based core with two skins characterised by CFRP laminates. At the end of the experimental campaign, some non-destructive tests were carried out on the samples in order to have a better interpretation and quantification of the internal damage. In detail, some visible inspection on the cross section of the sandwich specimen and a CT-Scan were executed.

Part3: Thin hybrid sandwich structures with bio-based cores

As consequence of the quasi-static and dynamic characterisation of thick bio-based cores, this experimental campaign is referred to the quasi-static characterisation of thin sandwich composite materials. The idea of this campaign derives from the desire to overcome a technological limitation of common core structures such as polymeric foams or honeycomb to produce thin cores. In this case, it is possible to combine the lightness of natural fibres with the good in plane and out of plane properties such as compression. Then, in this section a single layer bio-based core is coupled with two single layer CFRP skins. Three-point bending tests were carried out according to the ASTM standards on each sample typologies.

Part 4: Bio-hybrid composite laminates with improved mechanical properties

This part is focused on the design of hybrid laminates for structural application, in which an epoxy resin is reinforced by a combination of synthetic carbon fibres and natural hemp ones. This hybridisation was carried out in order to combine the advantage of both materials and improve the out of plane properties. In this experimental campaign four different stacking sequence were studied by varying the position of the natural fibres through the thickness. On these laminates a quasi-static mechanical characterisation was carried out, in detail flexural and ILSS tests. Moreover, dynamic impact tests were executed on each sample typologies. At the end of the experimental campaign non-destructive tests were carried out in order to estimate the damage extension and its localisation through the thickness.

Part 5: Tribological behaviour of hemp fibres

The study carried out in this section derives from the previous one. In case of structural application in which the composite material is subjected to tribological loads, and there is the risk of human touch with broken fibres that affect the human health, makes sense a study on the wear behaviour of natural fibres. In detail, a tribological experimental campaign was carried out on hemp/epoxy laminate and its behaviour was compared to that of glass/epoxy and carbon/epoxy composites.

3.13.1 Part 1: Continuous production of innovative core for sandwiches structures

In this part a new core material was produced. For its manufacturing Maeko hemp fibre was used, it is characterised by an areal density of 160 g/m^2 and is was impregnated with the SX 10 EVO epoxy resin. Before the impregnation process, hemp fabric was chemically treated with a 2% of NaOH solution at room temperature for 30 minutes. After this chemical treatment, the hemp fibres were copiously washed with water and then treated with a 1% acetic acid solution, then at the end of the chemical treatment, the natural fibres were dried in an oven at $60 \text{ }^\circ\text{C}$ for 12 hours. The production system of the natural core is shown in fig. 26 and it is mainly divided in five steps: fabric impregnation, resin jellification, semi-core forming, cutting and core assembling.

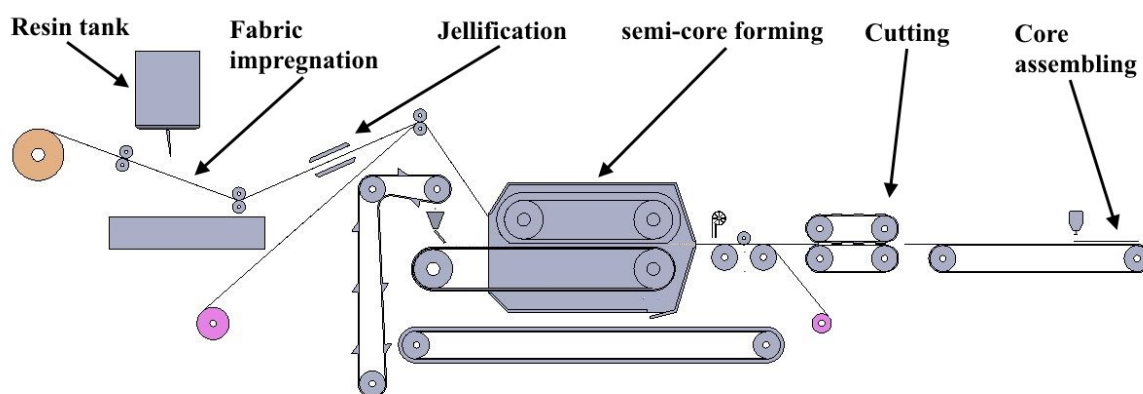


Fig.26: Schematisation of the production system of a new lightweight hemp core geometry.

The treated fabric wrapped on a roll, was impregnated by the epoxy resin and forced between two rolls in order to remove the exceeding resin. The impregnated fibres were heated before the formation phase in order to accelerate the polymerisation process and were forced to pass in a climatic room in which there is the formation zone. Then, the impregnated material in a state of jellification was forced in the formation zone. This zone is characterised by a caterpillar system which surfaces are modelled in order to obtain the desired core geometry. At the end of the formation phase, the polymerised semi-core was cooled through an air jet system and then was cut. An anthropomorphous robotic harm at the end of the production line, provides the superimposition of one or more semi-cores in order to produce a lightweight natural fibre core. The semi-core structures are characterised by a semi spherical geometry, they can be coupled each other by the contact between the peaks of the spherical geometry or by the contact between peaks and valleys of this geometry. The two different configurations of lightweight core structures are shown in fig. 27.



Fig.27: Core configurations: peak to peak assembly (a); peak to valley assembly (b).

During the impregnation and formation process, each semi-core was impregnated keeping constant the weight ratio between the impregnated fabric and un-impregnated one. In this way it is possible to evaluate the hemp fibre content that is almost 40% in weight for each layer. Moreover, with the two different superimposition processes it is possible to obtain two main core thickness and then two different values of the final density. The main characteristics of the two core structures are listed in table 14.

Table 14: Main properties of the new hemp core configurations

Core configuration	Weight fibre percentage [%]	Core thickness [mm]	Core density [g/cm³]
Peak to peak	40	5,40	0,18
Peak to valley	40	2,90	0,22

These materials are not still tested because this section is dedicated only on the production technology of lightweight natural fibre core materials.

3.13.2 Part 2: Hybrid sandwich structures with bio-based cores

This section is dedicated to the production of natural fibres core and the production of sandwich structures. For this experimental campaign the Fidia hemp fibres were employed. This reinforcement is characterised by an areal density of 380 g/m^2 and was impregnated with the SX 10EVO epoxy resin.

In this experimental campaign were produced cores with different thicknesses and density. A total of three thicknesses were produced by varying the number of plies that composes the core structure, with more detail cores with 2, 4 and 6 plies were produced. The density variation was obtained enlarging the mesh of the fabric, for this scope one alternative tow of fibre was manually extracted in the weft and warp direction of the fabric. In this way, the areal density of the natural reinforcement was reduced from 380 to 190 g/m^2 , then the final density of the core structure is halved. In fig. 28 are shown the two reinforcements.

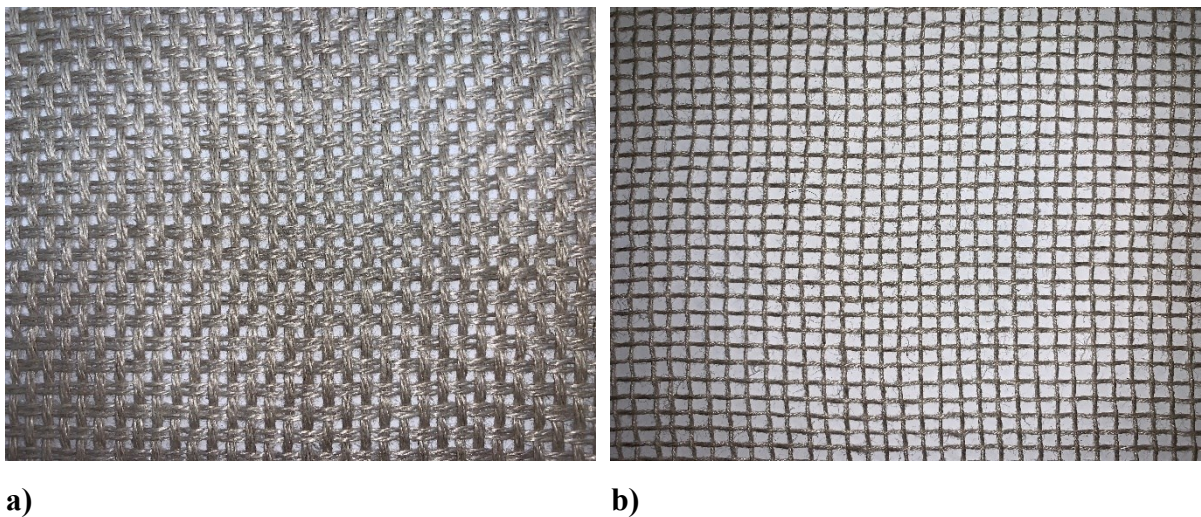


Fig.28: Not enlarged (a) and Enlarged hemp fabric (b).

Moreover, since a core structure for sandwich composite must be characterised by a low density, but also by good shear and compression properties, the aim of this experimental

campaign was focused on the production and mechanical characterisation of bio-based core structures with improved in plane and out of plane properties.

Before the impregnation phase, the hemp fabric was subjected to the same chemical treatment showed in the previous section, then the moisture content was reduced by an exsiccation in an oven at 60 °C for 12 hours. In fig.28 is reported an example of the hemp fabric before the impregnation phase.

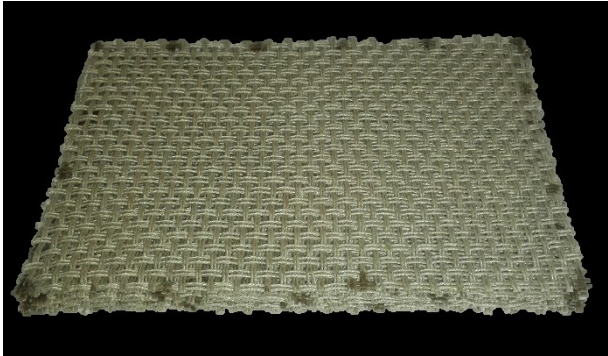


Fig.28: Not enlarged hemp fabric before the impregnation phase.

The impregnation of the reinforcement was carried out with the epoxy resin by using the hand lay-up technique, each layer of the single core specimen was impregnated, and its weight was evaluated in order to guarantee a fibre content of almost 40%. A particular attention has been paid in the mesh alignment during the stratification process, fig.29a and fig.29b show both normal and enlarged cores at the end of the stratification process.



a)



b)

Fig.29: Polymerised hemp cores: not enlarged (a); enlarged (b).

Then, all specimens were cured by using the compression moulding technology at room temperature for 24 hours. In table 15 are summarised the samples typologies and the main characteristics.

Table 15: Main properties of Not enlarged and Enlarged hemp cores

Label	Number of core plies	Weight [g]	Thickness [mm]	Density [g/cm³]	Fibre weight [%]
NSF_6P	6	81,46	9,93	0,63	40
NSF_4P	4	55,12	7,32	0,65	40
NSF_2P	2	26,24	4,66	0,60	40
SF_6P	6	39,25	8,76	0,37	40
SF_4P	4	26,88	6,64	0,37	40
SF_2P	2	13,28	4,41	0,33	40

In fig.29 are reported examples of the samples at the end of the curing phase, but in order to evaluate the dynamic behaviour of the sandwich structure, two skins were applied to the core surfaces. These skins were produced by using carbon fibres reinforced preregs supplied by Easy composites, their properties are reported in table 16.

Table 16: Carbon fibre prepreg mechanical properties

Property	Test Standard	results
Compressive strength [MPa]	BS EN ISO 14126 : 1999	483
Tensile strength [MPa]	BS EN ISO 527-4 : 1997	521
Tensile modulus [GPa]	BS EN ISO 527-4 : 1997	551
Flexural strength [MPa]	BS EN ISO 14125 : 1998	777
Flexural modulus [GPa]	BS EN ISO 14125 : 1998	46,7
Interlaminar shear strength [MPa]	BS EN 2563 : 1997	64,7
T _g onset (DMA) [°C]	ASTM 1-0003 Issue 3	121

A total number of 4 carbon fabric plies were used to produce skins 1 mm in thickness. The CFRP laminates were produced in autoclave with a pressure of 8 bar and a cure temperature of 120°C for 8 hours, in fig.30 are reported the main phases of their production.

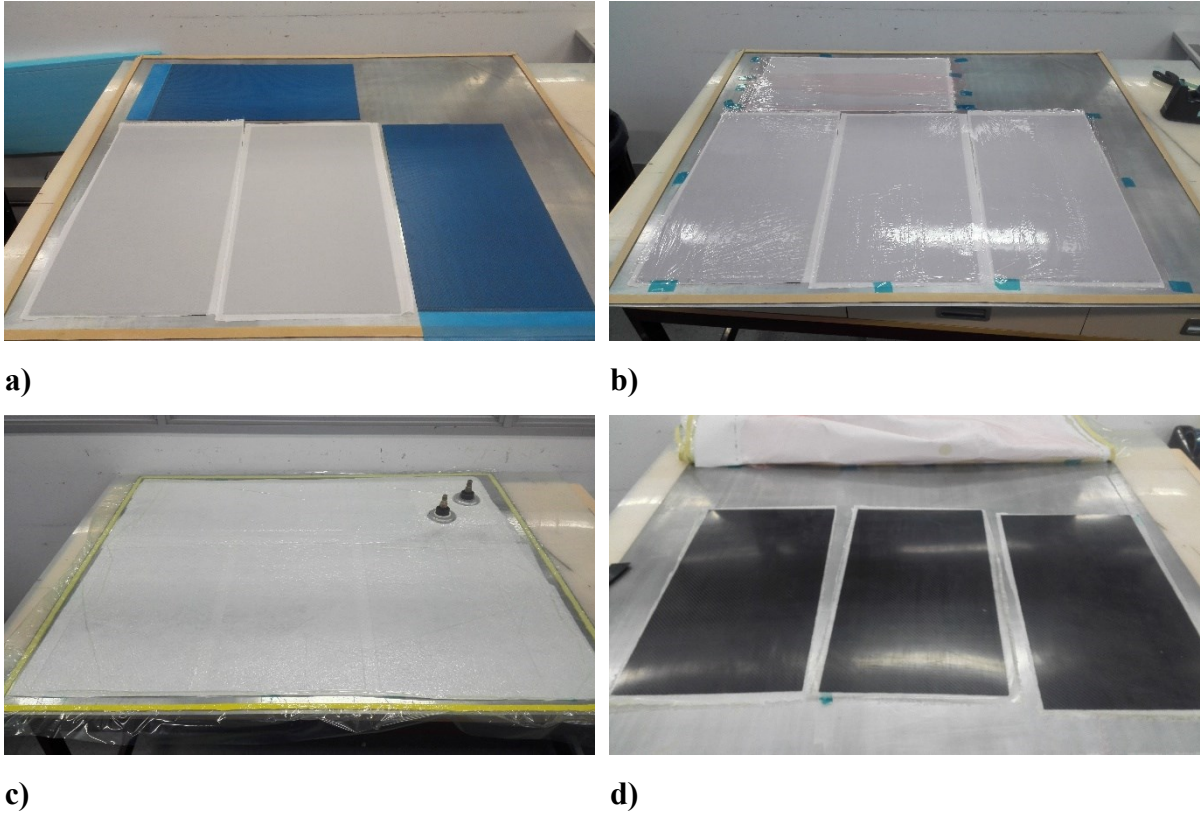
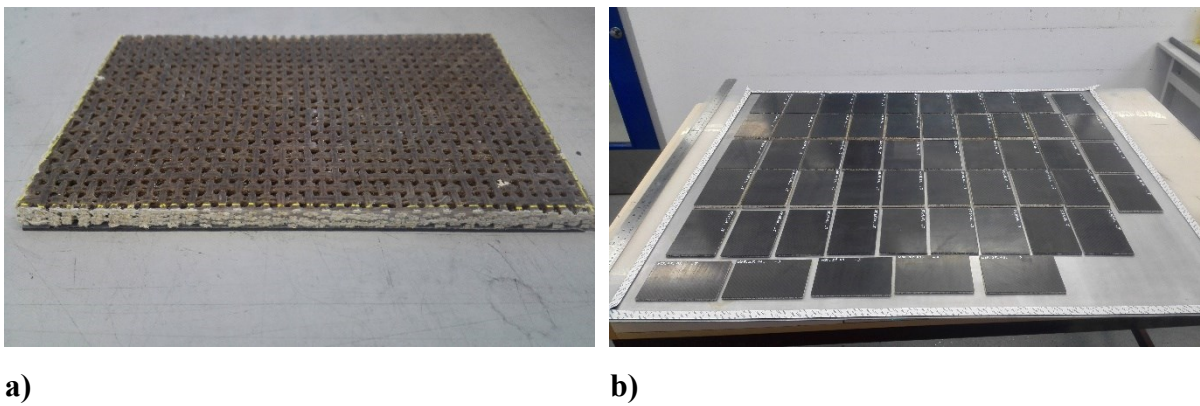


Fig.30: Sandwich skins production phases.

At the end of the polymerisation, all laminates were cut in plate 100 x 150 mm² in size by using a diamond cutter and were applied to the cores by means of an epoxy adhesive film supplied by Easy Composites [25] The skins and core assembling was executed in autoclave with a temperature of 120 °C and a pressure of 8 bar for 8 hours. In fig. 31 are reported all phases of the final sandwich composite production.



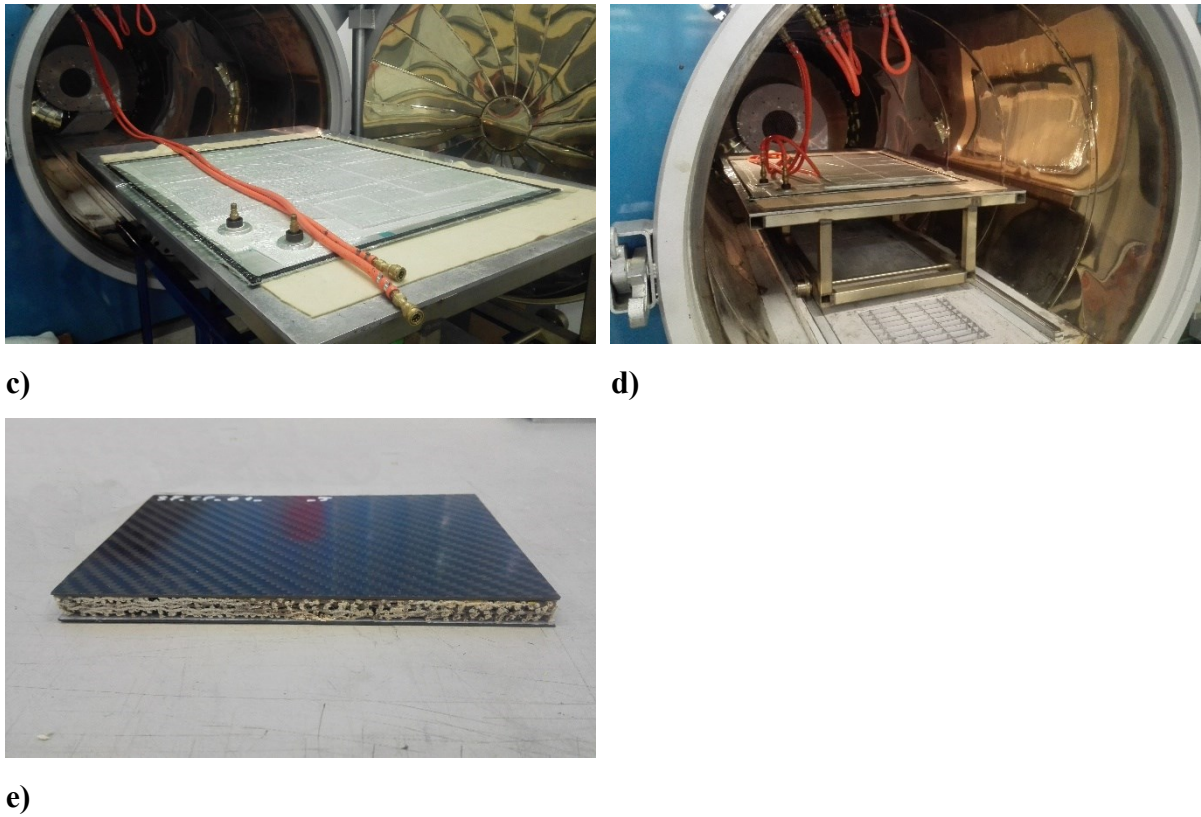


Fig.31: Hybrid hemp core sandwich assembling phases.

Therefore, two different families of sandwich composite structures were studied. These families differ each other by the core density that is one half of the other, but each sample of the same family differ each other by the core thickness. In order to evaluate the dynamic mechanical properties, some low velocity impact tests at different energy levels were carried out according to the ASTM standards.

3.13.3 Part3: Thin hybrid sandwich structures with bio-based cores

This section is an evolution of the previous part focalised on the study of the dynamic behaviour of bio-based core structures. The idea is the overcoming of the technological limitation of sandwich composites, related to the thickness of the mostly common polymeric foams and honeycomb core. Therefore, the aim of this part, is the production and the mechanical characterisation of thin sandwich structures, in order to evaluate the influence of a single layer of natural fibre core between two skins of CFRP laminates characterised by single layers.

As well as for the experimental campaign carried out in the part 2, also in this case natural fibres were used as core, in detail two natural fibres were employed. The first one is the Fidia hemp fibres, whilst the second one is a flax fabric supplied by Fidia S.r.l. Toray International carbon fibres were used as skin in the sandwich structure. The composite materials under inspection were produced by a combination of hand lay-up and vacuum compression moulding techniques. All reinforcements were impregnated with the SX 10 epoxy resin and placed on a mould plate with a size of 450 x 500 mm². At the end of the impregnation phase the sandwich structure was sealed in an elastomeric bag and the vacuum is applied, in fig.32 are reported some of the production phases of their production. Moreover, a further pressure was applied on the system in order to apply a total pressure of about 2 bar. Then the composite materials were cured at room temperature with a pressure of 2 bar for 24 hours, then, at the end of the cure cycle, all samples were cut in specimens with a diamond cutting.

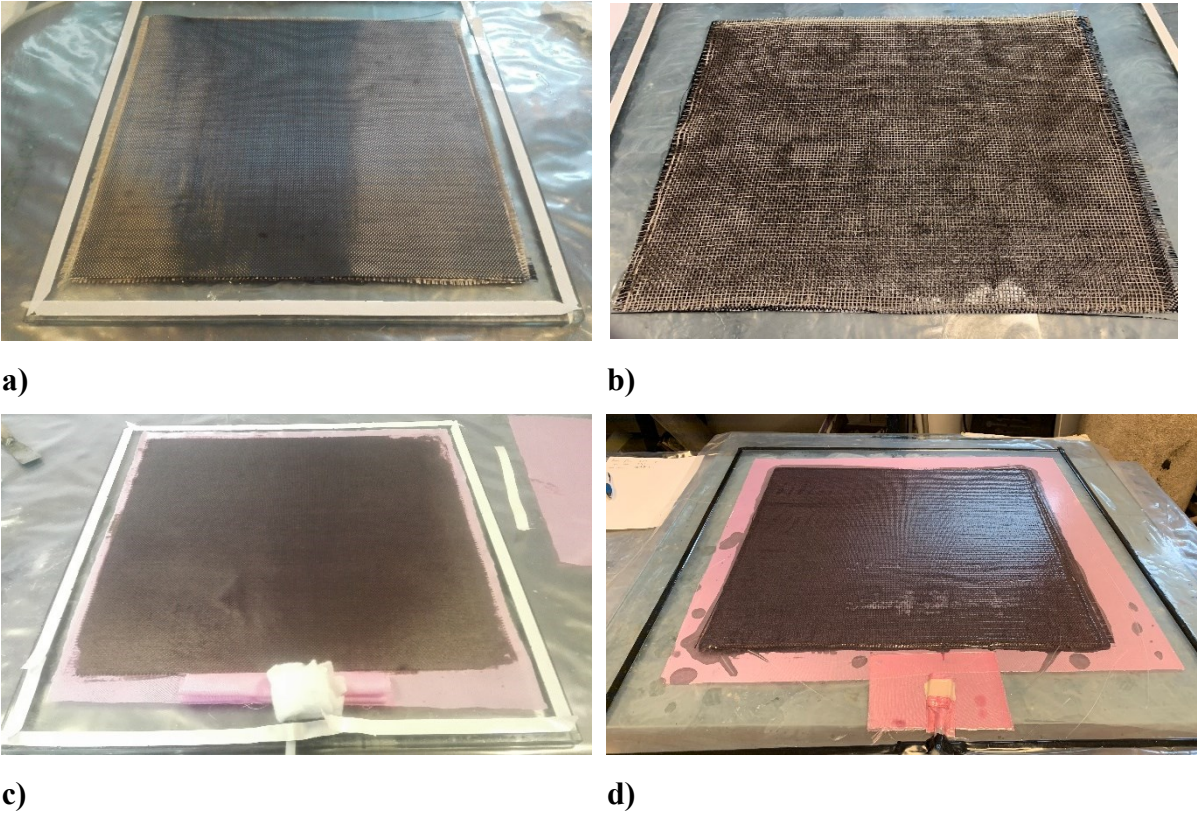


Fig.32: Thin hybrid natural/carbon fibres sandwich structures production phases.

Therefore, in this experimental campaign, three different families of composite materials were produced, the first one characterised by the reference CFRP laminate, the second ones are two sandwich samples with natural cores. On these materials, a comparison with the same

mechanical properties and with the same weight have been performed and a quasi-static test were carried out according to the ASTM standards. In table 17 are reported the main configurations produced in this experimental campaign.

Table 17: Classification and main properties of thin hybrid sandwich structures

Label	Reinforcement	Weight [g]	Thickness [mm]	Density [g/cm³]	Fibre weight [%]
CFRP 2P	2 Carbon plies	0,91	0.61	1,16	36,08
CFRP 4P	4 Carbon plies	1,81	0.92	1,48	49,40
C-H-C	Carbon/Hemp	2,36	1,68	1,11	55,56 (skins)
C-F-C	Carbon/Flax	2,24	1,38	1,09	55,56 (skins)

3.13.4 Part 4: Bio-hybrid composite laminates with improved mechanical properties

This section is focused on the design and the study of quasi-static and dynamic behaviour of hybrid laminates in which the reinforcement is a combination of the synthetic and natural fibres, in detail carbon and hemp fibres respectively. The hybridisation was carried out in order to combine the advantages of both materials improving the out of plane properties of traditional CFRP composite materials and reduce at the same time the carbon footprint introducing eco-friendly materials.

Woven Maeko hemp fabric and woven Toray International carbon fibres were hybridised with SX 10 EVO epoxy resin to produce hybrid laminates. Before the impregnation phase, the same chemical treatment illustrated in part1 was carried out on hemp fibres, moreover they were dried in an oven for 12 hours at 60 °C. As well as for the experimental campaign carried out in the third part, all composite laminates were manufactured by the combination of hand lay-up and vacuum compression moulding technique.

A total number of 15 plies of hemp and carbon fabrics were manually impregnated with the epoxy resin and placed in a mould sized 300 x 300 mm² by hand lay-up technique.

At the end of the stratification phase, the mould with the uncured laminates were sealed in an elastomeric bag under vacuum and placed in a hydraulic press under a pressure of 8 bar at 55 °C for 2 hours, then the laminates were left to cure at room temperature under a pressure of 8 bar for 24 hours. In fig.31 are reported the main production phases of hybrid laminates.

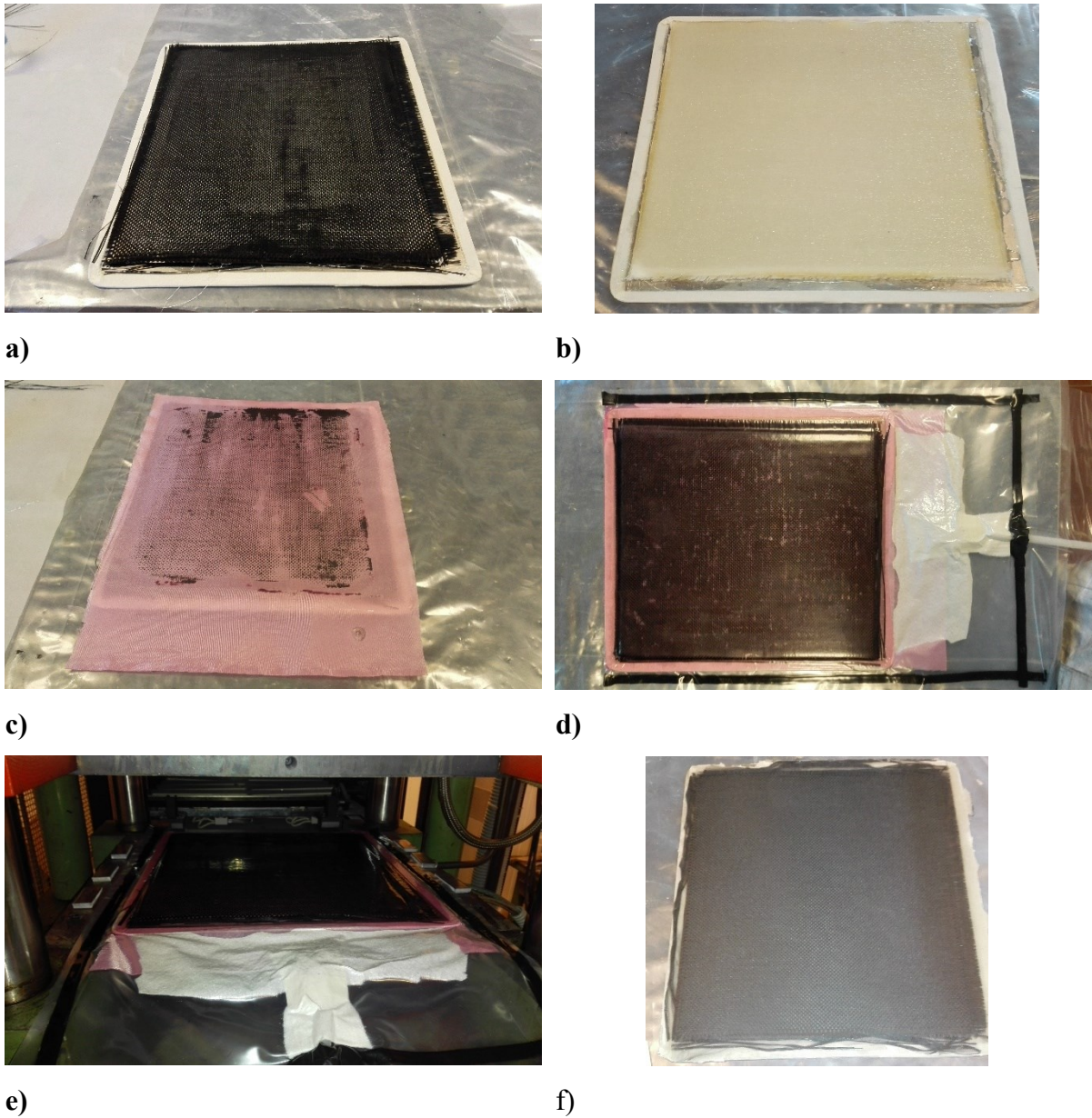








Fig.31: Hybrid hemp/carbon laminates production phases.

Six different configurations of composite materials were produced, their details are listed in table 18. Two of these typologies, with more detail composite materials reinforced by only carbon fibres labelled as C sample type, and laminates reinforced by hemp fibres alone labelled as H sample type, are employed as references. The other four typologies are hybrid laminates obtained by replacing three carbon plies with three hemp fabric layers. Both symmetric, configuration S and SU, and asymmetric, configuration A-CH and A-HC, laminates were considered.

Therefore, in this experimental campaign quasi-static and dynamic test were carried out in order to evaluate the influence of natural fibres on the flexural and impact properties of composite

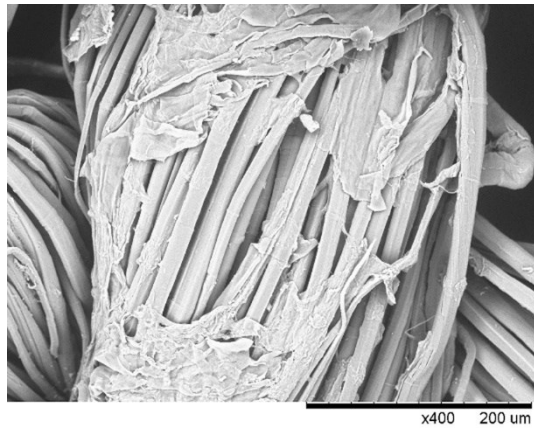
materials. Moreover, at the end of the tests, non-destructive tests were carried out on impacted samples in order to evaluate the internal damage extension and its localisation through the thickness of the hybrid composite.

Table 18: Classification and main properties of thin hybrid sandwich structures

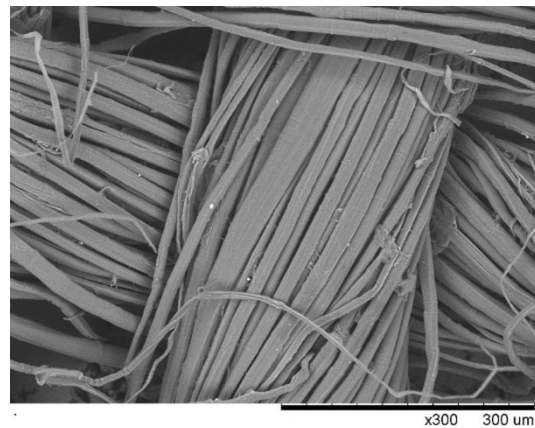
Label	Reinforcement fabric	Lamination	Stacking sequence	Thickness [mm]	Fibre volume fraction [%]
C	Carbon	Carbon control	[C ₁₅] 	2.72	61.1
S	Carbon/Hemp	Sandwich	[C ₆ H ₃ C ₆] 	3.12	53.7
A-HC	Carbon/Hemp	Asymmetric	[CH ₃ C ₁₁] 	3.12	53.2
A-CH	Carbon/Hemp	Asymmetric	[C ₁₁ H ₃ C] 	3.11	53.8
SU	Carbon/Hemp	Symmetric Uniform	[CHC ₅ HC ₅ HC] 	3.10	53.4
H	Hemp	Hemp control	[H ₁₅] 	3.68	46.6

3.13.5 Part 5: Tribological behaviour of hemp fibres

This section is focused on the characterisation of the wear behaviour of hemp/epoxy composite materials compared to that of glass/epoxy and carbon/epoxy composites. The experimental campaign derives from the study carried out in part 4. The idea was the replacement of the external ply with bio-based ones in all cases of tribological loads that can compromise the human health by dermatitis from contact or inhalation of broken fibres. Woven Maeko hemp fibres in form of fabric, Toray International carbon fibres and glass fibres were impregnated with SX 10 EVO epoxy resin in order to produce all samples typologies under inspection. As well as for the other experimental campaign, hemp fibres were chemically treated and then dried in an oven with a temperature of 60 °C for 12 hours. In fig. 32 are reported a SEM observation of the fibre surface before and after the chemical treatment.



a)



b)

Fig.32: Hemp tow surface before (a) and after (b) the chemical treatment.

The sample types under investigation are listed in Table 19. All laminates from which the specimens were obtained, have the same stratification sequence and the same number of plies equal to four.

Table 19: Main characteristics of all samples under inspection

Sample Type	Fabric	Matrix	Plies Number	Thickness [mm]	Fibre volume fraction [%]
H	Hemp	Epoxy	4	1,52	30,00
C	Carbon	Epoxy	4	1,56	29,70
G	Glass	Epoxy	4	1,80	34,20

The laminates were produced through the vacuum infusion process technique. At the end of the stratification, the dried plies were sealed in an elastomeric bag under vacuum, then the infusion process took place. The uncured laminates were left to cure under vacuum at room temperature for 24 hours.

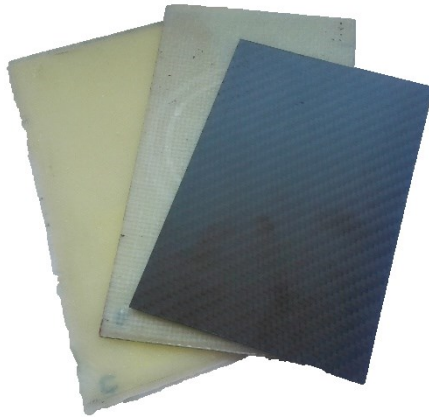


Fig.33: Hemp, glass and carbon specimen used for the experimental campaign.

Then, specimens 200 x 100 mm in size were obtained from the sample laminates and are shown in fig.33. Therefore, in this experimental campaign tribological tests and microgeometrical measurements were carried out in order to study how hemp fibre influence the wear behaviour of composite materials.

Reference

- [1] C. Hill, M. Hughes, Natural Fibre Reinforced Composites Opportunities and Challenges, *J. Biobased Mater. Bioenergy*. 4 (2010) 148–158. doi:10.1166/jbmb.2010.1079.
- [2] D.W. Lachenmeier, L. Kroener, F. Musshoff, B. Madea, Determination of cannabinoids in hemp food products by use of headspace solid-phase microextraction and gas chromatography-mass spectrometry, *Anal. Bioanal. Chem.* 378 (2004) 183–189. doi:10.1007/s00216-003-2268-4.
- [3] A. Shahzad, Hemp fiber and its composites—a review, *J. Compos. Mater.* 46 (2012) 973–986.
- [4] Tesla P100DL race car, (n.d.). <http://www.bcomp.ch/en/products/powerribs>.
- [5] L. Pil, F. Bensadoun, J. Pariset, I. Verpoest, Why are designers fascinated by flax and hemp fibre composites?, *Compos. Part A Appl. Sci. Manuf.* 83 (2016) 193–205.
- [6] Hemp chair-Werner Aisslinger, (n.d.). <https://www.yatzer.com/The-Hemp-Chair-by-Werner-Aisslinger>.
- [7] Hemp chair, Canvas Mariposa, (n.d.). <https://cuerodesign.com/product/canvas-butterfly-chair-canvas-mariposa/>.
- [8] J. Deferne, D.W. Pate, B. V Hortapharm, D.W. Pate, International Hemp Association essential fatty acids, 3 (1996) 1–48.
- [9] P. Cappelletto, M. Brizzi, F. Mongardini, B. Barberi, M. Sannibale, G. Nenci, M. Poli, G. Corsi, G. Grassi, P. Pasini, Italy-grown hemp: yield, composition and cannabinoid content, *Ind. Crops Prod.* 13 (2001) 101–113.
- [10] hemp cross-section, (n.d.). <https://iowahia.org/anatomy-of-hemp/>.
- [11] A. Thygesen, B. Madsen, A.B. Bjerre, Cellulosic Fibers : Effect of Processing on Fiber Bundle Strength Cellulosic Fibers : Effect of Processing on Fiber Bundle Strength, (2011). doi:10.1080/15440478.2011.602236.
- [12] A. Thygesen, A.B. Thomsen, G. Daniel, H. Lilholt, Comparison of composites made from fungal defibrated hemp with composites of traditional hemp yarn, *Ind. Crops Prod.* 25 (2007) 147–159.
- [13] M. Liu, A.S. Meyer, D. Fernando, D.A.S. Silva, G. Daniel, A. Thygesen, Effect of pectin and hemicellulose removal from hemp fibres on the mechanical properties of unidirectional hemp/epoxy composites, *Compos. Part A Appl. Sci. Manuf.* 90 (2016) 724–735.

- [14] D. Fengel, Wood and cellulose chemistry, *Holz Als Roh- Und Werkst.* 50 (1992) 340. doi:10.1007/BF02628639.
- [15] R.M. Rowell, A new generation of composite materials from agro-based fiber, in: *Polym. Other Adv. Mater.*, Springer, 1995: pp. 659–665.
- [16] H.L. Bos, M.J.A. Van Den Oever, O. Peters, Tensile and compressive properties of flax fibres for natural fibre reinforced composites, *J. Mater. Sci.* 37 (2002) 1683–1692.
- [17] TPP Industrial Hemp Guide, in Health Canada, 1998.
- [18] M. Liu, D. Fernando, G. Daniel, B. Madsen, A.S. Meyer, M.T. Ale, A. Thygesen, Effect of harvest time and field retting duration on the chemical composition, morphology and mechanical properties of hemp fibers, *Ind. Crops Prod.* 69 (2015) 29–39.
- [19] Maeko S.r.l., (n.d.). https://www.maekotessuti.com/?page_id=39.
- [20] Fidia S.r.l., (n.d.). http://www.fidiaglobalservice.com/ita/tessuti_lino_canapa.html.
- [21] Toray International S.r.l., (n.d.). <http://www.toray-intl.com/>.
- [22] M. Singla, V. Chawla, Mechanical properties of epoxy resin–fly ash composite, *J. Miner. Mater. Charact. Eng.* 9 (2010) 199.
- [23] M.S. Islam, The Influence of Fibre Processing and Treatments on Hemp Fibre/Epoxy and Hemp Fibre/PLA Composites, University of Waikato, 2008. <https://hdl.handle.net/10289/2627>.
- [24] Mike compositi S.r.l., (n.d.). <http://www.mikecompositi.it/category/336-resina-epossidica-sx10-evo-alta-resistenza.aspx>.
- [25] Easy Composite, (n.d.). <https://www.easycomposites.co.uk/#!/prepreg/component-prepregs/xpreg-xc110-prepreg-carbon-fibre-22-twill-210g.html>.

Chapter 4: Results and Discussions

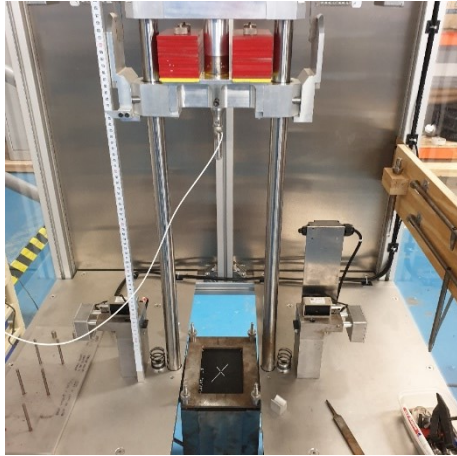
In this chapter, is going to be treated in detail the experimental set-up and the results of each section listed in the previous chapter. Then, in order to make easier the reading, this chapter is divided into four parts.

4.1 Part 2: Hybrid sandwich structures with bio-based cores

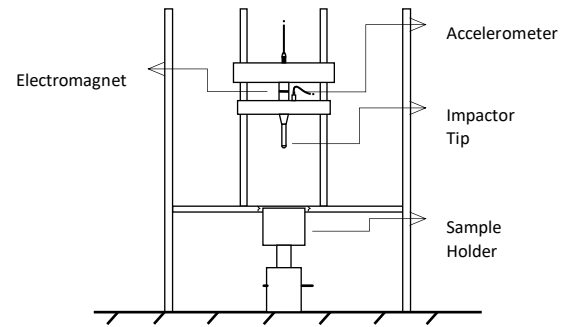
4.1.1 Impact tests

As above mentioned in chapter 3, low velocity impact tests are required in order to evaluate the dynamic mechanical properties of these hybrid sandwich structures. All tests were carried out in accordance with the ASTM D7136 standard.

The tests were executed using a home-made falling drop weight machine, equipped with an impactor tip of 16 mm diameter and a falling impact shuttle of 9.16 kg heavy. Furthermore, in order to avoid additional impacts of the shuttle on the specimen, the impact machine is equipped with an anti-rebound system that hold the shuttle after the first impact. fig.34 shows the impact test apparatus in which it is possible to see the sample clamped between two steel plates, fig.34b represents a schematisation of the experimental set-up.



a)



b)

Fig.34: Experimental set up (a) and schematisation (b) of the impact test.

The impact tests were carried out on a total number of 5 specimens for each sample typology. All samples are characterised by dimension of 100 mm x 150 mm as established by the ASTM standard, and, as showed in fig.34a, are clamped between two steel plates using bold serrated by hand in order to avoid any movement of the samples before and after the impact event.

All tests were carried out keeping constant the impactor mass that is equal to 9.16 kg, and different impact energy levels have been chosen: 10J, 25J and 45J obtained by varying the impactor tip height. Furthermore, additional impact tests were carried out at 50J in order to obtain the failure at penetration of the NSF_6P sample. Once selected the impact energies, the drop height and the impact velocities were evaluated using the potential energy eq. 17 and kinetic energy relations eq. 18.

$$E = mgh \quad \text{eq. 17}$$

$$v = \sqrt{2gh} \quad \text{eq. 18}$$

Where m is the impactor mass in (kg), g is the acceleration of gravity at sea level in (m/s^2) and h is the impact height (m).

The loading peak forces were measured using a piezoelectric load cell connected to a Pc through an amplifier. A Matlab routine was written in order to process all the impact data and at the end of the analysis force-time, force-displacement, displacement-time and velocity-time curves were obtained.

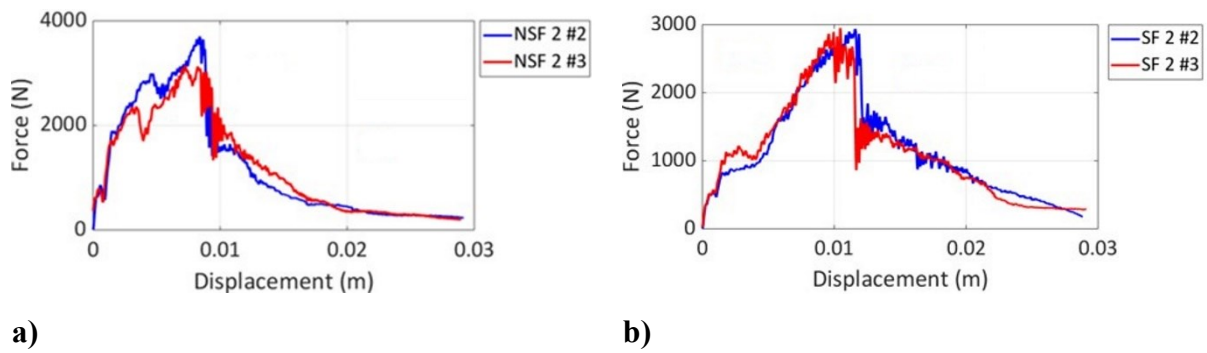


Fig.35: Impact test carried out at 45J on NSF_2P sample (a) and SF_2P sample (b).

fig.35 illustrates the impact force displacement curves, obtained from the impact tests at 45J on NSF_2P (fig.35a) and SF_2P (fig.35b) samples. For each sample typology, the minimum and maximum curves are reported. In both cases, it is possible to observe that the force displacement curves are open and a large area is subtended to the curves, these aspects suggest the failure at penetration for both sample typologies. Moreover, when the maximum force is reached, it is possible to observe in both cases a sharp load drop that corresponds with a growth and propagation of internal damage through the thickness. Focusing the attention to the loading section of the force displacement curves, it is possible to appreciate a first load drop in correspondence of almost 1000 N. This load drop testifies the creation of internal cracks that propagate through the thickness, with more detail, if the attention is focused on the SF sample (fig.35b) a plateau is detected in correspondence of the same loading force. This phenomenon can be justified by the lower rigidity that characterises the SF bio-based core. This aspect can be highlighted by the peak load that is 13.75% lower if compared to the NSF sample and by the displacement at failure that is 30% higher than the NSF sample.

This result confirms what observed about the maximum peak load, the absorbed energy E_a , and return coefficient, RC , values listed in table 20.

Table 20: Impact results of the test carried out at 45J on 2 layers hemp core

Sample	E_i [J]	F [N]	E_a [J]	RC [J/J]
NSF_2P	45	3416.17	34.66	0.229
SF_2P	45	2946.33	32.97	0.267

In the table is reported the peak load, detected for each sample typology, the absorbed energy E_a and the return coefficient that is defined as the ratio between the difference of the impact and the absorbed energies ($E_i - E_a$) and the impact one (E_i).

Other impact tests were carried out on thicker hemp core keeping constant the impact energy, then in fig.36 are reported the impact curves obtained from impact tests at 45J on the NSF_4P (fig.36a) and SF_4P (fig.36b) samples.

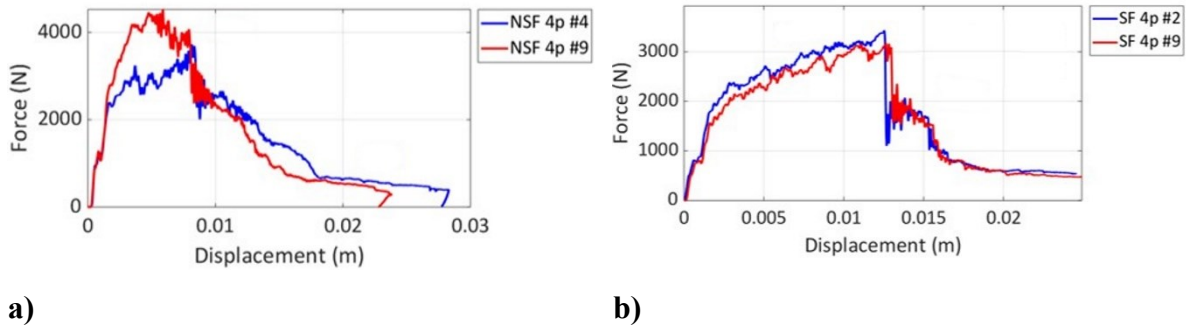


Fig.36: Impact test carried out at 45J on NSF_4P sample (a) and SF_4P sample (b).

From the force displacement curves it is possible to observe that if on one hand the SF sample demonstrates a failure at penetration, on the other the NSF sample shows a severe damage, but no penetration. At the same way, a peak load is detected in the loading section of the force displacement curves in correspondence of around 1000 N. Also in this case, if the attention is focused on the SF sample (fig.36b), it is possible to appreciate a sort of plateau in correspondence of this peak, but it is not so marked because the total number of the core plies is doubled, and then the overall rigidity of the hemp core is raised up. Furthermore, as well as the previous impact test, the SF sample shows a reduced peak force of almost 19.8% and a displacement at break that is 46.1% higher than the NSF sample. These results are indicative of a more ductile behaviour of the SF bio-based core if compared with the NSF one.

Table 21: Impact results of the test carried out at 45J on 4 layers hemp core

Sample	E_i [J]	F [N]	E_a [J]	RC [J/J]
NSF_4P	45	4121.56	44.78	0.005
SF_4P	45	3303.46	42.37	0.058

In table 21 are resumed the main results of the impact tests carried out on NSF_4P and SF_4P samples.

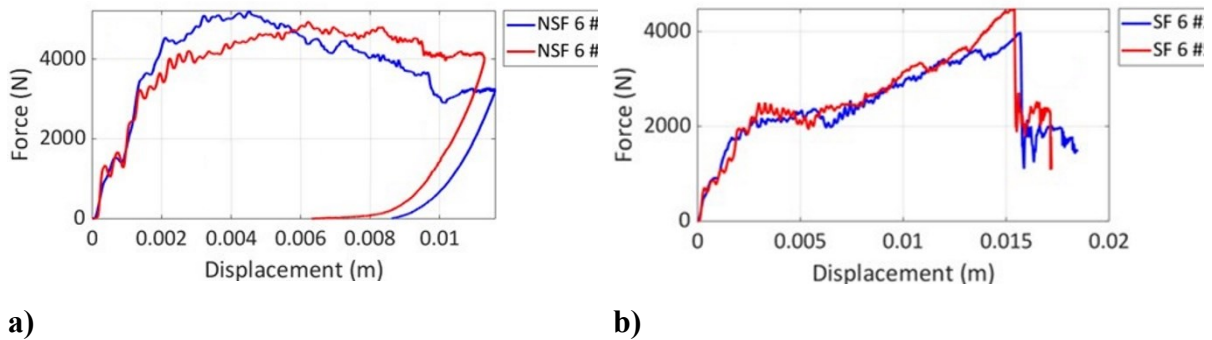


Fig.37: Impact test carried out at 45J on NSF_6P sample (a) and SF_6P sample (b).

Fig.37 shows the force displacement curves obtained from impact tests carried out at 45J on NSF_6P (fig.37a) and SF_6P (fig.37b) samples and table 22 summarises the main impact results.

Table 22: Impact results of the test carried out at 45J on 6 layers hemp core

Sample	E_i [J]	F [N]	E_a [J]	RC [J/J]
NSF_6P	45	5079.61	41.15	0.085
SF_6P	45	4226.99	44.90	0.002

For both sample typologies, it is possible to appreciate a good repeatability of the impact tests, and as well as for the 4 layers core case, a failure at penetration takes place for the SF samples whilst a severe damage without penetration occurs for the NSF sample. Looking at fig.37 it is possible to observe that the force suddenly reaches the maximum value in case of NSF sample (fig.37a), whilst increases smoothly up to the maximum value in case of SF sample (fig.37b). Furthermore, a peak load reduction of almost 16.8 % is detected for the SF sample if compared to NSF one and a displacement at break that is 29.2% higher than the NSF specimen. All these aspects, highlighted as well as the previous impact tests, a more ductile behaviour of the SF bio-based core.

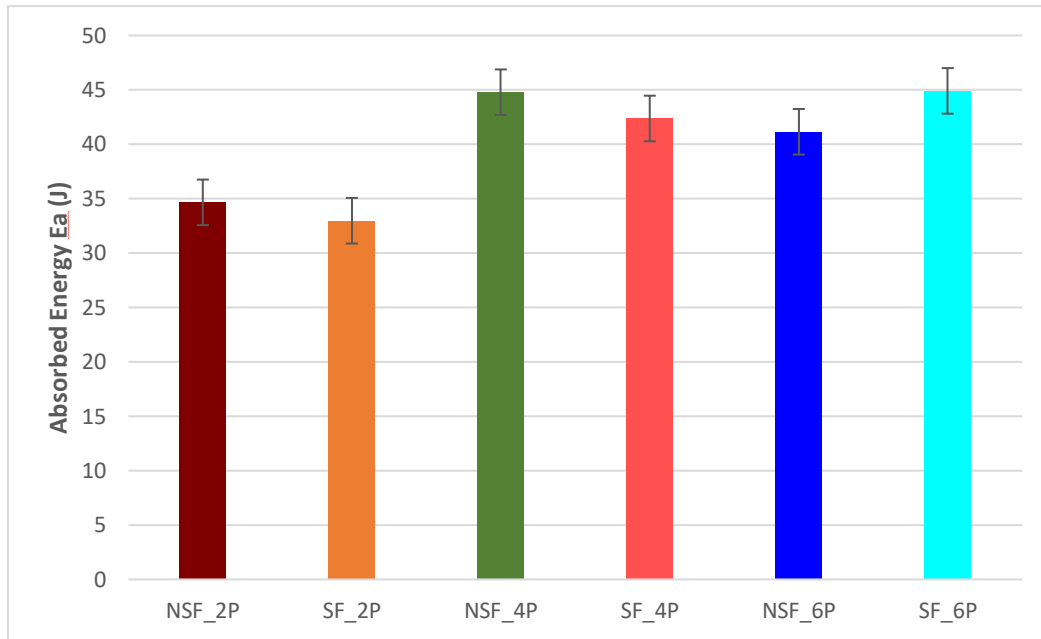


Fig.38: Mean value of the absorbed energy for each sample typology at the end of the 45J impact test.

In fig.38 are summarised the mean values of the absorbed energy obtained from the impact test at 45J carried out on each sample typology. From this graph, it is possible to observe that both sandwich structures with NSF_2P and SF_2P cores show the lowest value of absorbed energy, this aspect is linked to the load reaction capability of these two sample families. With more detail, only 77% and 73.3% of the impact energy were sufficient to reach the material limit and penetrate NSF_2P and SF_2P samples respectively. Analogous conclusions can be deduced for SF_4P and SF_6P samples, in which the 94% and the 99.8% of the impact energy is required to produce the failure of the specimens, then increasing the total number of core layers, a larger amount of energy is required to cause the failure of the specimen. On the other hand, if the attention is focused on the NSF_4P and NSF_6P samples, a reduction of the absorbed energy is detected when the number of core layers is raised up. Then, it is possible to conclude that the core density influences the impact behaviour of NSF sample typology.

4.1.2 Indentation tests

Additional indentation tests are then required to better understand the failure mechanism of NSF and SF hemp core. The tests were carried out according to the ASTM D6264 standard using an MTS Alliance RT/50 universal testing machine equipped with a 50 kN piezoelectric

load cell. The dimensions of both the sample typologies were established by the ASTM standard, then 150 mm x 150 mm square samples were tested with a hemispherical indenter tip with a diameter of 15 mm. As well as the specimen geometry, the testing speed was established by the standard and it was set to 4 mm/min.

A total of three curves were obtained for each sample typology, a first one at penetration, then other two curves in which the test was stopped when the 33% and 66% of the failure displacement was reached.

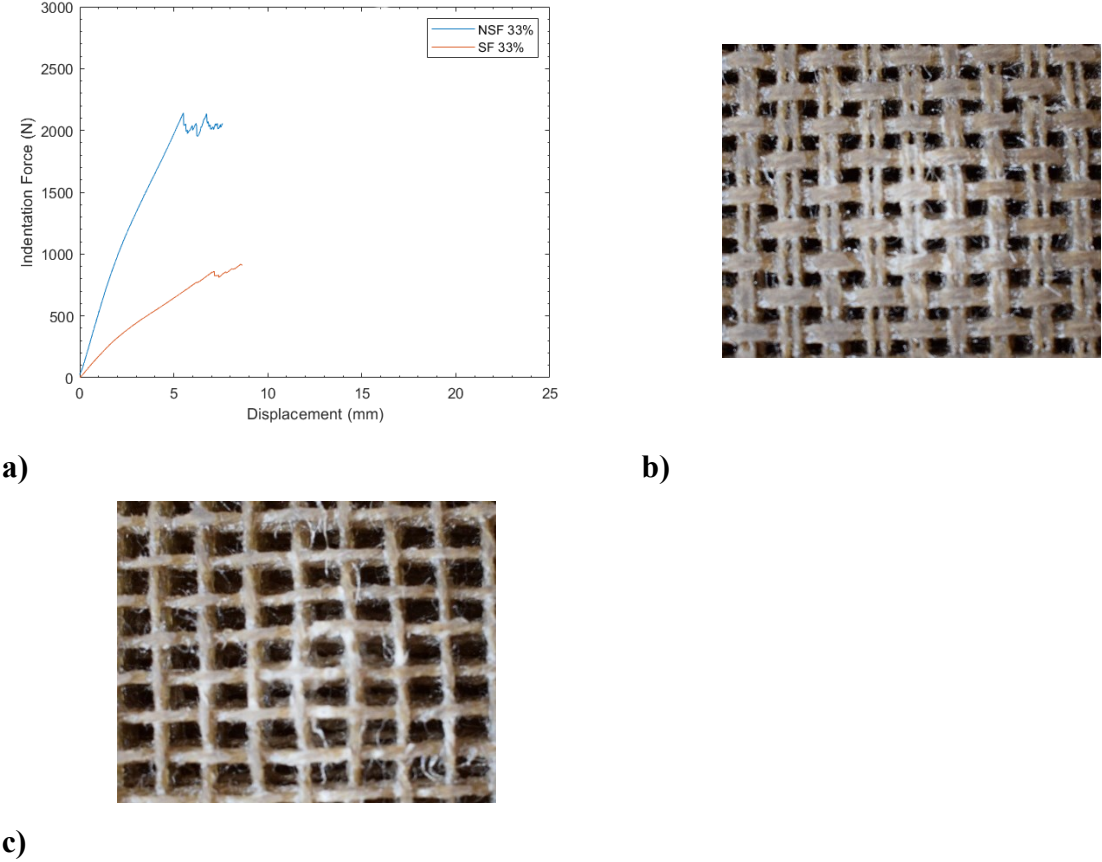


Fig.39: Indentation test 33% of the failure at penetration: indentation force displacement graph (a), NSF sample bottom surface (b), SF sample bottom surface (c).

In fig.39 are reported the 33% indentation curves and a magnification of the bottom surfaces of both the NSF sample (fig.39b) and SF sample (fig.39c). The indentation curves show, as well as for the impact test carried out on the sandwich structures, a maximum load reduction of SF sample of almost 57.5% in comparison with the NSF one and, at the same time, an improvement of the displacement of almost 36.7%. Focusing the attention on fig.39b and b, it is possible to appreciate that in both cases initial cracks start from the upper surface in contact with the

penetrator tip and propagate on the lower surface through the thickness. These cracks appear to be extremely localised, moreover no delaminations are detected at the end of this test.

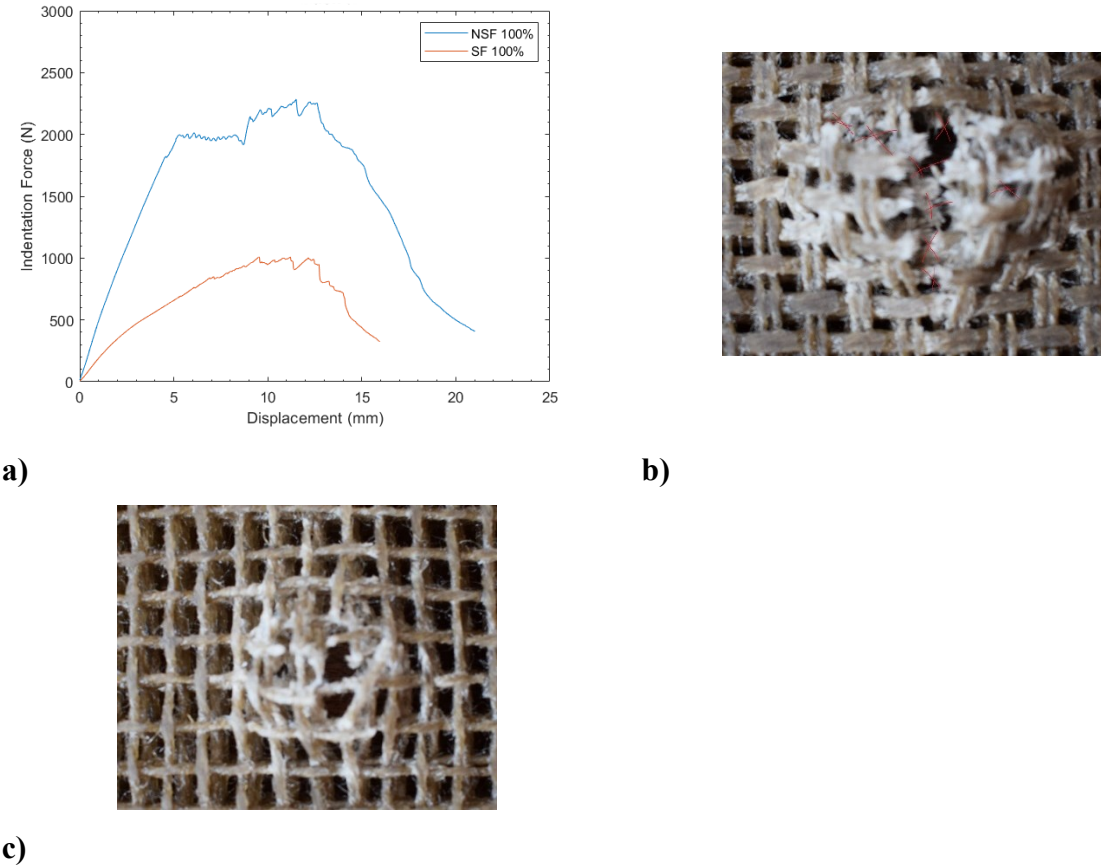


Fig.40: Indentation test at penetration: indentation force displacement graph (a), NSF sample bottom surface (b), SF sample bottom surface (c).

In fig.40 are reported the penetration force displacement curves and the magnification of the bottom surfaces of both the NSF and SF samples, respectively fig.40b and c. The indentation curves still demonstrate a peak load reduction of the SF sample of almost 55.5% in comparison with the NSF sample, whilst an improvement of only 5% of the displacement at failure is detected for the SF sample in comparison with the NSF one. At the end of the penetration test, both samples showed a defined indentation on the top surface in contact with the penetrator tip, on the other hand broken and bended fibres are appreciable on the bottom surfaces of both samples.

An additional failure mechanism can be observed from the SF sample magnification (fig.40c), in detail the penetrator breakthrough causes an in-plane hemp fibre bending both in warp and weft direction due to the low interaction between hemp tows at the intersection.

This mechanism justifies an additional contribute to the impact energy dissipation, indeed during the impact event part of the impact energy is used to plastically deform hemp core layers. This fibre bending mechanism that characterises the SF sample is responsible of a reduced damaged area.

4.2 Part 3: Thin hybrid sandwich structures with bio-based cores

4.2.1 Tensile tests

On the basis of a complete mechanical characterisation of thin sandwich structures, tensile tests were performed on all samples according to the ASTM D3039 standards, using the MTS Alliance RT/50 universal testing machine equipped with a 50kN piezoelectric load cell. The tensile tests were carried out on a total number of three specimen for each sample typology with a width and a length of 25 mm and 250 mm respectively. Moreover, as established by the ASTM standard, on each specimen four tabs were applied in the grip zone. Testing speed was chosen according to the standard equal to 2 mm/min, then the tensile stress was evaluated by using the eq. 19.

$$\sigma = \frac{F}{A} \quad \text{eq.19}$$

Where F is the load expressed in (N) and A is the cross section of the specimen in (mm^2). During the tensile test an extensometer was employed for the measurement of the strain at break. Then the elastic modulus was evaluated by the stress to strain ratio according to the following equation.

$$E = \frac{\Delta\sigma}{\Delta\varepsilon} \quad \text{eq.20}$$

Fig. 41 shows the typical force displacement curves of all sample typologies under inspection. Since in this part of the experimental campaign composite laminates and sandwich structures are compared, makes sense a simple force displacement comparison instead of the typical stress strain one.

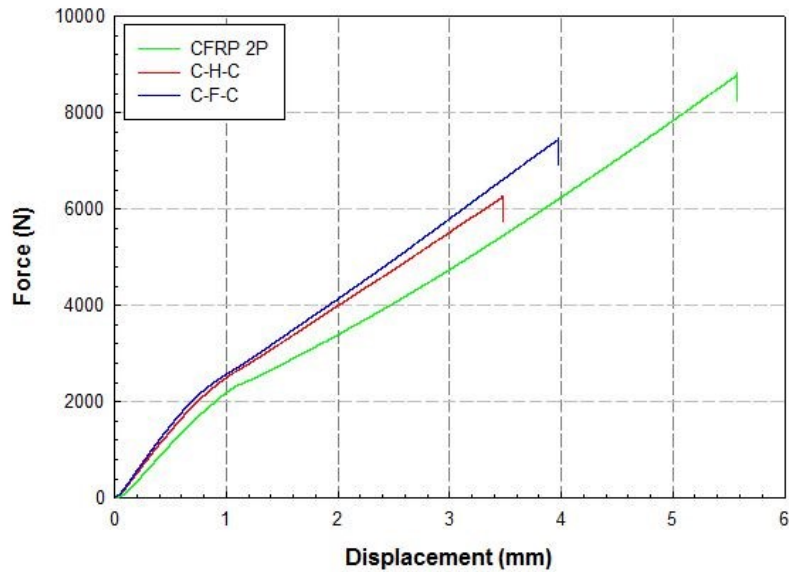


Fig.41: Typical force-displacement curves of each sample typology.

The chart shows that the addition of a natural fibre layer between the two carbon skins, does not influence the elastic behaviour of the hybrid laminate, indeed these plates respond elastically to the applied deformation with a linear load increasing. It is clear that there is a reduction of the mean value of the maximum load at break of almost 19,2% and 13% respectively for C-H-C and C-F-C configurations if compared to the carbon reference. In the hybrid composite structure, the two carbon skins are not in contact each other leading to internal delamination and then the premature fail of the single carbon layer. This issue is also linked to the smaller elongation at break that characterises the hybrid composites. Fig.41 shows also a slope increasing of the hybrid composite materials in comparison with the carbon laminate reference. In detail, the slope of C-H-C and C-F-C configurations is respectively 12,3% and 22,4% higher than the reference. This aspect is clear, considering that the addition of the natural fibre layer causes an increase of the total thickness, and then a larger cross section of the samples.

4.2.2 Three-point bending tests

Three-point bending tests were carried out according to the ASTM D790 standard, using the MTS Alliance RT/50 equipped with a 1 kN piezoelectric load cell. A total number of three

specimens for each sample typology were tested with a length and a width of 100 mm and 13 mm respectively. In all configuration, a three-point bending fixture was employed with both the loading nose and support characterised by a circular section with a diameter of 10 mm as established by the standard. As well as the fixture geometry, the testing speed was established by the standard, with more detail set to 2 mm/min. The ASTM standard recommend the support span that is equal to 44 mm and 53 mm respectively for hemp and flax core hybrid sandwiches. The support span of CFRP laminate was 20 mm in case of comparison with sandwich structures with the same mechanical properties and 58 mm in case of comparison with the same thickness. Moreover, additional three-point bending tests were carried out at the same support span equal to 30 mm in order to evaluate at the same load condition, the consequence of using a natural fibre layer between two single layers CFRP skins.

Then, the flexural stress (σ_f) was evaluated using eq. 21 in case of composite laminate and eq. 22 in case of sandwich structures.

$$\sigma_f = \frac{3 F L}{2 b s_c^2} \quad \text{eq.21}$$

$$\sigma_f = \frac{F L}{4 b s e} \quad \text{eq.22}$$

Where F is the load in (N), L is the support span in (mm), b is the width of the specimen in (mm), s_c is the thickness of the specimen in (mm), e is the distance between the neutral planes of the skins of the sandwich structure in (mm).

The flexural strain in both cases was evaluated using the following equation.

$$\varepsilon_f = \frac{6 D S_c}{L^2} \quad \text{eq.23}$$

Where D is the displacement of the crosshead in (mm). Then the flexural modulus of elasticity was evaluated by the stress to strain ratio according to eq. 24.

$$E = \frac{\Delta \sigma}{\Delta \varepsilon} \quad \text{eq.24}$$

Fig.50 shows the typical force versus displacement flexural curves of all the sample typologies under inspection. As it is possible to see from this figure, are not reported the flexural stress and strain because in this part of the experimental campaign, both composite laminates and sandwich structures are compared. Therefore, makes sense a simple force displacement comparison instead of the typical stress strain one.

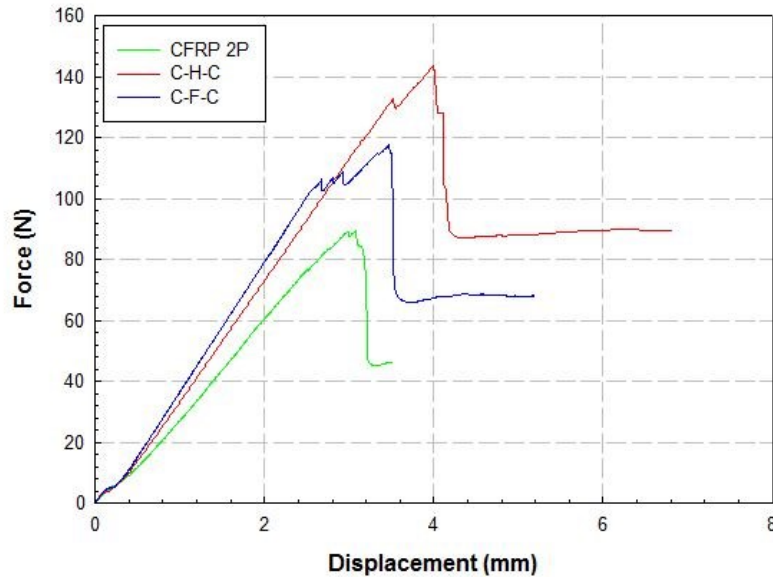


Fig.42: Typical bending force-displacement curves of each sample typology, case of comparison with the same mechanical properties.

Fig.42 shows the typical flexural force versus displacement for each sample typology. These curves show the typical behaviour of composite materials, in detail the composite materials show an elastic behaviour up to the failure of the specimen. The failure takes place in the compressive region due to the compression fibre instability. Moreover, from the chart in fig.42, it is possible to evaluate that there is a changing of the slope of the curves when hybrid sandwich structures are taken into account. With more accuracy, the hybrid laminates show a slope increasing that is almost 32% and 41% respectively for the C-H-C and C-F-C configurations if compared to the CFRP. Then, using the hybrid sandwich structures to obtain the same displacement, a higher force is required, this aspect is related to the improving of the flexural rigidity of the sandwich structure.

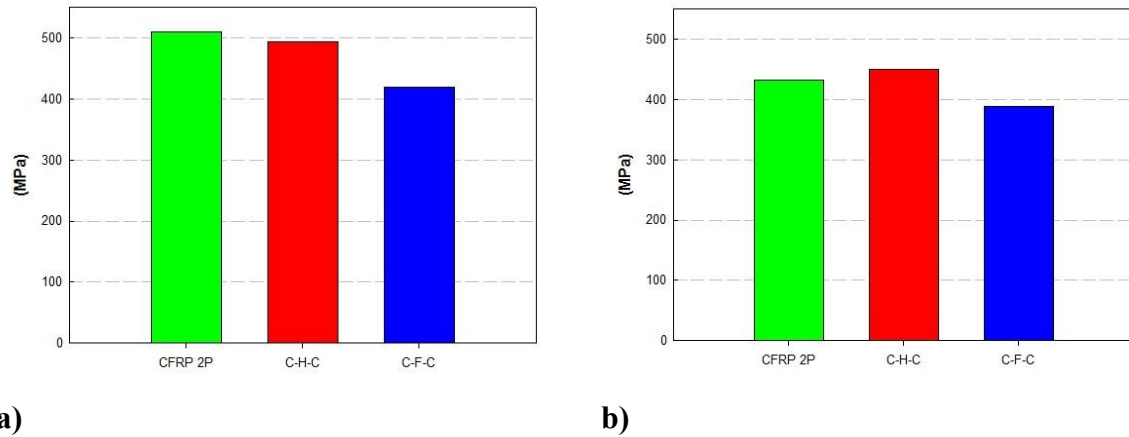


Fig.43: Mean value of the flexural stress of each sample typology (a), specific flexural stress of each family (b) in case of comparison with the same mechanical properties.

Fig. 43a shows the mean value of the flexural stresses for all samples under inspections, from this chart it is possible to evaluate that there is not an appreciable variation of flexural properties for all configurations under inspection, this aspect is clear because the failure of the specimen occur in the carbon layer where the load is applied. In fig. 43b are reported the specific flexural stresses obtained by the ratio between the bending stress and the density of the composite structures. From this chart it is highlighted an improvement of the specific flexural properties that is almost 5% if the hybrid C-H-C sandwich structure is compared to the CFRP one. Additional three-point bending tests were performed comparing each sample typology with the same weight. For these tests is not reported the flexural stress chart because, as well as for the previous case, the failure of the specimen is caused by the carbon fibre instability in the compression region, where the load is applied. Conversely the specific bending stresses are reported.

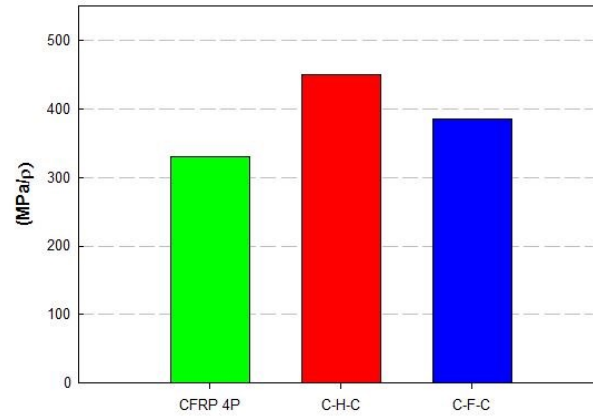


Fig.44: Specific flexural stresses of each sample typology, case of comparison with the same mechanical properties.

In fig.44 are shown the specific flexural stresses. From the chart it is possible to appreciate that both the sandwich structures demonstrate higher specific stress if compared to the carbon reference. With more detail, while the C-F-C configuration shows the best specific properties with an improvement of almost 36,5% compared to the carbon reference, the C-F-C structure demonstrates specific flexural properties that are almost 16,5% higher than the reference.

Then, at the end of the flexural tests, other bending tests were carried out maintaining a constant value of the support span. These tests were performed in order to evaluate with the same load conditions, the influence on the mechanical properties by the addition of a bio-based layer between two carbon skins.

In fig.45 are reported the typical flexural forces versus displacement of all samples under inspection. As well as for fig.42, also in this case, due to the comparison between composite laminates and sandwich structures, makes sense the presentation of flexural force versus displacement curves instead of the flexural stress strain ones.

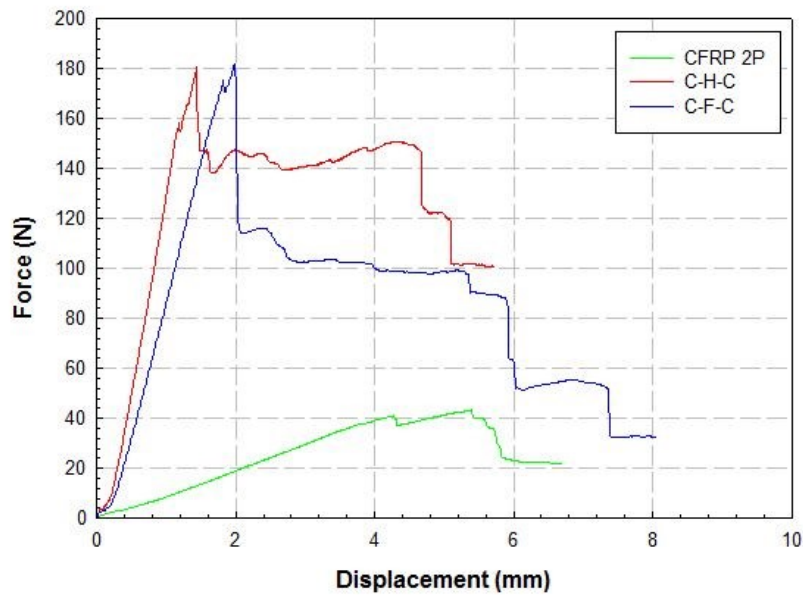


Fig.45: Typical bending force-displacement curves of each sample typology, case of comparison with the same mechanical properties under the same load conditions.

As well as for the fig.50 all sample typologies fig.45 shows the typical behaviour of composite materials, in detail, an elastic response to the applied deformation up to the failure is detected for each sample type. Moreover, as well as the comparison with the same mechanical properties, fig.45 shows an improving of the slope of the hybrid curves that is almost 1900% and 1300% respectively for the C-F-C and C-H-C sandwiches compared to the carbon reference. Then, when the different composite typologies are subjected to the same load condition, the addition of a natural fibre layer between two carbon plies, leads to a consistent increase of the rigidity of the composite structure. This aspect is confirmed by the force-displacement curves where, at the same value of the imposed displacement, a higher value of flexural force is required. In case of flexural tests performed at the same support span make sense a comparison between the specific forces of all samples under inspection. The specific force is obtained by the ratio between the flexural force and the weight of the specimen.

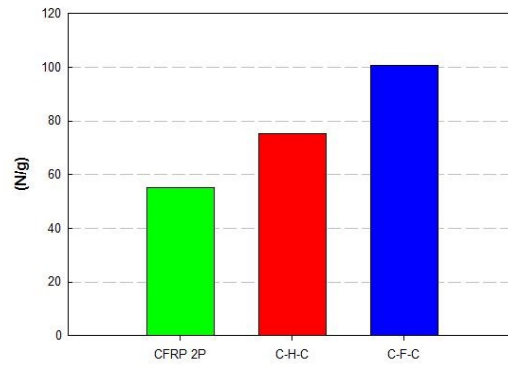


Fig.46: Mean values of the specific flexural force of each sample typology, case of comparison with the same mechanical properties under the same load conditions.

In fig.46 are reported the main value of the specific flexural forces. The chart shows an improvement of the specific force for both the hybrid sandwich structures, in detail the C-H-C configuration demonstrates a specific force that is almost 36% higher than the carbon reference laminate. The best results are indicated by the C-F-C samples with an increase of the specific mechanical properties of around 83% if compared to the reference. Therefore, even if the addition of a layer of natural fibre in the middle plane of the laminate causes a weight increase of the composite material, there is a significative improvement of the specific flexural properties under the same load conditions.

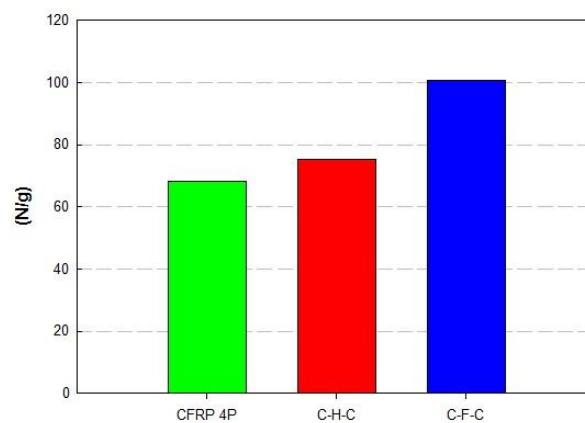


Fig.47: Mean values of the specific flexural force of each sample typology, case of comparison with the same weight under the same load conditions.

In fig.47 it is possible to observe the mean value of the specific forces as consequence of the bending test performed on samples with the same weight under the same load conditions. As

well as for the case showed in fig.46, hybrid sandwich structures demonstrate enhanced specific flexural properties. But this improvement is not so pronounced as in the previous case, indeed the C-H-C laminate shows an improvement of about 10% in comparison with the carbon reference, while the C-F-C demonstrates an improvement of 48%. These results are clear since the effective portion of carbon fibres in CFRP laminate which are resisting to the bending load is larger (4 carbon plies) if compared to the previous case (2 plies). However, even though a double number of carbon layers is employed, hybrid composite structures still offers higher specific flexural properties than both the carbon references.

4.3 Part 4: Bio-hybrid composite laminates with improved mechanical properties

4.3.1 Three-point bending tests

Three-point bending tests were performed according to ASTM D790 standard, using a universal testing machine (Instron 3369 equipped with a 50kN piezoelectric load cell in fig.48). These tests were carried out in the United Kingdom.



Fig.48: Instron universal testing machine.

The flexural tests were performed on a total number of 5 specimens for each configuration (see table 18 in Materials and methods Part 4 pag. 78) with a length of 210 mm and a width of 13.2 mm in case of carbon (C configuration) and hybrid laminates (A-CH, A-HC and SU configurations), and a length of 300 mm and a width of 18.2 mm in case of hemp composites (H configuration). Both loading nose and the supports are characterised by a circular section with a diameter of 10mm as established by ASTM standard. Testing speed and span length are chosen according to ASTM D790 standard and depend on the sample type: a testing speed of 18 mm/min and a span length of 180 mm in case of carbon composite (configuration C) and all hybrid composites were used, while a testing speed of 22 mm/min and a span length of 230 mm were adopted in case of hemp composites (H configuration). The flexural stress (σ_f), strain(ϵ_f) were evaluated according to the eq. 25 and eq. 23 showed in the part 3. Then the flexural modulus of elasticity was evaluated by the stress to strain ratio according to eq. 24.

$$\sigma_f = \frac{3 F_c L}{2 b S_c^2} \left[1 + 6 \left(\frac{D_c}{L} \right)^2 - 4 \left(\frac{S_c}{L} \right) \left(\frac{D_c}{L} \right) \right] \quad \text{eq. 25}$$

Where F_c is the load in (N), L is the support span in (mm), b is the width of the specimen in (mm), S_c is the thickness of the specimen in (mm) and D_c is the deflection of the centreline of the specimen. This equation is suggested by the ASTM standard when high vales of support span are used and when high anisotropic materials are tested.

At the end of bending tests, tested samples were embedded in the SX10 epoxy resin in order to conduct microscope inspections for understanding the failure mechanism of each sample type. At the end of the polymerisation at room temperature, the inspection surfaces, i.e. the sample cross section, were grinded firstly with 240p and 400p sandpaper for a period of 60 seconds and then polished with 9 μm and 3 μm diamond suspension for 120 seconds.

Then, the cast specimens were positioned on the microscope support and the failure zone was observed by using a LEICA M205 C stereomicroscope.

Flexural stress strain curves are indicative of the stress history, which is, in turn, linked to damage initiation and propagation, therefore, analysing the different curves it is possible to identify the differences in the behaviour of the two materials and understand how they can work simultaneously in the hybrid configurations.

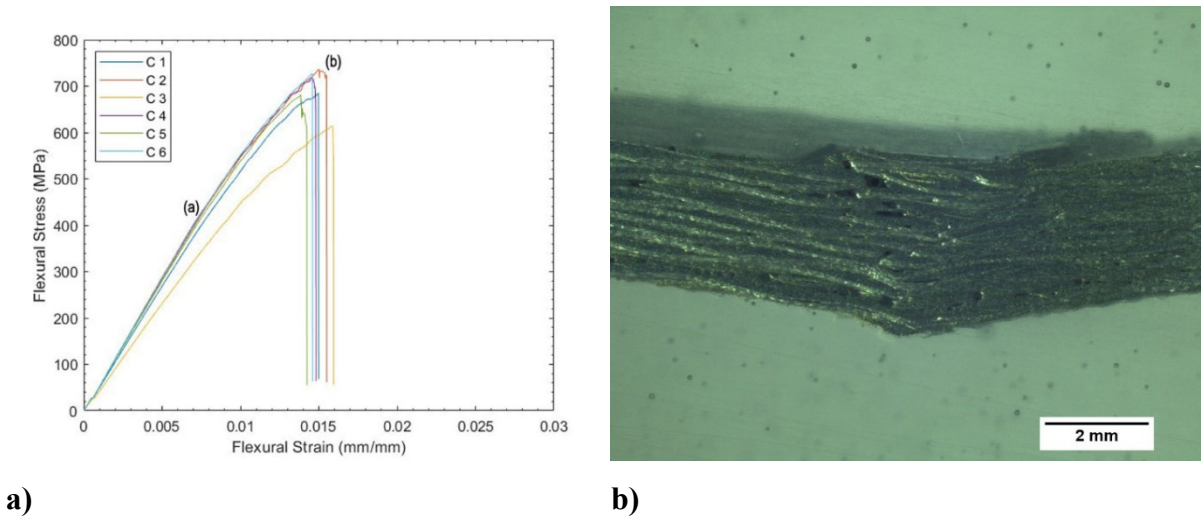


Fig.49: Flexural test on C configuration: flexural curves (a); failure zone microscope image (b).

Overall, from the curves in fig.49a, it is possible to observe the typical flexural behaviour of traditional carbon laminates: the laminate responds elastically to the applied deformation by linearly increasing the load without visible damage up to a critical point (a) which corresponds to the damage propagation phase, where cracks start to nucleate and grow in the compressive portion of the laminate, resulting in a slight progressive load decrease and a deviation from the linear trend. As it is possible to see from the micrography in fig.49b, these cracks propagate rapidly from the contact area throughout the thickness of the laminate, leading to the catastrophic failure of the specimen which is represented by the dramatic load drop of point (b) [1].

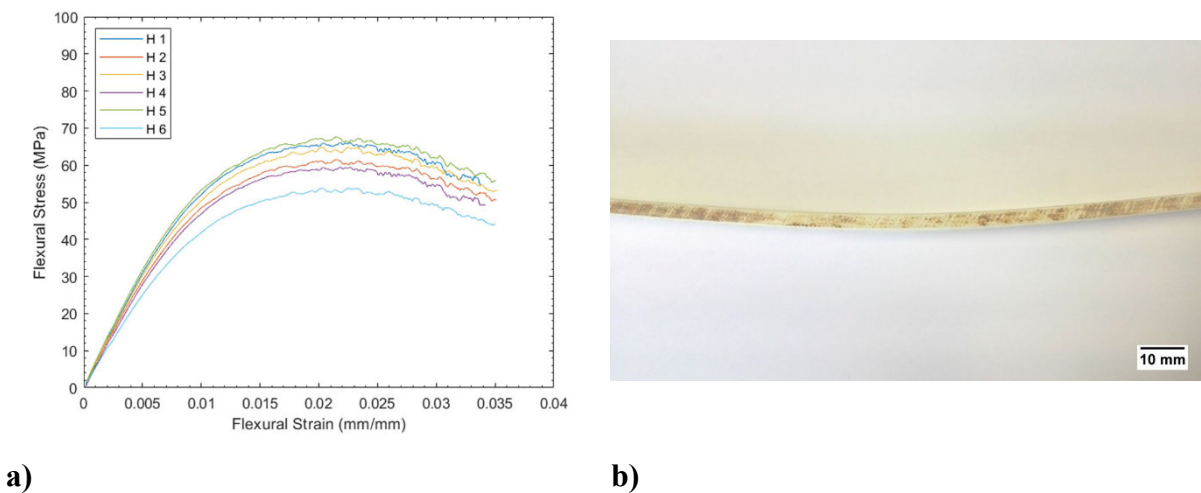


Fig.50: Flexural test on H configuration: flexural curves (a); failure zone microscope image (b).

The flexural behaviour of the hemp composite specimens (configuration H) is instead illustrated in fig.50a, where it is possible to observe a more ductile behaviour which is given by the specific multi-scale structure of natural fibres (NF) and typical of Natural Fibres Composites (NFC) [2,3]. In particular, the improved ductility of hemp fibres is the main cause of the change in behaviour observed for samples H, as these laminates are characterised by a lower flexural modulus (6.18 GPa, -89%), lower flexural strength (64.85 MPa, -90.7%) and larger displacement (0.035 mm/mm, 134.9%) in comparison with what observed for the traditional carbon reference (configuration C). The underlying mechanism behind the improved damping characteristics of NF is quite complex and previous works in literature have linked it with the yarn length available for fibre sliding and the with the combination of several hierarchical friction phenomena between cellulose and hemicellulose in each cell wall, between the different cell walls, between the fibres within the yarns and between the different yarns [4]. By considering this enhanced ductility as a possible mechanism to improve the out-of-plane properties of carbon laminates, it is important to underline that at the end of the three-point bending test, the hemp samples did not reach flexural rupture and were only plastically deformed (fig.50b) by the moving crosshead of the testing machine.

Based on the differences in the flexural response (stiff and brittle for the carbon laminates while soft and ductile for the hemp ones), it appears clear that by joining carbon and hemp fibres with a particular stacking sequence and by carefully tuning their relative volumetric fraction and position, it is possible to develop a hybrid material solution which would be characterised by a combination of strength and ductility.

In this context, as mentioned previously, the position along the laminate's thickness of the hemp layers plays a fundamental role in the development of the equivalent properties of the hybrid laminate and therefore, each configuration will be analysed in depth by comparing its performance to the traditional CFRP. Moreover, since the failure mode will also be affected by the combination of hemp and carbon layers due to the different maximum bending moment that each component will withstand (that will depend on their relative position), the initial fracture might not necessary lie on the top surface layer, therefore the results from the flexural tests will be analysed together with the micrographies of the samples[5].

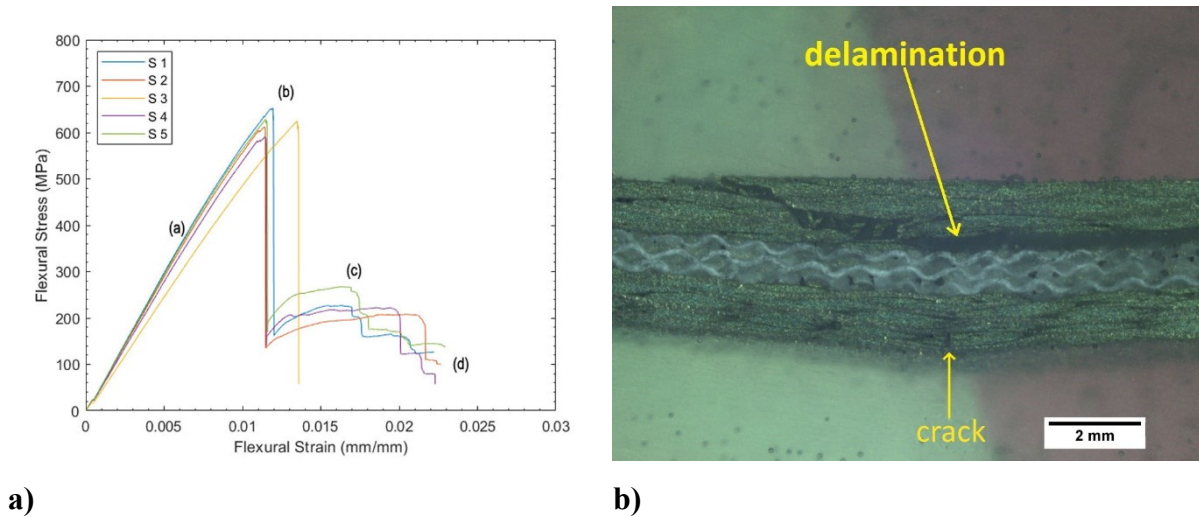


Fig.51: Flexural test on S configuration: flexural curves (a); failure zone microscope image (b).

In particular, fig.51 illustrates the results of the flexural tests carried out on the symmetric samples (Configuration S) from which it is possible to observe the results of the combination between carbon and hemp and when the latter is positioned in the central portion of the laminate.

As it is possible to see from the curves of fig.51a, the hybridisation process results in a mixed flexural behaviour, showing an increase in the maximum strain (0.0223 mm/mm, 49.7%) and a slight decrease in the flexural strength (624.87 MPa, -10.9%). As expected, the interaction between the two different materials also leads to a modification in the failure mode of the laminate, as it is possible to see from fig.51a. Indeed, since the hemp layers are positioned in correspondence with the mid plane, the laminate at first responds elastically with the same modulus of the full carbon samples (point a) (59.75 GPa) until it reaches a critical value (point b, 624.87 MPa), then damage starts to propagate within the upper portion of the laminate leading to a large drop in the stress-strain curve. Unlike the traditional CFRP (configuration C) however, the crack does not propagate throughout the entire thickness of the sample, as shown in fig.51b, but it stops when it reaches the hemp layers and bends at the interface between the carbon and the hemp layers resulting in a plateau at around 200 MPa (point c). During the propagation of the delamination, the load slightly increases until it reaches a second critical point which corresponds to the opening of cracks in the bottom portion of the laminates leading to the sudden failure of the entire sample (point d).

The results from the symmetric laminate (S configuration) showed that the hybrid configuration allows for a combination of different failure mechanisms and damage propagation mechanisms

which are caused by the mismatch in mechanical properties between carbon and hemp layers. It is important to underline that being placed in the midplane, the hemp layers did not affect the material's response in the elastic portion of the stress-strain curve as demonstrated by the very close values of flexural modulus and the maximum load recorded during the tests, which are in line with what previously reported in literature for basalt/carbon hybrid laminates [5]. Figs.52 and 53 represent the results of the three-point bending tests on samples A-CH and A-HC, that were carried out to investigate how the hemp layers affect the flexural behaviour of the hybrid material when they are placed in the tensile or compressive portion of the laminate, respectively.

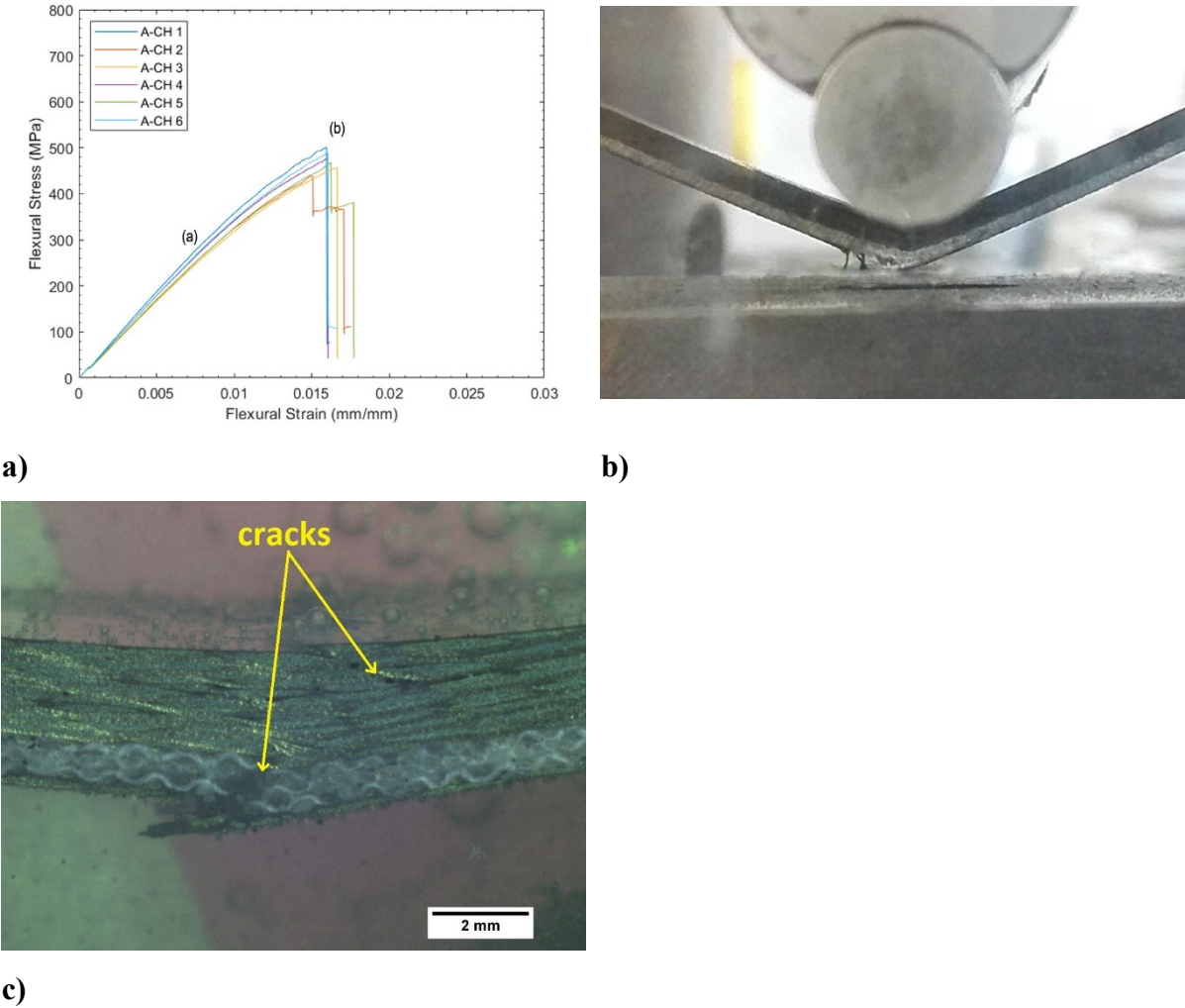
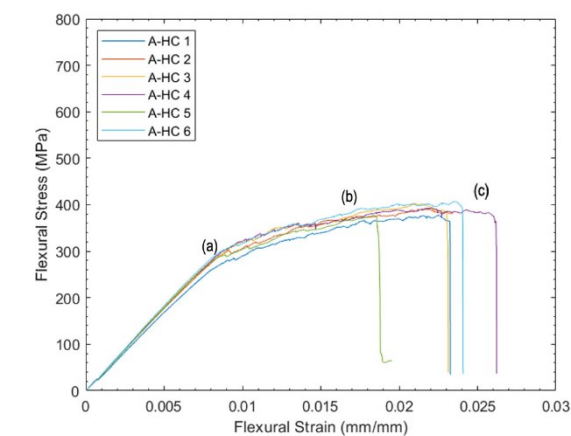


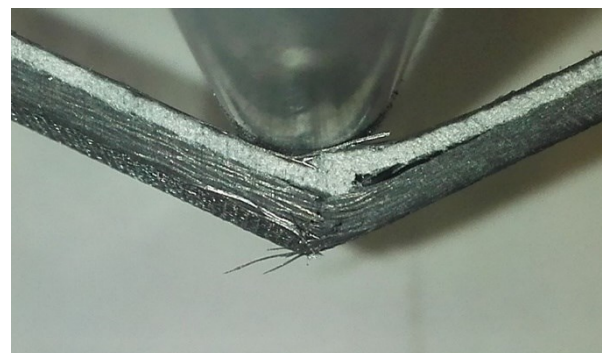
Fig.52: Flexural test on A-CH configuration: flexural curves (a); failure zone during the bending test (b); failure zone microscope image (c).

As it is possible to observe from fig.52, the presence of the natural fibres in the tensile portion of the laminate (samples A-CH) seems to negatively affect the performance of the composite, showing a decrease in flexural modulus (34.15 GPa, -38.3%) and strength (473.13 MPa, -32.5%) in comparison with the control CFRP samples and a slight decrease in terms of strength in comparison with the symmetric hybrid configuration (-12%, S sample type). While this is expected due to the lower stiffness of hemp 38 -70 GPa of hemp fibres [6], 230 – 250 GPa of carbon fibres [7] less expected are the values of the maximum strain which are very close to the ones of the control sample (0.015 mm/mm). This behaviour can be explained by analysing the micrography of figs.52b and c, which represent the typical cross section of a sample A-CH during and after the test, respectively. As it is possible to see from the images, the load drop corresponds with the crack growth from the compressive portion of the laminate (carbon) which propagates through the thickness of the sample. Unlike the symmetric sample (S configuration), in this case the hemp layers are not able to bend the crack because the stresses are too high at that distance from the neutral axis, therefore the damage propagates through the hemp portion overcoming its tensile strength and, consequently, causing catastrophic tensile failure. These results are in line with what observed in literature by Zhang et al in their study on hybrid carbon/glass laminates [8]. It is important to underline that in two out of five samples, it is possible to see some crack bending around the carbon/hemp interface but this phenomenon is not able to dissipate much energy as demonstrated by the very short plateau that leads to the inevitable collapse of the sample.

Inverting the reciprocal position of carbon and hemp (i.e. A-HC configuration, hemp layers in the compression portion of the laminate), the behaviour of the sample changes radically as illustrated in fig.53.



a)



b)

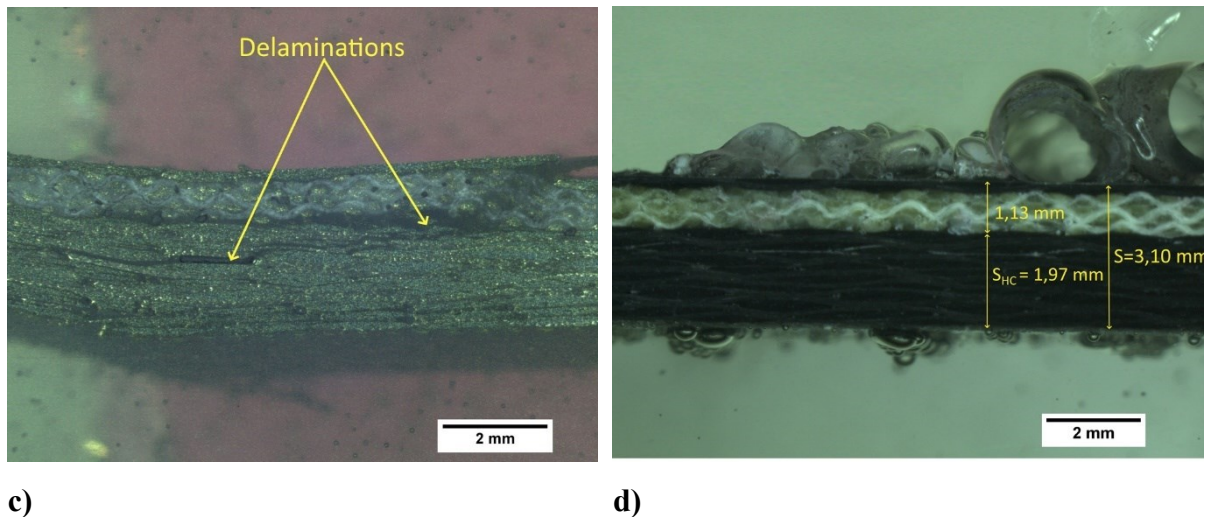


Fig.53: Flexural test on A-HC configuration: flexural curves (a); failure zone during the bending test (b); failure zone microscope image (c); thickness of bundles of carbon and hemp layers (d).

Indeed, observing the stress strain curves relative to the A-HC samples, it is possible to observe a first linear trend (point a) which corresponds with the one observed for the A-CH samples (respectively 290 MPa and 300 MPa against 450 MPa of configuration C) and it is the result of the interaction between the two materials. However, while in the previous case the presence of the carbon layers in the compressive portion led to the generation of cracks that in turn led to critical failure, in the A-HC configuration, the curves do not show a specific peak, but present sign of large deformation after a threshold value is reached (point a) which is given by the higher strain at failure of the hemp fibres. After this point, damage starts to grow at the interface between hemp and carbon, causing a large delamination (see fig.53b) that leads to the detachment of the hemp layers (see fig.53c) and translates into the very long and smooth plateau of point b. Similar results were observed by Subagia et al for carbon/basalt hybrid laminate loaded in flexure when the more ductile basalt fibres are placed in the compressive side of the laminate [5].

At this point, the effective section of the sample that responds to the imposed deformation is only the bottom carbon portion of the laminate which will resist until the critical stress is reached (point c), leading to the total failure of the specimen. One could argue that if only the carbon is resisting to the applied displacement and the hemp layers are effectively not being tested, it is not clear why the two configurations fail at different values of sigma. However, it is important to notice that the evaluation of the flexural stress does not take into account the separation of the top portion of the laminate due to the generation of the large delamination observed in the A-HC hybrid configuration. Indeed, by measuring the effective dimension of

the portion of carbon fibres which is resisting to the bending load after the delamination has grown up to point c, it is possible to evaluate the real stress acting on the carbon layers by considering the difference in the thickness of the two laminates (laminates C and A-HC) and the relative maximum load before failure.

According to the ASTM standard D790, the flexural strength will be a function of the perpendicular load F , the span L , the width b and the thickness S of the laminate. If we assume that this value will be the same for both samples C and samples HC, we can write that:

$$\sigma_{max} = \frac{3 F_C L}{2 b s_C^2} \left[1 + 6 \left(\frac{D_C}{L} \right)^2 - 4 \left(\frac{s_C}{L} \right) \left(\frac{D_C}{L} \right) \right] = \frac{3 F_{HC} L}{2 b s_{HC}^2} \left[1 + 6 \left(\frac{D_{HC}}{L} \right)^2 - 4 \left(\frac{s_{HC}}{L} \right) \left(\frac{D_{HC}}{L} \right) \right] \quad \text{eq. 26}$$

considering that the width and span of the samples in the two configurations are the same and that the average values of the maximum Load are equal to 300 N and 165 N for the configurations C and A-HC respectively, it is possible to evaluate the thickness of the carbon portion which is necessary to reach the failure of the fibres as:

$$S_{HC}^2 [F_C L^2 + 6 F_C D_C^2 - 4 F_C D_C S_C] + S_{HC} [4 S_C^2 F_{HC} D_{HC}] - S_C^2 [F_{HC} L^2 + 6 F_{HC} D_{HC}^2] = 0 \quad \text{eq. 27}$$

By substituting the values of the two loads and considering that S_C represents the total thickness of sample C, it is possible to calculate the value S_{HC} as equal to 2.00 mm, which represents exactly the thickness of the bundle of carbon layers (1.97 mm, see fig.53d) which resists to the bending load once the delamination separates it from the hemp layers.

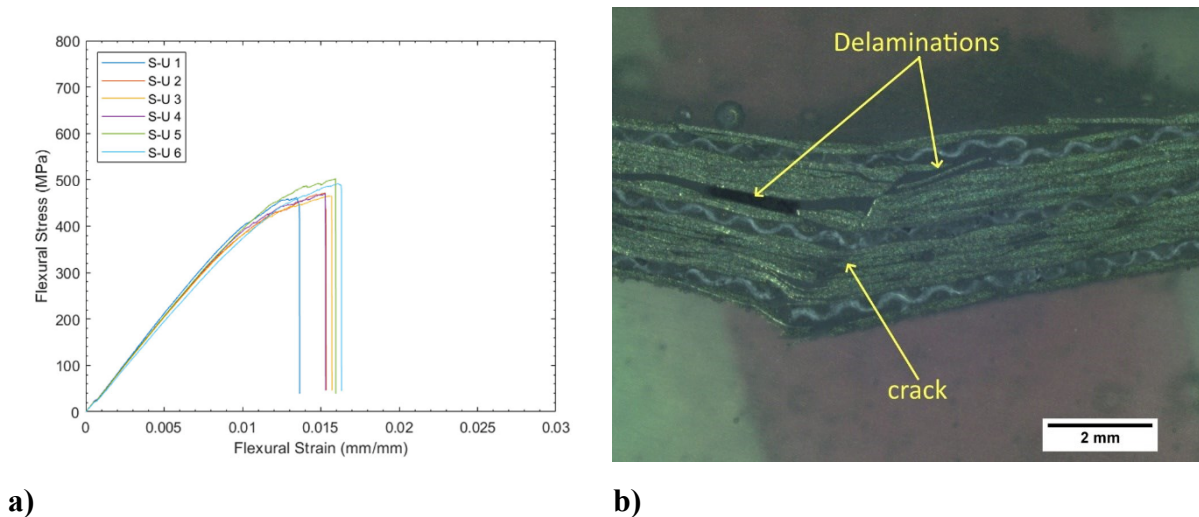


Fig.54: Flexural test on S-U configuration: flexural curves (a); failure zone microscope image (b).

The results from last configuration tested, i.e. uniform distribution of the hemp layers within the sample thickness (configuration S-U) are reported in fig.54. In this case, the hybrid material presents a behaviour which is very close to the one shown for the configuration A-HC and illustrated in fig.52a in terms of Flexural Modulus (40.36 GPa), flexural strength (471.38 MPa) and maximum strain (0.0155 mm/mm), showing a brittle behaviour with catastrophic failure after the critical stress is reached. Analysing the micrographies relative to these samples (see fig.54b), it is possible to observe that the presence of multiple carbon/hemp interfaces leads to a large number of delamination at different depths within the laminate and intralayer cracks that propagate from the compressive portion of the laminate to the bottom surface at 45 degrees resulting, in the catastrophic tensile failure of the bottom hemp layer and, consequently, of the entire sample.

4.3.2 ILSS tests

In order to evaluate the interlaminar shear strength of each sample type, three-point bending tests in short beam configurations were carried out using a universal testing machine (Instron 3369, fig.48) according to ASTM D2344 standard. Five specimens for each configuration were tested and the specimens size were chosen according to the above mentioned standard: 30 mm in length and 15 mm in width for carbon and hybrid composites specimens (C, A-CH, A-HC

and SU configuration) and 38 mm in length and 19 mm in width for hemp composites (H configuration).

All tests were carried with a traverse speed of 1 mm/min and a span to thickness ratio 5:1 was set in order to emphasise the shear contribution between the layers, then a span length depending on the type of sample was adopted: 15 mm in case of carbon and hybrid samples (C, A-CH, A-HC and SU configurations) and 19 mm in case of hemp composite (H configuration). Shear stress was evaluated by means of the eq. 28.

$$\tau = \frac{3}{4} \frac{F}{b S_c} \quad \text{eq. 28}$$

Where F is the load in (N), b is the width of the tested specimen in (mm), S_c is the thickness of the laminate in (mm).

It is not surprising that these two reference materials present a very different interlaminar behaviour, with a very brittle shear fracture for the carbon laminate and an almost flexural response of the hemp laminate, which is the only one that present a failure mechanism that seems to include flexural damage as it shows perpendicular cracks in the tension portion of the laminate (see fig.55).

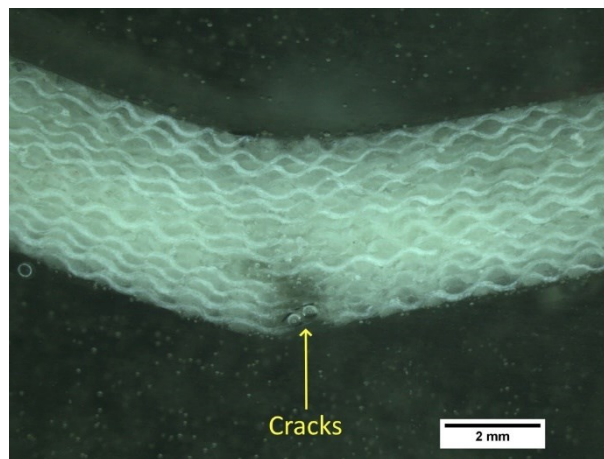


Fig.55: ILSS test on H configuration. Microscope image of the failure zone.

As for the carbon/hemp hybrid laminates, the curves relative to the ILSS tests are presented in fig.56 and show a shear behaviour which is very close to the one shown by the traditional carbon laminate (configuration C) for all the different samples, with a variation of the maximum shear strength which falls below 11%. The only hybrid configuration that shows a clear

difference from the carbon reference is the A-HC sample, that it is characterised by a lower value of ILSS (-23.9%).

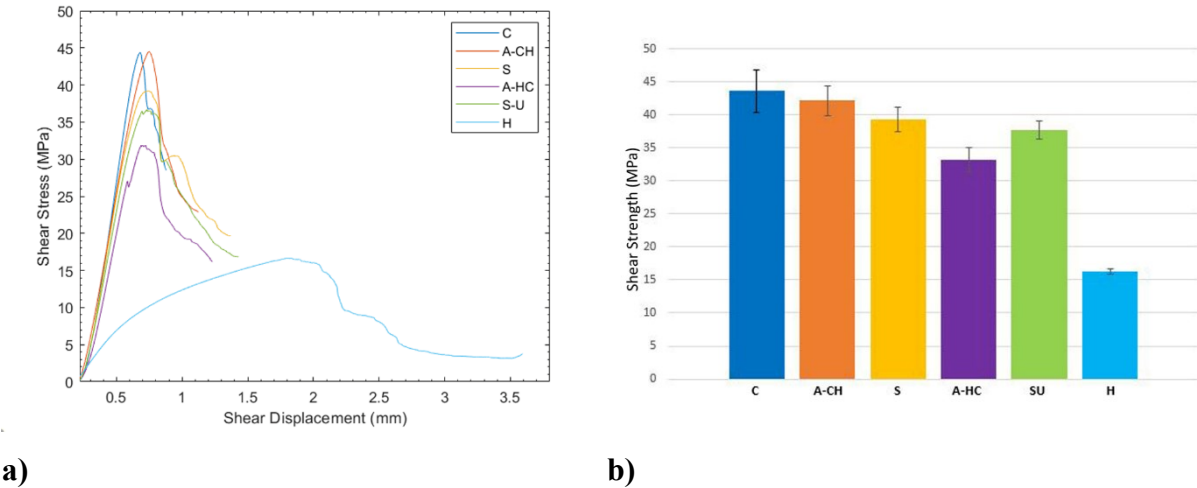


Fig.56: ILSS test on all configuration: Interlaminar shear stress curves (a); mean value of the shear strength (b).

Analysing the curves relative to this configuration (fig.57), it is possible to observe the presence of a double peak in three out of five curves which can be related with the opening of delamination at the interface between carbon and hemp before the critical collapse of the structure and observed during the flexural tests (see fig.57b).

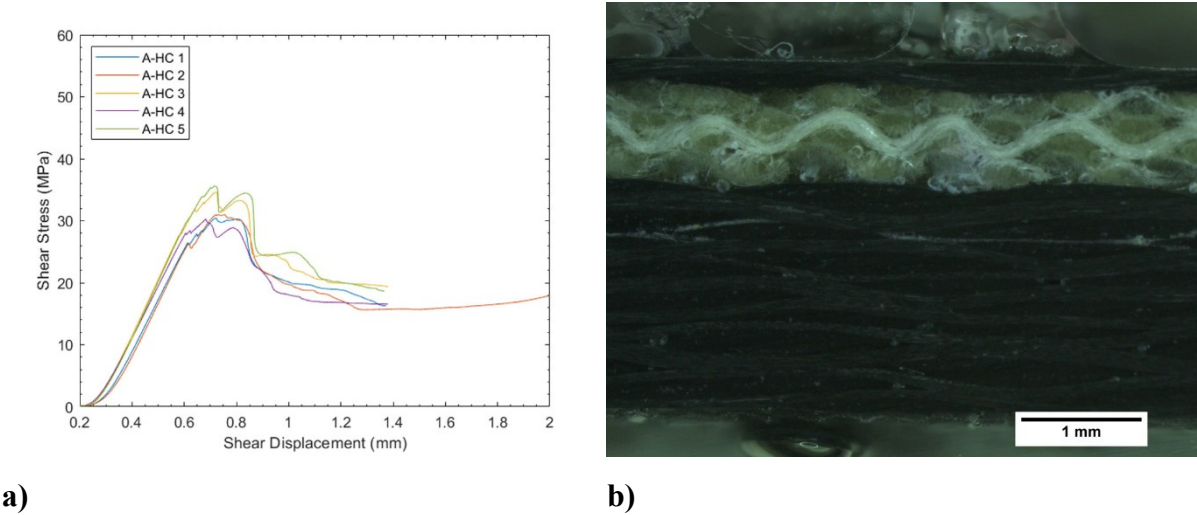


Fig.57: ILSS test A-HC configuration: interlaminar shear stress curves (a); microscope image of the tested specimen (b).

From these results, it is possible to conclude that the hybridisation process is able to modify the flexural response of the material by changing the failure mechanism mostly due to the combination between the brittle failure of carbon and the smoother, gradual deformation of the hemp fibres. It is possible to tune the flexural modulus, by keeping it very close to the one of pure carbon (by placing the hemp layers close to the neutral axis), or lower it by using an asymmetric hybrid configuration and, more importantly, it is possible to include additional energy dissipation mechanisms by adjusting the position of the hemp layers along the laminate's thickness in order to activate crack bending mechanisms. As for the ILSS, the shear behaviour of carbon is less affected by the presence of the natural fibres, however the A-HC configuration shows a decrease in shear strength due to the presence of large delamination at the carbon/hemp interface. In the following table are resumed the main results of the quasi-static characterisation by the comparison between references and hybrid composites.

Table 23: Main results of the quasi-static characterisation on the hybrid laminates

Configuration	$\Delta\%$ flexural strength	$\Delta\%$ flexural strain	$\Delta\%$ elastic modulus	$\Delta\%$ shear strength
S Vs C	-10,9	49,7	5,9	-9,7
H Vs C	-90,7	134,9	-89	-62,7
A-CH Vs C	-44,1	57	-38,3	-23,9
A-HC Vs C	-32,5	11,4	-49,5	-3,3
S-U Vs C	-32,7	4	-28,5	-13,5

4.3.3 Damping tests

In order to evaluate the energy absorption properties of the samples, damping tests were carried out. The damping test measures the attitude of the laminates to dissipate energy after an external excitation by evaluating the logarithmic decrement of the out of plane displacement during a free oscillation. The damping tests were performed for a total of 5 times for each sample typology.

A single cantilever configuration was considered, with all specimens (with a length of 100 mm and a width of 10 mm in order to obtain a slender beam) clamped at one end. A laser transducer ($\mu\epsilon$ optoNCD T2300) focused 5 mm far from the free edge were used to measure the time-domain oscillations of the specimen.

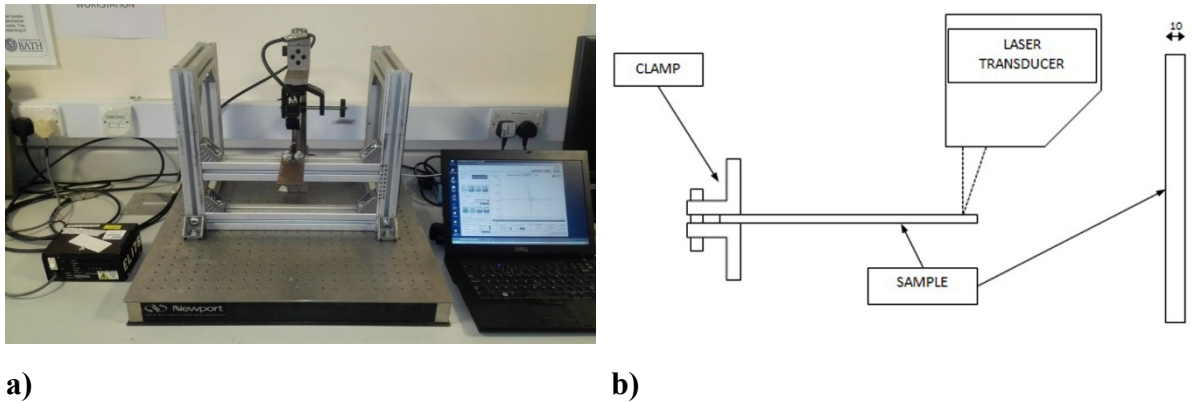


Fig.58: Damping test apparatus (a); schematisation of the experimental set-up (b).

Fig.58 shows the damping test apparatus (fig.58a) and the schematisation of the test set-up (fig.58b). A Matlab routine was written in order to acquire the time-domain signal, and then evaluate the logarithmic decrement δ and the damping ratio ζ . According to eq. 29, the logarithmic decrement can be expressed as:

$$\delta = \frac{1}{n} \ln \frac{A_i}{A_{i+n}} \quad \text{eq. 29}$$

where n is the number of peaks taken into account for the logarithmic decrement evaluation, A_i is the amplitude of the i -th oscillation and A_{i+n} is the amplitude of successive peaks. The damping ratio was then evaluated according to eq. 30.

$$\zeta = \frac{1}{\sqrt{1 + \left(\frac{2\pi}{\delta}\right)^2}} \quad \text{eq. 30}$$

Principal aim of the tests was to analyse how the different stacking sequences and materials affect the energy dissipation attitude of the laminates.

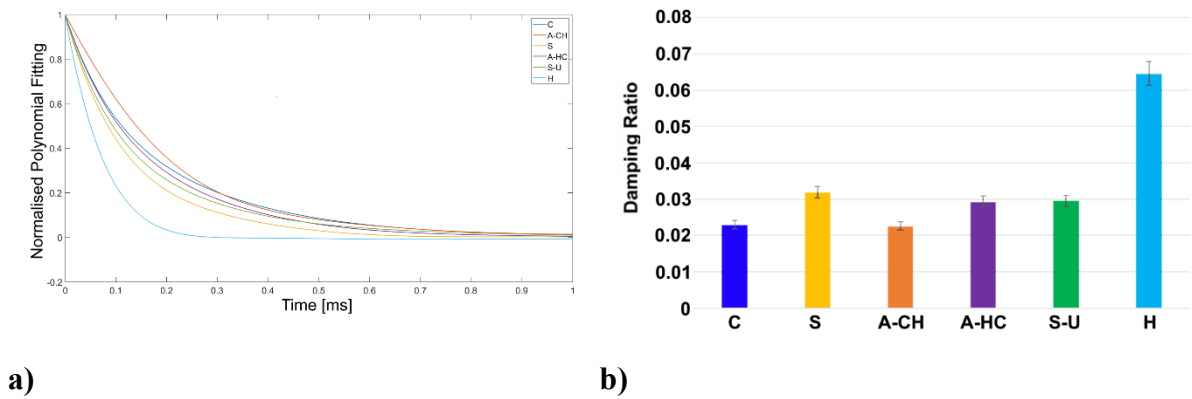


Fig.59: Logarithmic decrement curves (a); damping ratio chart (b).

Fig.59a shows the logarithmic decrement curves carried out from the damping tests. Analysing these results, it is possible to conclude that the introduction of the hemp layer in the CFRP laminate leads to an increase of damping properties in comparison with traditional Carbon laminates (C configuration). Indeed, excluding A-CH type samples which showed the same trend of the control configuration C type, the damping ratio histograms (fig.59b) showed an increase in absorption performance. S type showed an interesting behaviour that was between C and H sample type. It was possible to appreciate this behaviour even in the logarithmic decrement plot (fig.59a), where the S type is clearly in the middle between C and H sample type.

It is well known from literature, that in order to increase the absorption performance of a composite material by mean interleaving or hybridisation, the best configuration is the one with a layer in the middle plane of the laminate [9]. Damping tests were in good accordance with this, with the highest absorption shown by the S configuration (+40%). The principal drawback of such configuration is that the highest shear stresses are in correspondence of the interfaces between hemp and CFRP, with possible weakness towards onset delamination (S-U type is affected by the same issue).

A possible solution, considering the other configuration tested, was given by the A-HC samples with the hemp layer located on the top surface. This configuration showed increased damping properties (+28%), not too far from the S type, with a similar increase of the SU type (+29%) compared to the control configuration C type.

4.3.4 Impact tests and internal damage detection

Impact tests were carried out using a home-made falling drop weight machine, equipped with an impactor tip of 16 mm diameter and an impactor mass of 2.66 kg (the experimental set-up is reported in fig.34). Moreover, in order to avoid possible further impacts, the impactor rig is equipped with an anti-rebound system that hold the shuttle after the first impact. The impact tests were performed according to ASTM D7136 standard.

The impacts were carried out on a total number of 5 specimens for each sample typology. Rectangular specimens 100 mm x 150 mm in dimension were cut according to the ASTM standard and clamped between two steel plates using bold serrated by hand in order to avoid any movement of the samples.

All tests were carried out keeping constant the impactor mass at 2.66kg and three different impact energy levels were chosen in this experimental campaign: 5J, 10J and 20J obtained by varying the impactor height.

Non-destructive tests were carried out using a Phased array transducer. In order to focalise the ultrasound waves generated by the array, the transducer was coupled with a delay line 30 mm thick, then the assembly was coupled with the specimen under inspection, using an ultrasonic gel in order to avoid the acoustic impedance mismatch between the air and the specimen and then facilitate the ultrasound waves propagation fig.60.

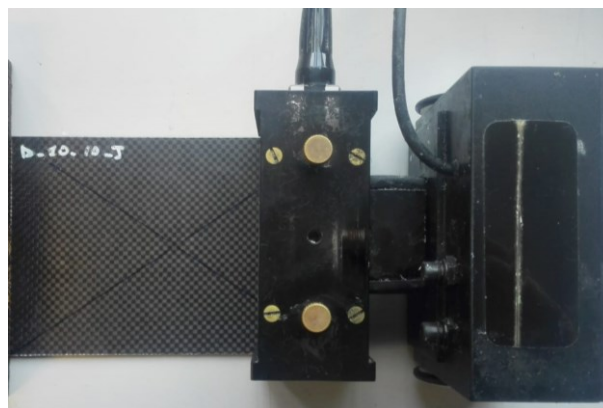


Fig.60: Non-destructive test, Phased array apparatus.

Since in this experimental campaign hybrid laminates are studied; an issue is related with the choice of the acoustic impedance because two different fibre typologies with two different speeds of sound are coupled. The acoustic impedance was evaluated using the eq. 31.

$$Z = C_0\rho \quad \text{eq.31}$$

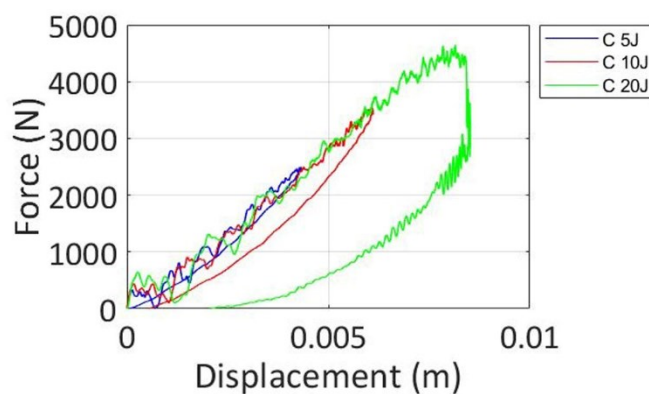
Where C_0 is the speed of sound of the material under inspection in (m/s), ρ is the density in (g/cm^3).

By using the above equation, it was found that the two acoustic impedances are similar in a range of 5700 – 6000 (MRayls), this aspect means a good wave propagation within the thickness, and then a non-appreciable wave propagation mismatch through the two materials [10].

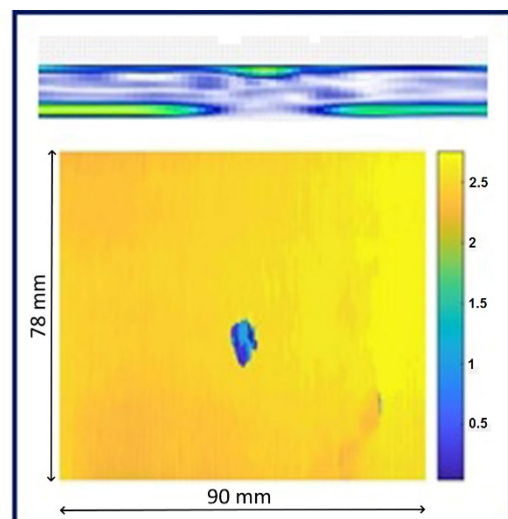
For the experimental set-up, the Phased Array was positioned on the specimen and coupled with a wheel encoder in order to acquire a C-Scan image. The assembly was connected to a PC and the data were acquired and processed using a DSLFIT focus stream software.

Two outputs are obtained from the data processing, with more detail a B-Scan which shows the cross section of the specimen permitting the damage location through the thickness, a C-Scan that is a top surface of the sample that leads to the damage extension and depth evaluation.

Moreover, using the IMAGE J software, the carbon/hemp surface interfaces were found starting from the cross sections of the resin cast samples. Then, with the same technique, the damaged regions were individualised from the B-Scan. These results were confirmed by the colour bar of the C-Scan images, in this way was possible to have a better interpretation of the failure mechanism of all sample typologies.



a)



b)

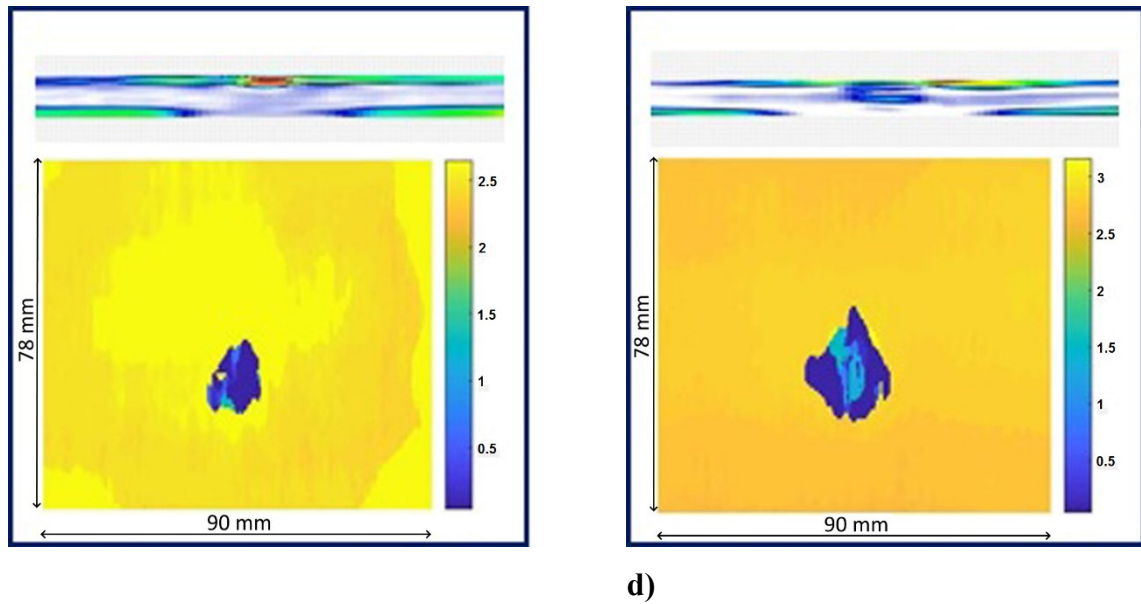


Fig.61: Impact test on C configuration: force-displacement curves (a); B-Scan and C-Scan 5J (b); B-Scan and C-Scan 10J (c); B-Scan and C-Scan 20J (d).

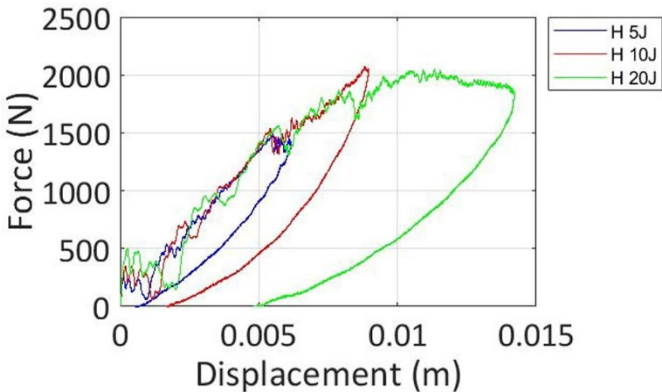
Fig.61a illustrates the force displacement curves obtained from the impact tests on the carbon control sample (C configuration) at the three different energies of 5, 10 and 20J and shows the typical behaviour of a traditional composite samples subjected to low velocity impact (LVI) [11]. Indeed, analysing the curves for the 5 and 10J, it is possible to observe that the samples show an almost completely elastic behaviour with a very small area in the force-displacement curves that suggests that the majority of the impact energy is given back to the impactor during the rebound of the shuttle. This result confirms what observed in the trend of the absorbed energy, E_a , and return coefficient, RC , values listed in Table 24.

Table 24: Impact results of configuration C at the end of the test

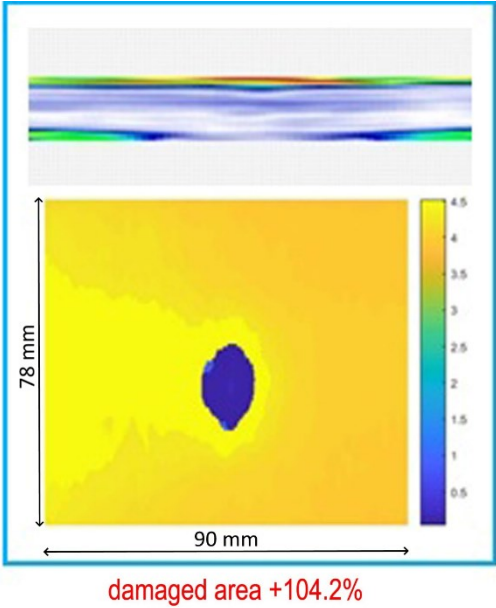
E_i [J]	F [N]	E_a [J]	RC [J/J]
5	2492.7	0.69	0.862
10	3554.7	2.72	0.727
20	4713.1	13.54	0.323

In the table it is also reported the peak load, F , detected for each level of impact energy, E_i . The return coefficient was defined as the ratio between the difference of the impact and absorbed energy ($E_i - E_a$) and the impact ones (E_i).

When the impact energy is raised to 20J, it is possible to observe a sharp drop in the force-displacement curve which corresponds with the growth and propagation of internal damage in the compressive portion of the laminate, which is similar to what observed during the flexural tests. In order to correlate the information from the LVI with an assessment of the structural integrity of the sample fig.61b, c and d show the extent of the internal delamination of the impacted samples for the three energy levels. As it is possible to see from the images, even though the curves did not show any evident sign of internal damage, both 5J and 10J images are indeed damaged, showing signs of a delaminated area which increases with the increase of the impact energy and it is positioned in the layers underneath the impact location (i.e. compressive portion). Raising the energy to 20J leads to a large damage, increasing the defective area by more than seven times (755.7%) in comparison with the 5J impact, confirming the brittle behaviour of traditional CFRP (C configuration).



a)



b)

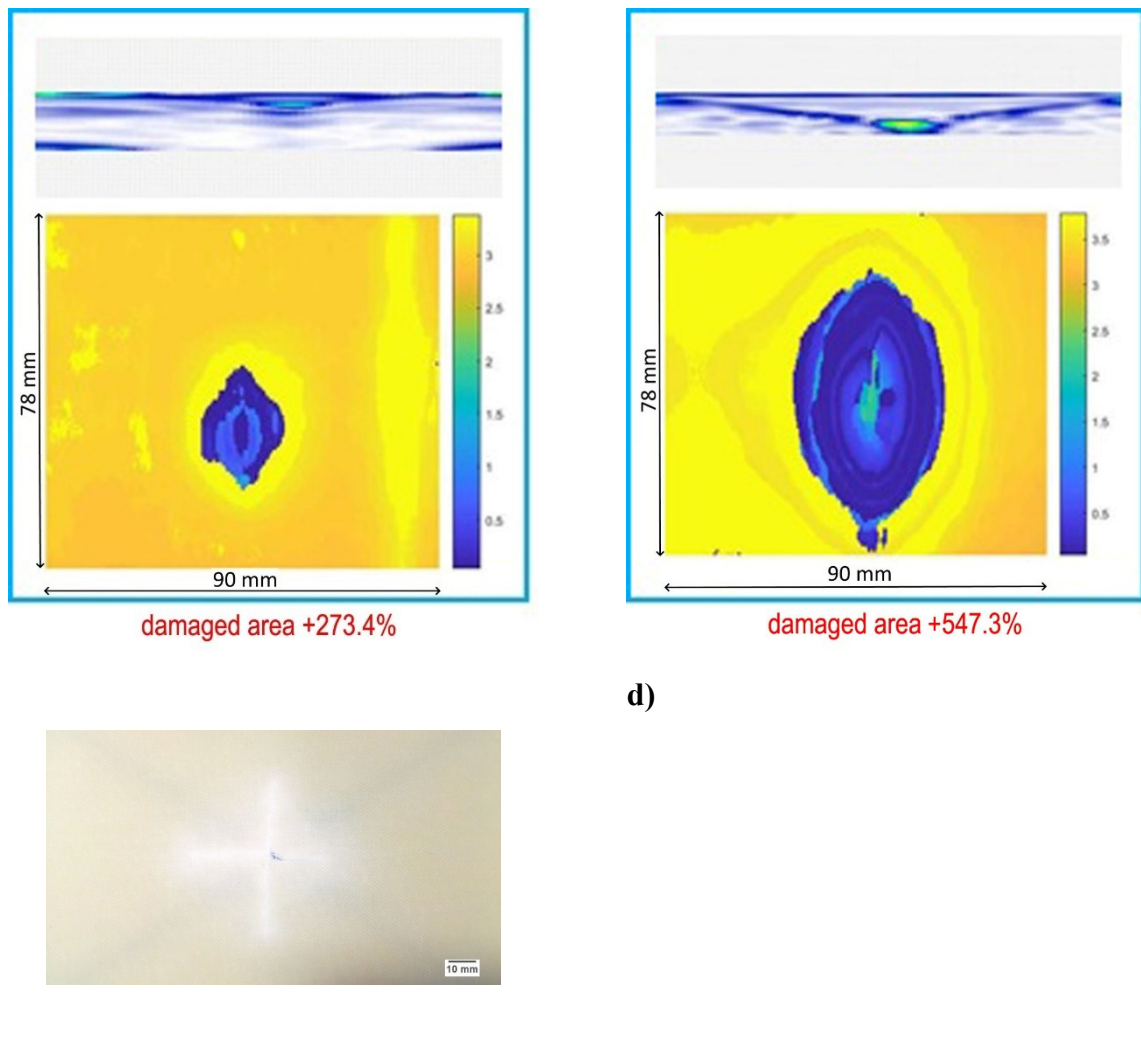


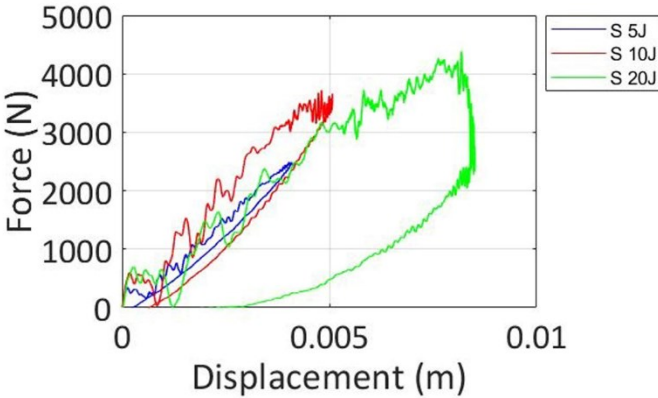
Fig.62: Impact test on H configuration: force-displacement curves (a); B-Scan and C-Scan 5J (b); B-Scan and C-Scan 10J (c); B-Scan and C-Scan 20J (d); impacted H configuration specimen (e).

Fig.62 illustrates the force displacement curves obtained from the impact tests on the hemp control sample (H configuration) at the three different energies of 5, 10 and 20J and Table 25 summarises the main results.

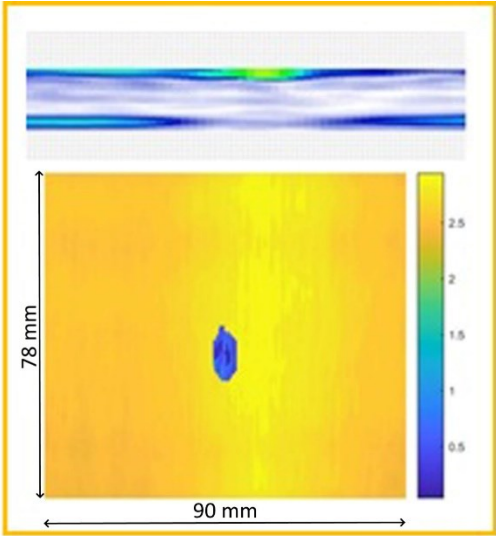
Table 25: Impact results of configuration H at the end of the test

E_i [J]	F [N]	E_a [J]	RC [J/J]
5	1544.4	1.99	0.602
10	1933.8	5.62	0.438
20	2090.4	14.64	0.268

While sample C showed a typical brittle response, the results from the hemp laminates (H sample type) indicate a typical ductile behaviour, showing lower values of the peak forces for all the tested energies (-38%, -45.6% and -55.6% in comparison with configuration C) and larger displacements (+27.7%, +39.2% and +36.7%) and contact time. This behaviour can be explained considering the very high damping characteristic of the hemp fibres which are given by their higher strain to failure in comparison with carbon fibres [12] together with fibres pull out phenomena resulting in a permanent plastic deformation of the laminate which is associated with a higher energy absorption for the 5J and 10J impacts (+188.8%, +106.6%). When the impact energy is raised to 20J, this difference starts to become less consistent (+8.1%) due to the brittle failure of the C samples which allows the CFRP to absorb more energy via the creation of fibre damage and the propagation of multiple cracks. Analysing the internal state of the laminate with the Phased Array images (fig.62b, c, d), it is also possible to observe a very large delaminated area (+104.2% and +273.4% for 5 and 10J in comparison with the carbon laminates) which becomes macroscopically visible at 20J (see fig.62e).



a)



damaged area +83.9%

b)

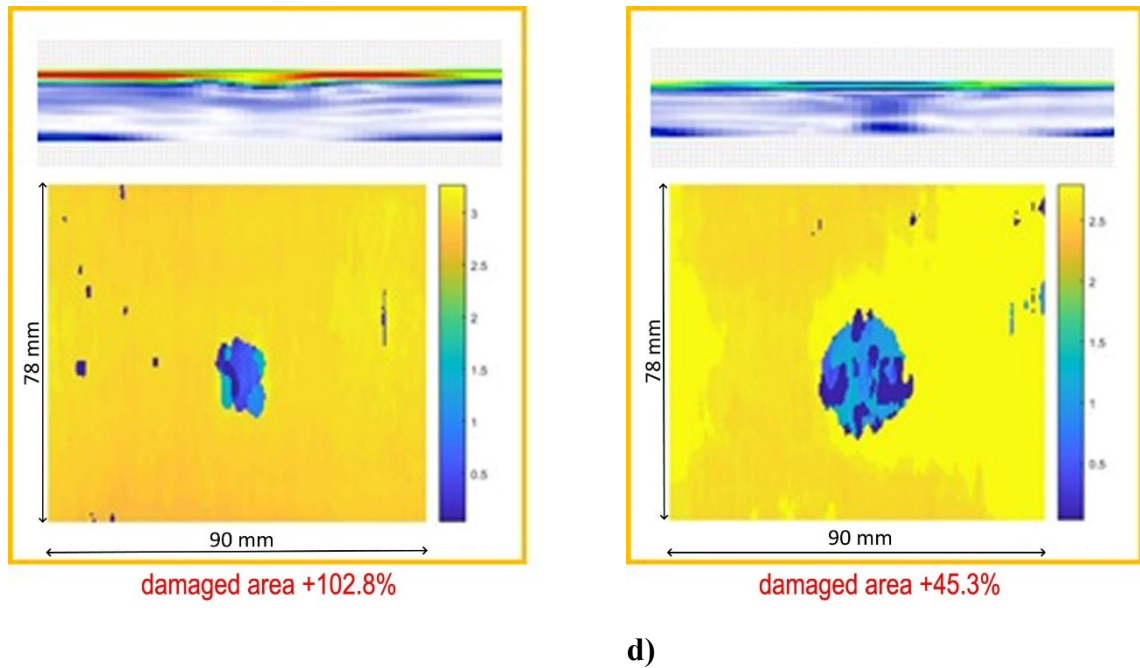


Fig.63: Impact test on S configuration: force-displacement curves (a); B-Scan and C-Scan 5J (b); B-Scan and C-Scan 10J (c); B-Scan and C-Scan 20J (d).

As for the hybrid laminates, fig.63a illustrates the results obtained for the symmetric samples (configuration S) together with the analysis of the internal damaged areas recorded after the impact tests (fig.63b, c, d). As it is possible to see from the curves (fig.63a) and from the phased array images (fig.63b, c, d), all the impacts resulted in an internal delamination whose extent increased with the impact energy. As already mentioned in the discussion relative to the flexural analysis, the presence of the hemp layers at the midplane does not affect the elasticity of the laminate, which follows the same trend observed for the configuration S in its initial linear response. However, when the critical load is reached, the presence of the hemp layers changes the response of the material, leading to larger damage growth at both the interfaces between carbon and hemp. In particular, while for the impact at 5J all the damage is limited at the upper interface (compressive portion, see fig.63b), when the energy is raised to 10J, cracks start to propagate from the bottom interface (see fig.63c), leading to carbon fibre damage in the tensile portion of the laminate when the impact energy is raised up to 20J (see fig.63d).

Table 26: Impact results of configuration S at the end of the test

E_i [J]	F [N]	E_a [J]	RC [J/J]
5	2540.2	0.83	0.835
10	3745.9	3.77	0.623
20	4439	14.77	0.261

Looking at Table 26, it is possible to note that, the above said mechanism translates into larger energy absorption if compared with traditional carbon laminates (configuration C) with increases equal to +19.8%, +38.6% and +9.1% for 5,10 and 20J respectively, but it must be considered that this additional energy absorption mechanism leads to internal damaged areas with an increase equal to +83.9%, +102.8% and +45.3%, respect to configuration C, lowering the residual properties of the laminate.

The response of sample A-CH to LVI is illustrated in fig.64 and summarised in table 27.

Table 27: Impact results of configuration A-CH at the end of the test

E_i [J]	F [N]	E_a [J]	RC [J/J]
5	2371.8	0.98	0.803
10	3200.3	3.53	0.647
20	4381.7	13.53	0.323

As already discussed in the previous sections, placing the hemp layers in an asymmetrical configuration affects the failure method of the laminate, especially in the case of large deformations. Analysing the force-displacement curves (fig.64a), it is possible to see that, similarly to what observed during the flexural tests, this configuration presents a slight decrease in terms of peak force (-4.8%, -9.9% and -7%) and a slight but consistent increase in the maximum displacement (+2.5%, +2.6% and +4.3%). However, unlike the flexural case, in this case the presence of the hemp layer allows for an additional dissipation mechanism which is caused by the accumulation of damage at the carbon/hemp interface, leading to similar values to those of configuration C for all the energetic levels. In terms of failure mode, the analysis of the B-Scan (see fig.64b) shows that for the 5 J impact the damage is concentrated on the bottom portion of the laminate, showing a small delamination at the lower interface with some fibre

damage in the last carbon ply (see fig.64b). When the energy is raised to 10 J, the damage keeps accumulating at the interface and a large delamination starts growing, leading to an abrupt increase in the damage extension (see fig.64c). The accumulation of damage reaches critical levels for the 20 J impact (see fig.64d), leading to fibre damage at the lower interface with a visible bump on the bottom surface as shown in fig.64c.

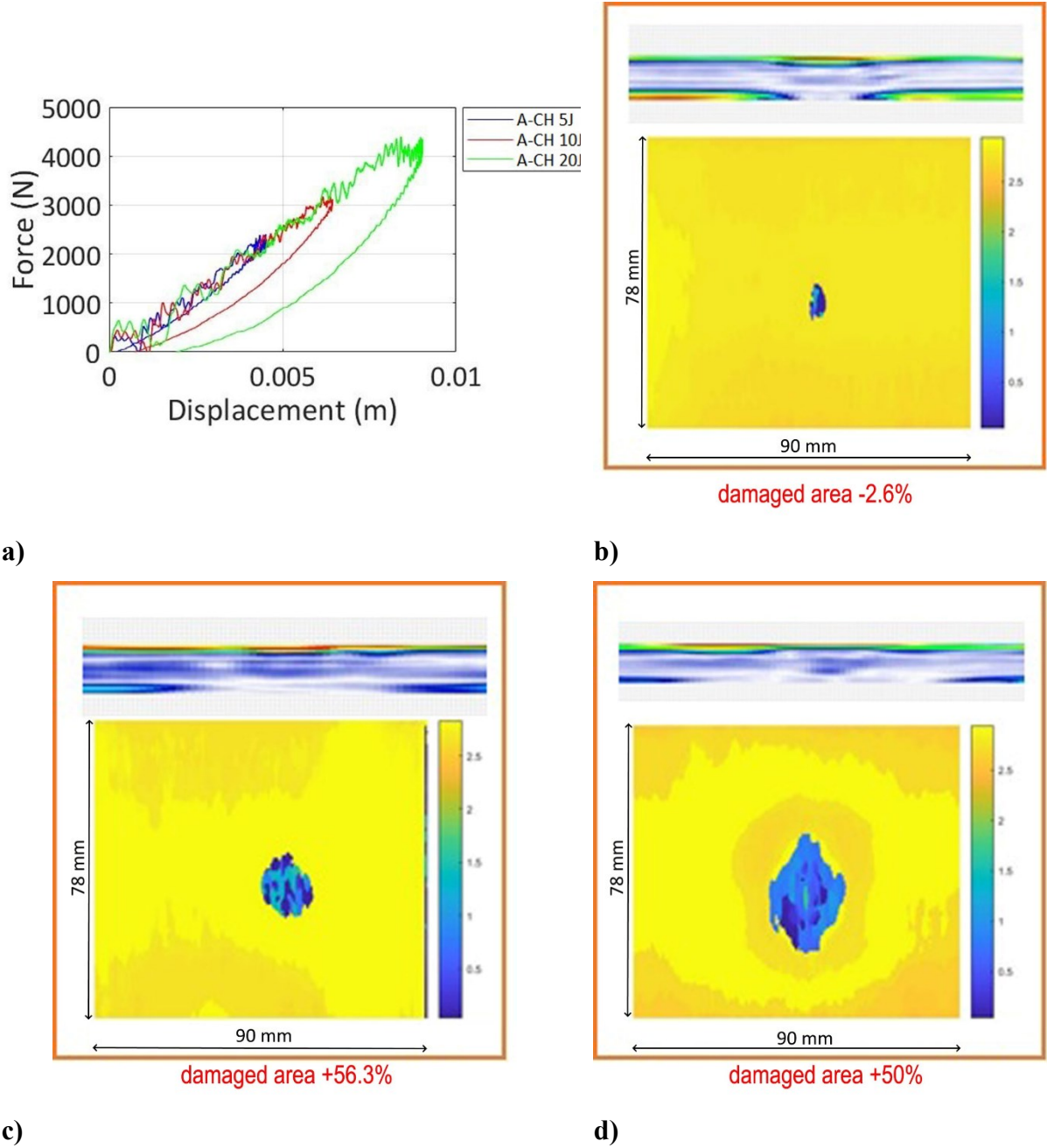


Fig.64: Impact test on A-CH configuration: force-displacement curves (a); B-Scan and C-Scan 5J (b); B-Scan and C-Scan 10J (c); B-Scan and C-Scan 20J (d).

As discussed for the flexural behaviour, also for the impact behaviour the asymmetric configuration gives a different response when the hemp layers are positioned in the compression region (configuration A-HC). The results are reported in fig.65 and Table 28.

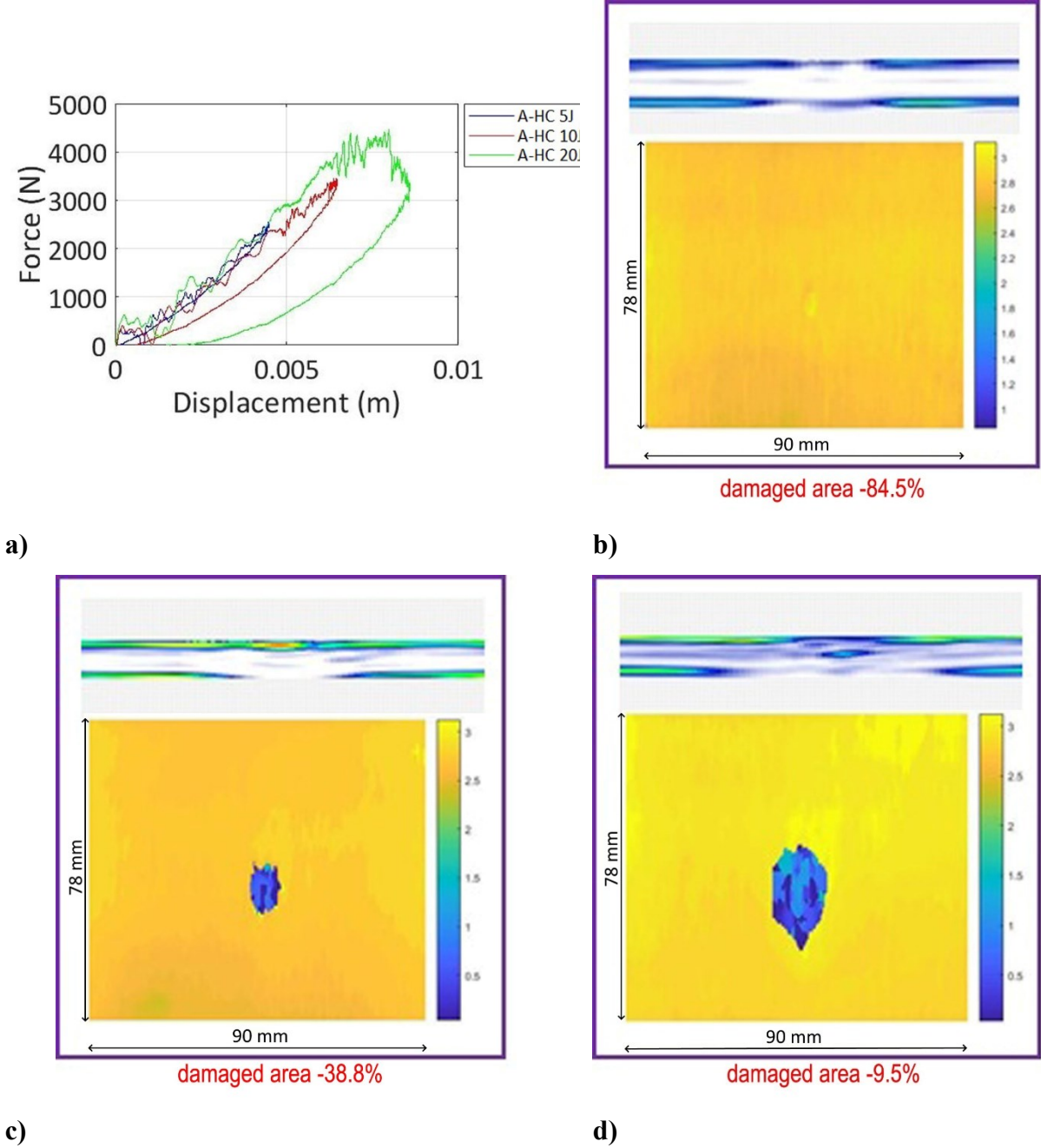


Fig.65: Impact test on A-HC configuration: force-displacement curves (a); B-Scan and C-Scan 5J (b); B-Scan and C-Scan 10J (c); B-Scan and C-Scan 20J (d).

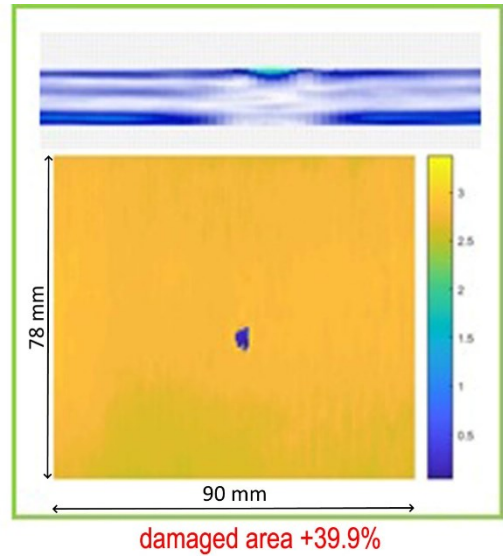
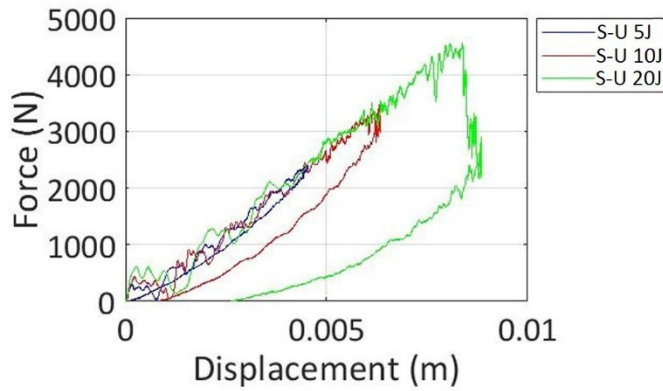
Table 28: Impact results of configuration A-HC at the end of the test

E_i [J]	F [N]	E_a [J]	RC [J/J]
5	2494.3	0.59	0.882
10	3510.6	2.79	0.720
20	4404.2	13.01	0.349

In particular, in this case it is possible to observe that the presence of the more ductile material in the proximity of the impact location allows for the larger deformation of the area surrounding the contact zone which translates with a more efficient energy transfer between the penetrator tip and the laminate. This mechanism leads to the absorption of a consistent portion of the impact energy in the deformation of the hemp layers thanks to their improved damping characteristics which, in turn, reduces the extent of the internal damage for all the tested energies. This behaviour is particularly evident looking at fig.65b where the Phased array images are reported. From these, it is possible to observe the absence of any kind of damage for the 5J impact and just a small delamination for both the 10J and 20 J impacts which accounts to -38.8% and -9.5% in comparison with the traditional carbon laminate.

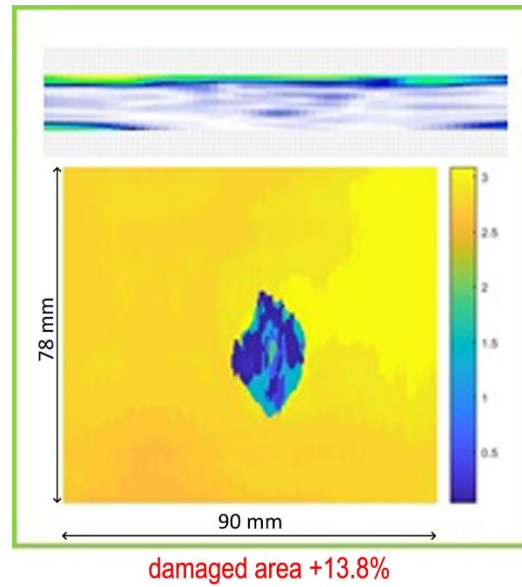
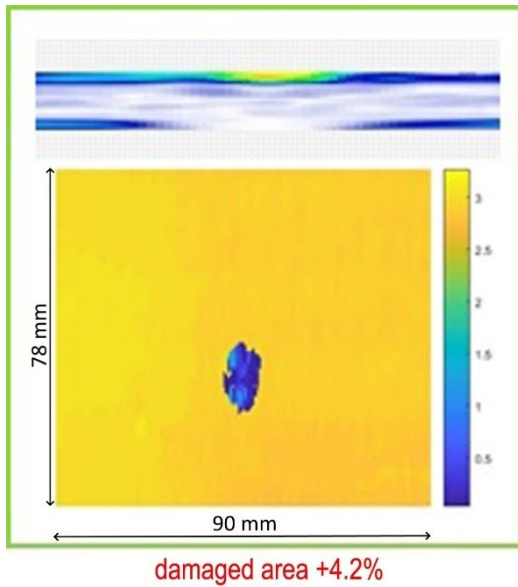
Based on the results observed for both the symmetric and asymmetric configurations, it appears clear that the presence of the carbon/hemp interface modifies the behaviour of the hybrid laminate, allowing for different energy dissipation mechanisms (larger energy absorption associated with larger delamination at the interface or constant energy absorption associated with smaller delamination) which can be tuned according to the relative position between the carbon and hemp layers. Similar results can be found in literature for hybrid aramid/glass laminates, for which it was observed that when the more ductile aramid layer is positioned at the front surface (similar to the configuration A-HC), a portion of impact energy is dissipated via plastic deformation of the aramid, while when the glass is placed on the impact surface (similar to configuration CH) the stiffness of the top layer leads to a reduction in the energy absorbed by local deformation and consequently in a more brittle fracture [13].

In this context, it is of particular interest to analyse the results obtained from samples S-U which present more interfaces since the three layers of hemp are uniformly distributed along the laminate's thickness rather than concentrated in a single portion as in configuration S, A-CH and A-HC.



a)

b)



c)

d)

Fig.66: Impact test on S-U configuration: force-displacement curves (a); B-Scan and C-Scan 5J (b); B-Scan and C-Scan 10J (c); B-Scan and C-Scan 20J (d).

Analysing the curves (fig.66a) and the phased array images (fig.66b, c, d) together with the data reported in Table 29, it is possible to observe that for the 5 J impact the amount of energy absorbed is very close to the one of the traditional carbon laminates and the damage is mostly concentrated in the bottom interface of the first layer of hemp, located in the tensile portion of the laminate.

Table 29: Impact results of configuration S-U at the end of the test

E_i [J]	F [N]	E_a [J]	RC [J/J]
5	2410.9	0.71	0.858
10	3335.8	3.27	0.673
20	4517.2	11.72	0.414

Increasing the impact energy to 10 J, the mechanism observed previously (a single delamination in correspondence with the hemp layer as observed for example in the configuration A-HC) loses its efficiency and part of the energy is transferred through the thickness and concentrates at the top interface of the second and third hemp layers. The importance of the role of the interface in hybrid laminates is in line with what observed by Nisini et al on their work on carbon/flax/basalt laminates [14]. When the energy is raised to 20 J the hemp layers are not able to dissipate the impact energy and part of the energy is spent to grow additional damage in the carbon portion underneath the third hemp layer, causing fibre damage with the relative loss of structural integrity.

4.4 Part 5: Tribological behaviour of hemp fibres

In this section, three different fibre typologies were used. In detail hemp, carbon and glass fibres composites were produced instead of hybrid hemp/carbon composite materials, in order to evaluate the wear behaviour of natural fibres compared to that of traditional composite materials.

4.4.1 Indentation tests

For each sample typology, indentation tests were preliminary carried out in order to evaluate the elastic behaviour of the sample surfaces. In these tests, a martensitic stainless-steel AISI 440C ball, 8 mm in diameter, (its properties are listed in table 30) was pressed against the sample surface with a crosshead speed of 0.5 mm/min at room temperature by means of a universal testing machine (MTS alliance RT/50). Each specimen was supported from a rigid

steel plate end each test was repeated three times. So, three laminates for type of composite were manufactured.

Table 30: Indenter Properties

Stainless steel AISI 440C				
Density [g/cm³]	Tensile Strength [MPa]	Young Module [GPa]	Rockwell Hardness	Roughness R_a [μm]
7,70	1900 – 2000	210	57 – 60	0,01 – 0,15

The choice in the use of a ball (8 mm in diameter) as indenter tool was to ensure the same contact conditions that characterised the tribological tests carried out in this experimental campaign.

No significative differences between experimental indentation curves of the specimens of the same sample type were observed, this validate the reproducibility of test results. Therefore, fig.67 presents the typical load versus displacement of indentation curves for each sample type. For each sample type, the typical curve plotted in fig.67 represents the intermediate curve between three obtained from three specimens of the same type.

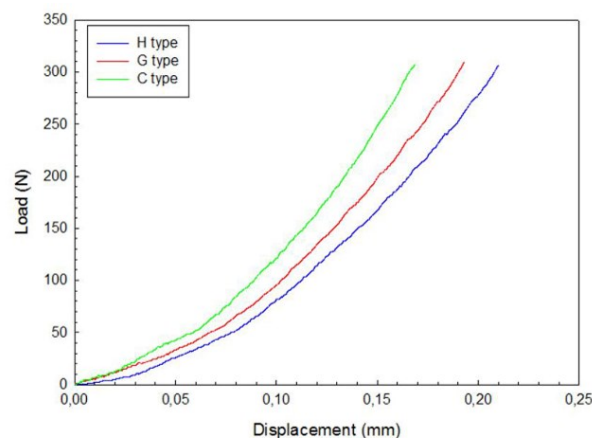


Fig.67: Typical indentation load versus displacement curves of each sample type.

From the results, it is clear that the hemp type is characterised by a softer behaviour than the others. The hemp fabric shows a lower out of plane rigidity (due to the hemp fibres properties) and this involves in a greater tendency to accommodate the deformation induced by the pin.

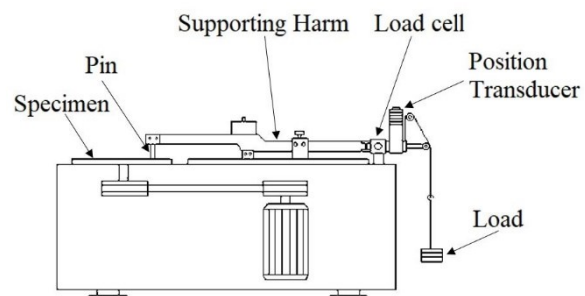
This consideration will be useful for the next sections, when the results of the tribological tests will be illustrated.

4.4.2 Tribological tests

The tribological behaviour was evaluated by using a pin-on-disk apparatus (Ducom TR20-LE) at room temperature according to ASTM G99–95a standard. The apparatus consists of a rotating disk, a pin holder, a loading rig and a measuring equipment for friction force and wear depth (fig.68) [15]. During the test, a fixed steel ball (8 mm in diameter) was used as pin and pressed against the rotating specimen under a fixed normal load of 10, 20, 50 and 70 N. The friction force and the wear depth were continuously measured during the sliding time by the measuring equipment of the Ducom TR20-LE.



a)



b)

Fig.68: Ducom TR20-LE machine (a) tribological test schematisation (b).

All tribological tests were conducted at established constant peripheral speed of 210 mm/s by varying the applied load and the track radius (20, 24, 28, 32 mm), as listed in table 31. The sliding speed value was chosen considering that the application of carbon or glass and especially hemp composites is not for kinematic couples (as bearing), so it was chosen a value of the sliding speed adequate to simulate the velocity of an accidental contact with a rigid body as the rubbing at which an interior component made in composite material, for example, can be subjected. In addition, by using a pyrometer to measure the temperature in the contact point

between pin and laminate, it was revealed that the sliding speed of 210 mm/s allowed the reaching of a temperature always lower than 50°C (T_g of resin is 80°C), therefore the effect of the temperature on the matrix properties can be considered negligible. The rotation speed of the disk and the test time was chosen to ensure that for each track radius the total number of revolutions is the same.

At the end of tribological tests, each wear track was observed by means of a stereomicroscope (OLYMPUS SZ60 - PT) to have its global view and an optical microscope with a greater magnification (ZEISS AxiosKop 40) in order to obtain a more detailed track visual.

Table 31: Pin-on-disk test conditions

Experimental Conditions	Sample Type											
	H Type				C Type				G Type			
Applied Load [N]	10	20	50	70	10	20	50	70	10	20	50	70
Wear track radius [mm]	20	24	28	32	20	24	28	32	20	24	28	32
Time [min]	96	115	134	153	96	115	134	153	96	115	134	153

Figs.69-72 show typical curves of the wear depth and the dynamic coefficient of friction versus the number of revolutions for all the load conditions under investigation and for each sample type. The dynamic coefficient of friction was determined as the ratio between the measured friction force and the applied normal load. Also for this test, for each sample type, the typical curves plotted in figs. 66-69 represent the intermediate curve between three obtained from three specimens of the same type.

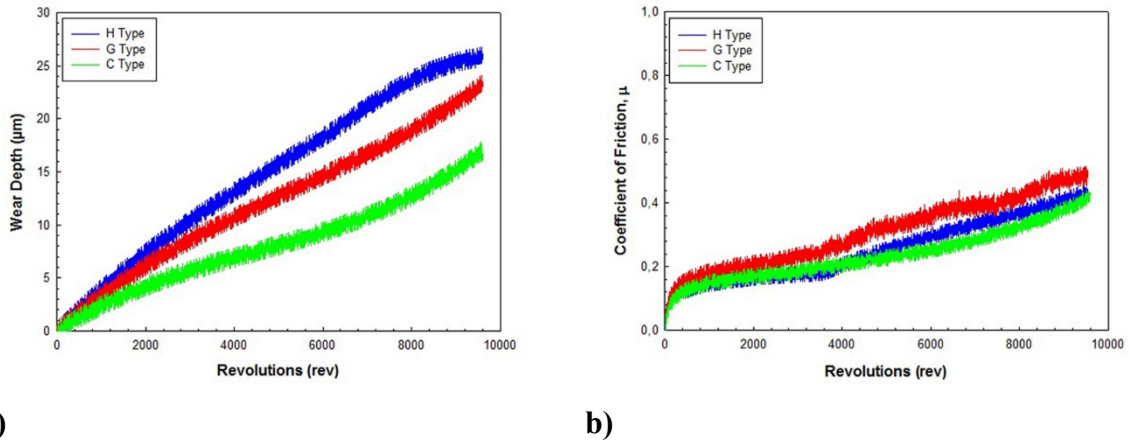


Fig.69: Wear depth (a) and friction coefficient (b) vs number of revolutions under a normal load of 10 N.

Concerning the wear depth trend, all the curves of the test carried out with a load of 10 N (fig.69a), show a similar behaviour especially in the initial tract (short-time). Under this low load and short sliding time condition the wear response was given from the resin, as confirmed from the similar trends of the coefficients of friction showed fig.69b. This means that under a load of 10 N the tribological behaviour was mainly given by the matrix that was the same for each typology.

However, looking at fig.69a the hemp composite type possess a slightly worse wear behaviour than the others due to a lower rigidity that characterised this sample type, as evidenced in fig.67. The upper surface of each specimen is mainly constituted by resin and then only after the removal of the resin layer, the wear behaviour change because the fibres begin to manifest its effects on the sliding contact conditions with the pin. Indeed, the final slope of the curves is positive for both glass and carbon composite instead of the one observed for the hemp composite that is almost zero; this might suggest that as the sliding time or the test load increases the trends of the wear depth could be inverted.

Indeed, looking at fig.70, when a higher load was used (20 N) and the sample started to show a major wear depth damage, the fibre type begins to manifest its tribological effect. In particular, the glass fibres highlighted a very lower wear resistance than the others and its coefficient of friction curve become to differ from the others (fig.70b).

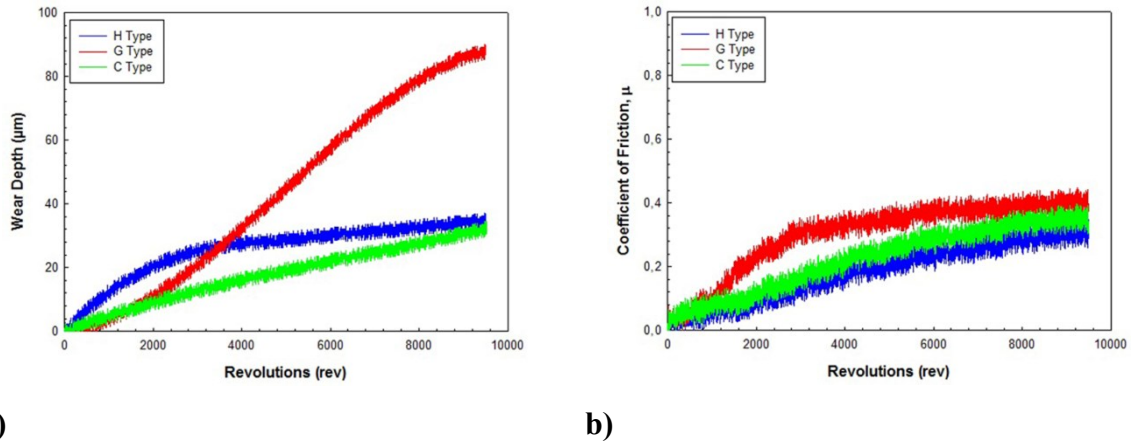
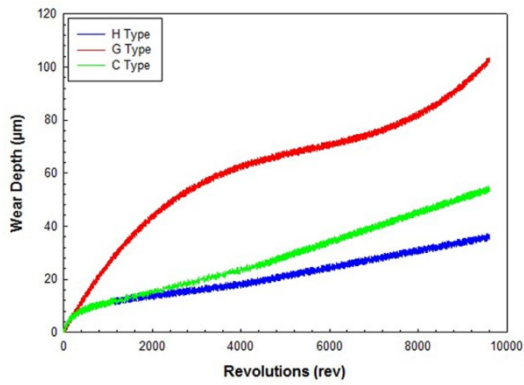
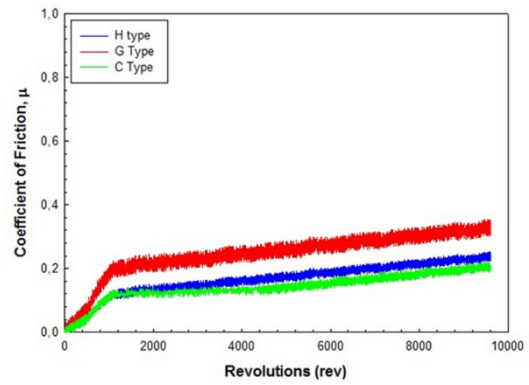


Fig.70: Wear depth (a) and friction coefficient (b) vs number of revolutions under a normal load of 20 N.

Looking at fig.70a, when a normal load equal to 20 N was used, the H type starts to show its interesting behaviour over the G type and its curve tends to the one of the C type. In particular, under a load of 20 N, it is possible to observe that the carbon and natural type curves show a similar trend instead of the one of the glass type. Therefore, respect to the previous conditions (10 N) it is possible to highlight two main curve behaviour blocks: one showed from the glass type and another showed from the carbon and hemp composite type. This difference, is more evident as the normal load increases, as shown in figs.71 and 72. In both cases the glass types showed the worst wear behaviour and its curves are characterised by the higher wear depth and coefficient of friction values. It is also interesting to note that despite the previous load conditions, as the load increases (see figs.71 a and 72a) the wear depth curves of the carbon and hemp composites type are perfectly superimposed up to around 1200 revolutions (211,0 and 241,1 m for 50 N and 70 N respectively), after this point the curve of the H type emphasised its better wear behaviour.



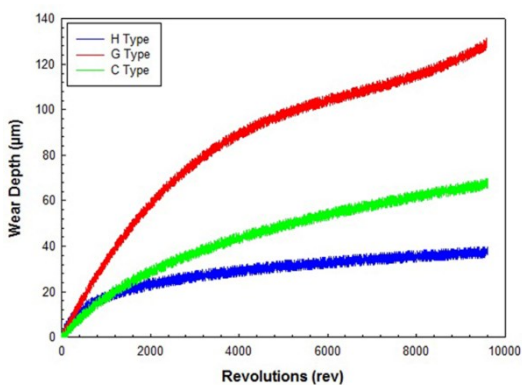
a)



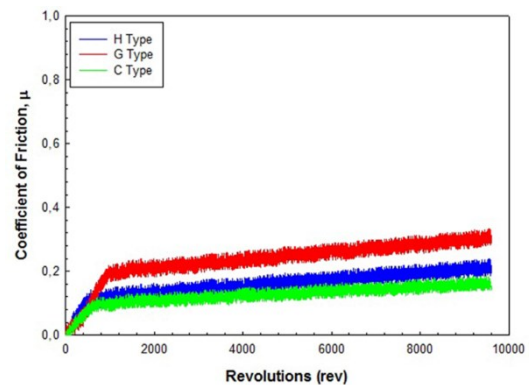
b)

Fig.71: Wear depth (a) and friction coefficient (b) vs number of revolutions under a normal load of 50 N.

The advantage in the use of hemp composites in long time conditions is also clear looking at fig.72, where the curves concerning the tribological tests carried out with a normal load of 70 N are reported. Indeed, both the glass and carbon type curves show a final positive slope instead of the curves of the H type that has got a zero slope in the final tract. This means that predictably as the test time will increase, the wear depth will further increase for the glass and carbon composite type instead of the one of the hemp type that tends to keep its constant value.



a)



b)

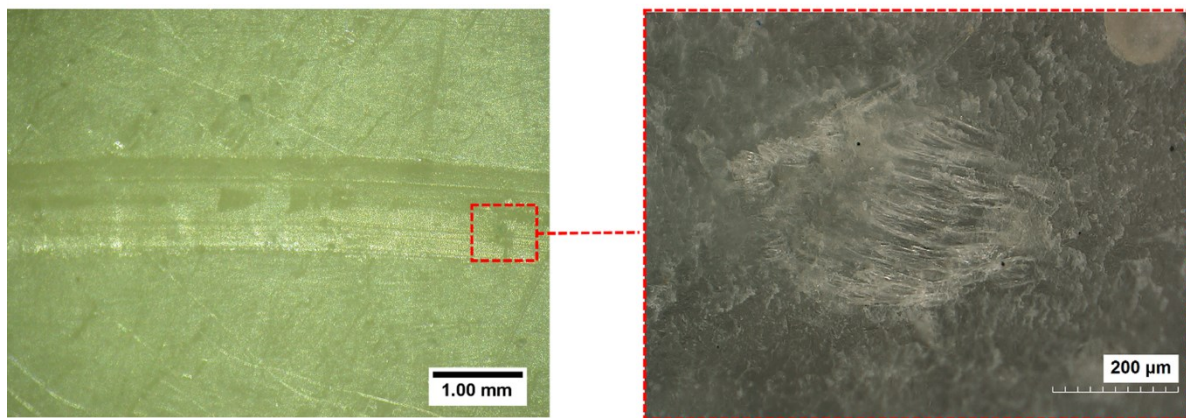
Fig.72: Wear depth (a) and friction coefficient (b) vs number of revolutions under a normal load of 70 N.

By comparing figs.71 and 72, it is also possible to observe that the final wear depth of the H type under normal loads of 50 and 70 N (high load) is quite similar instead of the ones showed from the other composite types.

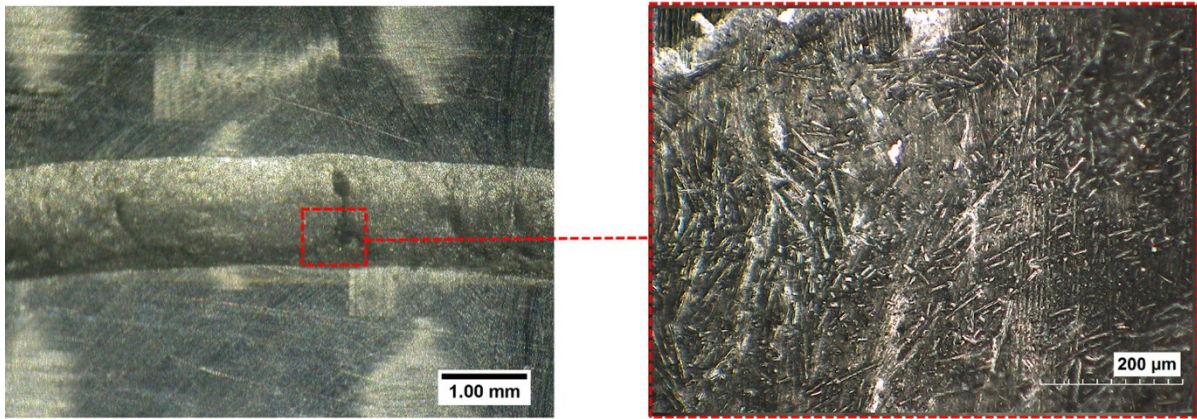
In these load conditions, as the tests time increases (long time conditions) the H type starts to emphasise its interesting wear properties, indeed in both cases it showed the best wear resistance.

To corroborate the results of the wear curves, it is also interesting to observe same typical damaged area at the end of the tests carried out at 70N. fig.73 shows comparative microscope images for each sample type.

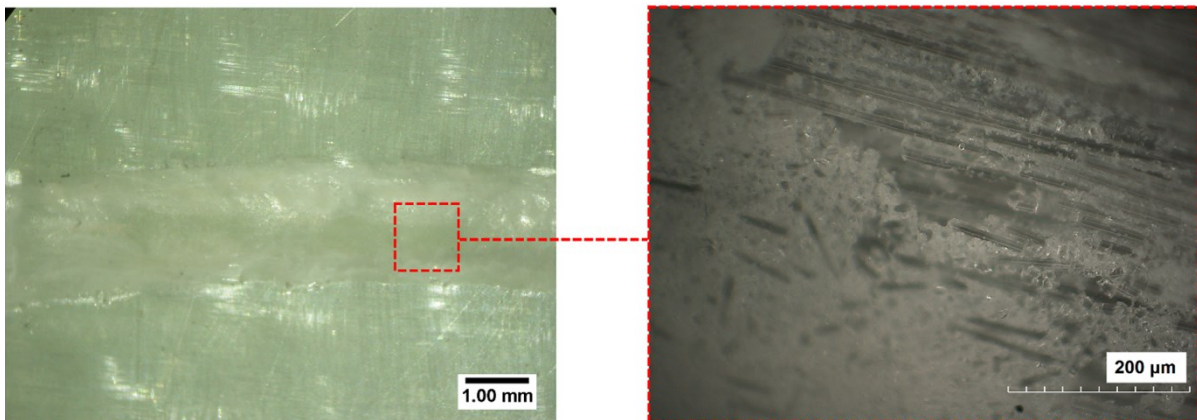
From these images, it is clear the presence of broken fibres for the specimen having glass and carbon fabric as reinforcement (fig.73b and c), this has a double effect: on the tribological point of view the pin affects the fabric involving in its damage that generates a three bodies wear mechanism[16] and on the practical point of view, the presence of synthetic broken fibres can lead health problems and environmental pollution. Therefore, when the test time increases the top matrix layer was completely removed and the underlying fabric fibres started to show their wear resistance behaviour that reached its maximum when the hemp fabric was used. In this case, due to the no-brittles behaviour of the natural fibres, there are evidences of any broken fibres but just a fabric distortion along the sliding direction was observed, as shown in fig.73a.



a)



b)



c)

Fig.73: Wear track details of hemp (a), carbon (b) and glass (c) composite specimens.

Finally, fig.74 summarises, for each sample type, the mean value (obtained as mean of three values shown by three specimens of the same sample type) of the coefficient of friction measured at the end of the tests versus the applied normal load. From this, it is possible to observe that as the normal load increases, the coefficient of friction values decrease. This can be explained considering that under low load conditions (10 N) the wear mechanism is mainly adhesive and then the presence of resin on the ball surface could involve in the highest values of the coefficient of friction. On the other hand, when the applied load increases the ball affects the fabric and the abrasive wear mechanism begins to be prevalent, this could justify the decreasing of the coefficient of friction versus the load. In particular, after long sliding time the wear damage can generate a three-body mechanism due to the presence of broken fibres that,

as in the case of C and G types, it could facilitate the sliding of the ball on the rotating specimen; this involved in a further decreasing in the coefficient of friction.

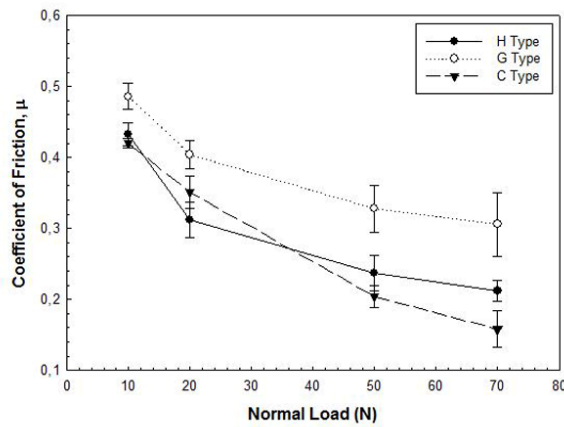


Fig.74: Values of coefficient of friction versus the applied normal load for each composite type.

On the basis on these considerations it could be interesting to better understand the wear behaviour of the fibres type under investigation without consider the matrix contribute to the wear resistance. To do this, additionally tribological tests on un-impregnated single fabrics were also carried out by using the same testing equipment used before. Under a constant peripheral speed of 210 mm/s a normal load of 10 N was applied until an evident fabric damage or a constant wear depth was achieved.

Fig.75 shows the typical trend of the percentage dimensionless wear depth versus the number of revolutions curves for each sample type; the dimensionless wear depth was evaluated as the ratio between the wear depth and the specimen thickness. For each sample type, the typical curve plotted in fig.75 represent the intermediate curve between three obtained from three specimens of the same type.

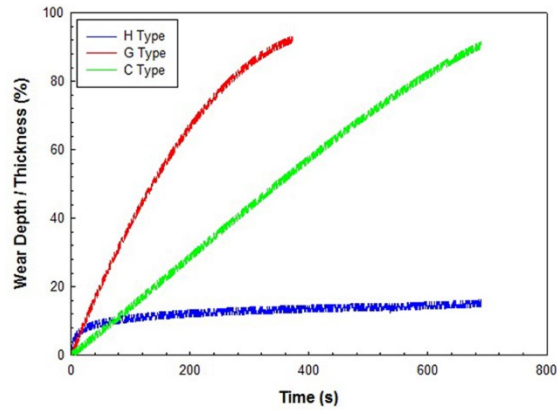
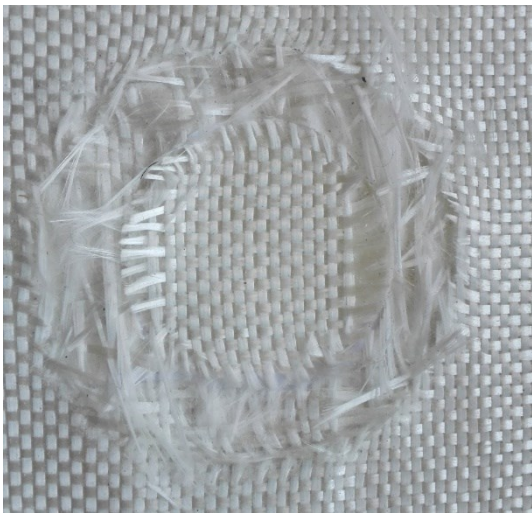


Fig.75: Dimensionless wear depth curves versus the sliding time for each un-impregnated fabric type.

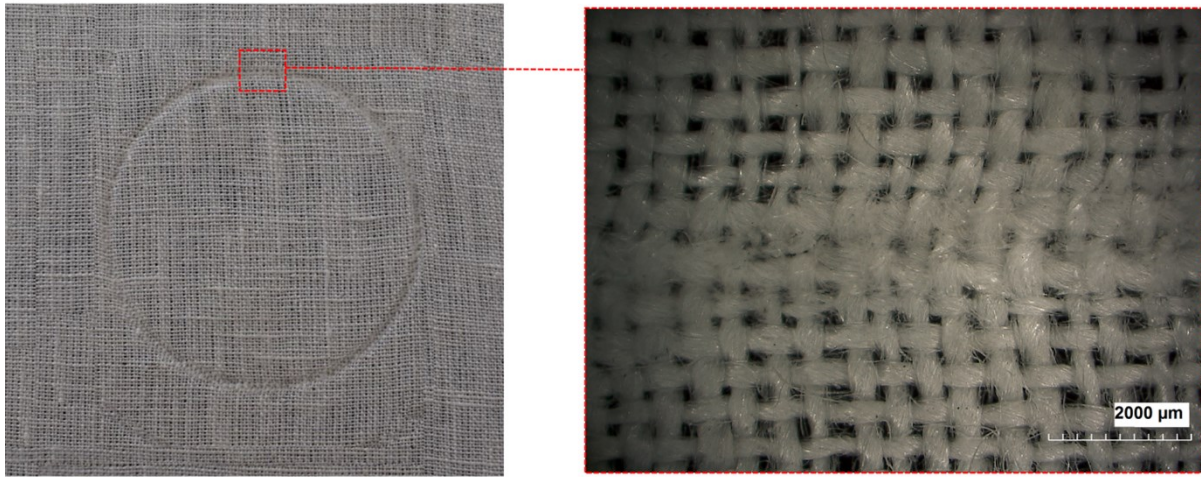
The curves confirm what was above explained: the hemp fabric possesses a better wear resistance than glass and carbon one indeed only the 10 % of the total thickness results to be affected by the wear. In the other cases, the pin quickly destroyed the fabrics, as showed in fig.76. In addition, in the case of the hemp fabric more than broken fibres it is evident a fabric distortion along the sliding direction.



a)



b)

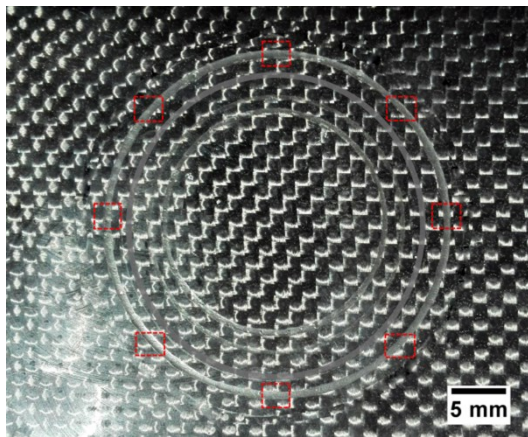


c)

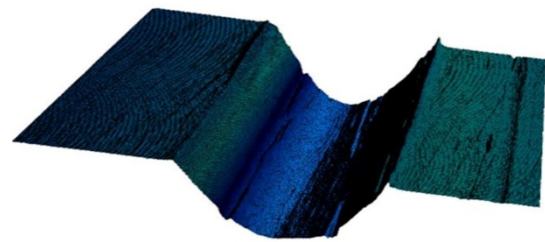
Fig.76: Un-impregnated samples at the end of the test: glass (a), carbon (b) and hemp (c) fabric.

4.4.3 Microgeometrical measurements

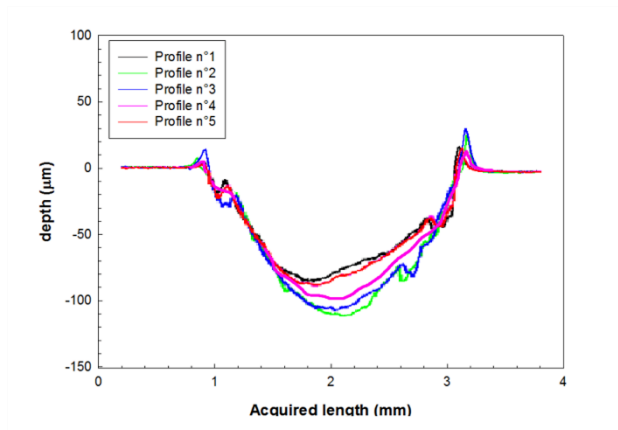
In order to determine the loss of volume, the depth and the width of each wear track were evaluated by means the confocal microscope by using 10X as magnification (see fig.77). The wear track surfaces were acquired by means of a confocal microscope (Leica DCM 3D) in order to scan the wear tracks and to evaluate its depth (d) and its width (w), as shown in fig.77 [17].



a)



b)



c)

Fig.77: Diametric sample areas on the wear tracks acquired via confocal microscope (a) and an example of one of their 3D representation (b) from which single profiles are extracted (c).

For this purpose, for each wear track and for each specimen, eight areas ($4 \times 20 \text{ mm}^2$), as the ones indicated with rectangular areas in fig.77a, were acquired (fig.77b) and five profiles (fig.77c) were extracted from each area. Therefore, the depth and the width of the wear tracks were measured for each single profile and their mean values were evaluated.

The wear behaviour was evaluated by comparing the curves of the wear depth over the number of revolutions and the loss of volume (ΔV) at the end of the tests. Each acquired surface (fig.77b) was analysed using a routine written in MATLAB code in order to evaluate the volume of the tracks and then the final loss of volume (ΔV).

The results in terms of mean and standard deviation values for each specimen are listed in tables 32-34. The values of depth and width reported in each table represent the mean and the standard deviation obtained from 40 profiles at different locations of the same track, i.e. of the same specimen as showed in fig.77. Looking at these values, it is possible to observe that in terms of width and depth the track is almost regular.

Comparing the values of tables 32-34, that represent the same measurement on different specimens, i.e. specimen 1, 2 and 3, it is worth to note that the variability of the measurement and then of the test is very small.

Table 32: Depth and width of the wear tracks for each sample type of the specimen n°1

Applied Load [N]	Sample H				Sample G				Sample C			
	Depth [μm]		Width [mm]		Depth [μm]		Width [mm]		Depth [μm]		Width [mm]	
	Mean	St. Dev.	Mean	St. Dev.	Mean	St. Dev.	Mean	St. Dev.	Mean	St. Dev.	Mean	St. Dev.
10	26,11	1,48	0,870	0,02	22,99	1,65	0,83	0,01	16,60	0,47	0,72	0,03
20	34,60	1,73	1,050	0,03	87,80	0,73	1,66	0,03	31,60	1,50	1,00	0,04
50	35,90	1,79	1,070	0,01	102,60	1,47	1,80	0,03	53,20	1,44	1,30	0,01
70	36,60	0,86	1,065	0,13	129,00	1,68	2,01	0,01	66,59	1,28	1,30	0,03

Table 33: Depth and width of the wear tracks for each sample type of the specimen n°2

Applied Load [N]	Sample H				Sample G				Sample C			
	Depth [μm]		Width [mm]		Depth [μm]		Width [mm]		Depth [μm]		Width [mm]	
	Mean	St. Dev.	Mean	St. Dev.	Mean	St. Dev.	Mean	St. Dev.	Mean	St. Dev.	Mean	St. Dev.
10	27,10	1,38	0,890	0,03	23,10	1,55	0,84	0,02	16,90	0,48	0,75	0,02
20	35,50	1,64	1,060	0,02	87,90	0,44	1,76	0,02	32,30	1,35	1,08	0,03
50	36,80	1,56	1,073	0,01	103,60	1,48	1,88	0,03	54,10	1,48	1,38	0,02
70	37,10	1,11	1,076	0,11	129,48	1,56	2,31	0,02	67,49	1,32	1,40	0,03

Table 34: Depth and width of the wear tracks for each sample type of the specimen n°3

Applied Load [N]	Sample H				Sample G				Sample C			
	Depth [μm]		Width [mm]		Depth [μm]		Width [mm]		Depth [μm]		Width [mm]	
	Mean	St. Dev.	Mean	St. Dev.	Mean	St. Dev.	Mean	St. Dev.	Mean	St. Dev.	Mean	St. Dev.
10	25,92	1,45	0,831	0,01	21,78	1,60	0,79	0,02	16,36	0,51	0,70	0,02
20	33,49	1,78	1,042	0,04	86,52	0,79	1,58	0,04	30,48	1,56	0,96	0,03
50	34,84	1,72	1,066	0,02	100,96	1,40	1,73	0,02	51,89	1,41	1,25	0,04
70	35,98	0,83	1,055	0,12	126,15	1,62	1,94	0,03	65,42	1,35	1,28	0,05

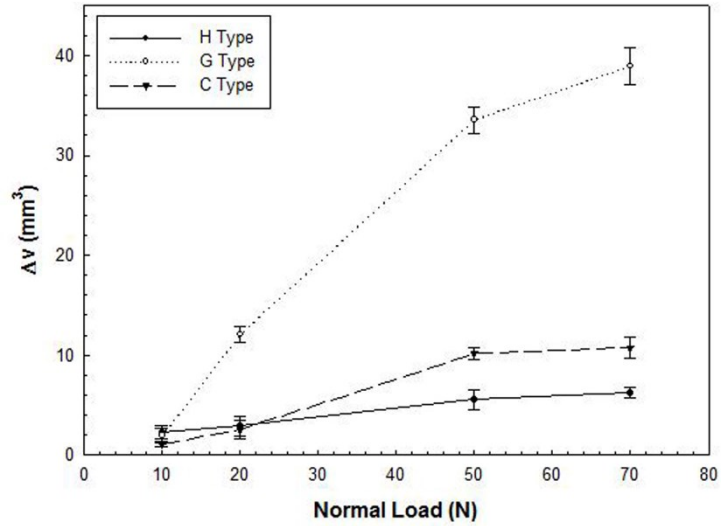


Fig.78: Volume variation for each load conditions.

From fig.78, it is possible to observe that the loss of volume (ΔV) versus the applied load increases in a different way for each sample type, showing that for the hemp one, its increases in the slightest way reaching the lowest values. This result further highlighted the interesting wear behaviour of the natural fibre composite under investigation.

Reference

- [1] C. Andreades, P. Mahmoodi, F. Ciampa, Characterisation of smart CFRP composites with embedded PZT transducers for nonlinear ultrasonic applications, *Compos. Struct.* 206 (2018) 456–466. doi:10.1016/j.compstruct.2018.08.083.
- [2] M. JOHN, S. THOMAS, Biofibres and biocomposites, *Carbohydr. Polym.* 71 (2008) 343–364. doi:10.1016/j.carbpol.2007.05.040.
- [3] F. Reux, I. Verpoest, *Flax and Hemp Fibres: A Natural Solution for the Composite Industry*, Paris, 2012.
https://books.google.it/books/about/Flax_and_Hemp_Fibres.html?id=s_eJYgEACAAJ&redir_esc=y.
- [4] F. Duc, P.E. Bourban, C.J.G. Plummer, J.-A.E. Månson, Damping of thermoset and thermoplastic flax fibre composites, *Compos. Part A Appl. Sci. Manuf.* 64 (2014) 115–123. doi:10.1016/j.compositesa.2014.04.016.
- [5] I.D.G. Ary Subagia, Y. Kim, L.D. Tijing, C.S. Kim, H.K. Shon, Effect of stacking sequence on the flexural properties of hybrid composites reinforced with carbon and basalt fibers, *Compos. Part B Eng.* 58 (2014) 251–258.
doi:10.1016/j.compositesb.2013.10.027.
- [6] I. Sanal, D. Verma, *Construction Materials Reinforced with Natural Products*, in: *Handb. Ecomater.*, Springer International Publishing, Cham, 2019: pp. 2119–2142.
doi:10.1007/978-3-319-68255-6_75.
- [7] H. Ku, H. Wang, N. Pattarachaiyakoop, M. Trada, A review on the tensile properties of natural fiber reinforced polymer composites, *Compos. Part B Eng.* 42 (2011) 856–873.
doi:10.1016/j.compositesb.2011.01.010.
- [8] J. Zhang, K. Chaisombat, S. He, C.H. Wang, Hybrid composite laminates reinforced with glass/carbon woven fabrics for lightweight load bearing structures, *Mater. Des.* 36 (2012) 75–80. doi:10.1016/j.matdes.2011.11.006.
- [9] A. Martone, V. Antonucci, M. Zarrelli, M. Giordano, A simplified approach to model damping behaviour of interleaved carbon fibre laminates, *Compos. Part B Eng.* 97 (2016) 103–110. doi:10.1016/j.compositesb.2016.04.048.
- [10] A.H.G. Cents, D.W.F. Brillman, G.F. Versteeg, P.J. Wijnstra, P.P.L. Regtien, Measuring bubble, drop and particle sizes in multiphase systems with ultrasound, *AIChE J.* 50 (2004) 2750–2762. doi:10.1002/aic.10203.
- [11] F. Rizzo, F. Pinto, M. Meo, 3D bio-inspired hierarchical discontinuous CFRP with enhanced ductility, *Compos. Struct.* 226 (2019) 111202.
doi:10.1016/j.compstruct.2019.111202.
- [12] M. Liu, A. Thygesen, J. Summerscales, A.S. Meyer, Targeted pre-treatment of hemp bast fibres for optimal performance in biocomposite materials: A review, *Ind. Crops Prod.* 108 (2017) 660–683. doi:10.1016/j.indcrop.2017.07.027.
- [13] R. Park, J. Jang, Impact behavior of aramid fiber/glass fiber hybrid composites: The effect of stacking sequence, *Polym. Compos.* 22 (2001) 80–89. doi:10.1002/pc.10519.

- [14] E. Nisini, C. Santulli, A. Liverani, Mechanical and impact characterization of hybrid composite laminates with carbon, basalt and flax fibres, *Compos. Part B Eng.* 127 (2017) 92–99. doi:10.1016/j.compositesb.2016.06.071.
- [15] G. RAJARAM, S. KUMARAN, T.S. RAO, Sliding Wear Behavior of Al-Si/Graphite Composite, *Tribol. Trans.* 54 (2010) 115–121. doi:10.1080/10402004.2010.528854.
- [16] A.P. Harsha, U.S. Tewari, Two-body and three-body abrasive wear behaviour of polyaryletherketone composites, *Polym. Test.* 22 (2003) 403–418. doi:10.1016/S0142-9418(02)00121-6.
- [17] S.C. Amico, W. Brostow, M. Dutta, T. Góral, J.T.N. de Medeiros, L.V. Silva, J.R. de Souza, Composites of polyester + glass fiber residues vs. composites with mineral fillers, *Compos. Interfaces.* 19 (2012) 511–522. doi:10.1080/15685543.2012.762197.

Chapter 5: Conclusions

This Ph.D thesis has been focused on manufacturing techniques of natural hemp fibre composite materials both in hybrid laminate and hybrid sandwich structure configurations. Then a wide investigation on the mechanical properties of the produced composite has been performed through quasi-static, dynamic and tribological tests. Several aspects of these hybrid composite materials were studied, with more detail their tensile and flexural properties, the effect of the presence of hemp-carbon interface in hybrid laminate on the interlaminar shear, and the capability of hybrid laminates to dissipate energy by means of damping tests. Dynamic properties were evaluated through low velocity impact tests on both laminate and sandwich configuration and dynamic surface wear resistance was studied through tribological tests.

- Focusing the attention on the experimental campaign carried out on the **hybrid sandwich structures with bio-based cores** in part 2, it is possible to conclude that as consequence of the impact tests at penetration carried out at 45J, globally, the SF sample shows a reduction of the peak force in comparison with the NSF sample that is almost 13,7%, 19,8% and 16,8% respectively for the 2, 4 and 6 layers samples. Furthermore, an increasing of the displacement at failure is detected indeed the 2, 4 and 6 SF hemp core layers show an improvement of 30%, 46,1% and 29,2% if compared with the NSF sample. These aspects are representative of a more ductile behaviour of the SF samples caused by its density and fabric geometry.

Focusing the attention on the absorbed energy, it is possible to observe that the absorbed energy increases when the number of the total core layers rise up in case of SF sample, whilst. If the attention is focused on the NSF sample, a reduction of the absorbed energy is detected when the number of core plies increase then, in that sample typology the impact behaviour is influenced by the core density.

From the indentation tests it is possible to conclude that at the end of the loading portion of the indentation curves, some localised cracks propagate through the core thickness. When the penetration load is reached a severe indentation is localised on the top core surface that is in contact with the penetrator tip, on the other hand, broken and bended fibres are appreciable on the bottom surfaces of both sample typologies.

Furthermore, an additional failure mechanism is detected for the SF sample, the penetrator breakthrough causes an in-plane hemp fibre bending both in warp and weft direction due to the low interaction between hemp tow at the intersection. This mechanism can be an additional contribute to the impact energy dissipation when its amount is not enough to cause the failure of the sandwich structure. Indeed, during an impact event, part of the impact energy can be used to plastically deform the hemp core layers.

- Regarding the research on **thin hybrid sandwich structures with bio-based cores**, it is a natural evolution of the previous work. The guideline of the entire PhD thesis is the extension of the application fields of natural fibre, then in order to overcome the classical limitation of sandwich structures related to the core thickness, the idea was the replacing of traditional core materials with a single porous layer of natural fibres. This in order to obtain a thin laminate in sandwich configuration. Then, in this experimental campaign, three different sample typologies were produced: a first hybrid laminate in sandwich configuration, characterised by one layer of hemp fabric between two single carbon layer skins, labelled as C-H-C; the second one is the same of the C-H-C configuration but a flax layer is placed between the two skins and is labelled as C-F-C; then a reference laminate with 2 and 4 carbon plies in case of comparison with the same mechanical properties and the same weight respectively.

The tensile test results do not reveal a better behaviour of hybrid composite compared to the 2 plies carbon laminate. The tensile properties are lower than the reference, indeed a reduction of almost 19% and 13% was detected for C-H-C and C-F-C respectively, moreover, a weight rising up is detected and it is attributed to the addition of the natural fibre layer. But, in semi-structural application, flexural and impact mechanical properties are of greater interest, then from the flexural tests carried out on each family at the same mechanical properties and at the same weight, it is possible to conclude that the C-H-C configuration demonstrates specific stress properties of almost 5% higher than the 2 plies carbon laminate in case of comparison at the same mechanical properties. On the other hand, a larger improvement is shown when the comparison is performed keeping constant the weight of all specimen typologies, in that case the C-H-C laminate demonstrates specific flexural stresses that are 36,5% higher than the 4 plies carbon reference. Positive results are revealed from the C-H-c configuration when the same comparisons mentioned before are made keeping constant the support span. In this case, when the comparison was performed at the same mechanical properties, the C-H-C composite material shows a specific flexural force that is 36% higher than the 2 plies carbon reference,

whilst in case of comparison carried out keeping constant the support span and the weight of the samples, the C-H-C configuration reveal the specific flexural properties that are almost 10% higher than the 4 plies carbon reference. Then, in this last case, the improvement is less than the previous case (36%) but it is clear since the total number of the carbon plies that characterise the reference is twice the previous case. However, even though a double number of carbon layers is used, the hybrid configuration still offers improved specific flexural properties.

- Focusing the attention on the **Bio-hybrid composite laminates with improved mechanical properties** treated in the part 4, all samples under inspection have been subjected to a complete experimental campaign in order to evaluate the flexural and impact behaviour of hybrid configurations. A total number of six families of hybrid laminates were produced keeping constant the synthetic/natural fibre content, in detail three of fifteen carbon plies were replaced with hemp ones in order to obtain both symmetric and asymmetric laminate configurations. The mechanical properties of bio-hybrid samples in terms of flexural, damping and impact behaviour were extensively investigated and compared with traditional CFRP and HFRP references. The results proved that the presence of hemp fibres successfully influenced the failure mechanism of these laminates, making the proposed bio-hybrid composites very attractive for future structural applications.

From the mechanical characterization the following main conclusions can be drawn:

The hybridisation process was able to modify the flexural response of the reference carbon composite material by changing the failure mechanism mostly due to the combination between the brittle failure of carbon and the smoother, gradual deformation of the hemp fibres. It was pointed out that it is possible to tune the flexural modulus, by keeping it very close to the one of pure carbon by placing the hemp layers close to the neutral axis, i.e. the symmetric S configuration, or lower it by using asymmetric hybrid configurations. Comparing with the reference CFRP samples, the S hybrid configuration also showed an increase of around 49.7% and a slight decrease of around 10.9% of the maximum strain and flexural strength respectively. Furthermore, it was observed that it is possible to include additional energy dissipation mechanisms by adjusting the position of the hemp layers along the laminate's thickness in order to activate crack bending mechanisms; for example, the best results were shown when the hemp fibres were placed on the top side, i.e. configuration A-HC. In this case, the absorbed energy at bending improved of around 20.5% in comparison with the reference CFRP sample.

From the bending tests carried out on short beams, it was observed that the shear behaviour is less affected by the presence of the natural fibres, however only the sample type with the hemp on the bottom side, i.e. configuration A-CH showed a slight decrease in shear strength due to the presence of large delamination at the carbon/hemp interface.

The results of damping tests, proved that the hybridization with hemp leads to an increase of damping properties in comparison with traditional CFRP laminates, except for the configuration in which the hemp fabrics are placed on the bottom side. The highest absorption performances were exhibited when the hemp layers are placed close to the neutral axis, i.e. configuration S. In this case, an improvement of around 40% of the damping ratio respect to the CFRP reference samples were observed.

From the LVI tests appeared that that the presence of the carbon/hemp interface modifies the behaviour of the hybrid laminate, allowing for different energy dissipation mechanisms (larger energy absorption associated with larger delamination at the interface or constant energy absorption associated with smaller delamination) which can be tuned according to the relative position between the carbon and hemp layers. Of particular interest two cases can be mentioned: the one with the symmetric configuration with the hemp layers close to the neutral axis, i.e. configuration S, in which for each impact energy value, no significant deviations from the CFRP reference samples in terms of absorbed energy and damage extensions were detected. This means that in this stacking configuration, in the investigated experimental windows, three layers of hemp can represent a suitable replacement of the same number of carbon layers. The second case is the asymmetric stacking configuration with the hemp layers placed on the impacted side, i.e. configuration A-HC. In this case it was observed that the presence of a more ductile material in the proximity of the impact location allowed the larger deformation of the area surrounding the contact zone which translates with a more efficient energy transfer between the penetrator tip and the laminate. This mechanism leads to the absorption of a consistent portion of the impact energy in the deformation of the hemp layers. Indeed, the reduction of the internal damage extension for all the tested energies was observed, reaching for the case of impact energy of 5J the absence of any kind of internal damages.

- Regarding the experimental campaign treated in part 5 on **tribological behaviour of hemp fibres**, it is an extension of the dynamic characterisation of the bio-hybrid laminates. In all cases in which synthetic structural composite materials are subjected to tribological loads that can compromise the human health by dermatitis from contact or inhalation of broken fibres, the

idea was the replacement of the external traditional fibre ply with a natural fibre one. Then, in this experimental campaign tribological tests were performed on three different composite materials: carbon and glass reinforced composite as references and hemp fibre composite as case study. The results highlight the best wear behaviour of hemp reinforced composites, indeed, under higher load conditions (50 and 70 N) there are no evidence of any broken fibres, but just a fabric distortion along the sliding direction. This aspect is more evident in long time tribological tests, where the better hemp fibre wear behaviour is emphasised. This good wear behaviour is given by the no brittle behaviour of natural fibres, that bend under the pin transient protecting the inner layers. Then, from this study the better wear behaviour of natural fibres with respect to other common synthetic fibres used as reinforcement is evident, furthermore uncovered natural fibres that can appear on the composite surface after wear or scratch damage of the external surface of a composite laminate, are not as dangerous for human health as some synthetic materials like glass or carbon fibres. This aspect makes the hemp fibre hybrid composites an interesting candidate in all applications in which a composite product is in contact with the human body.

Then is possible to conclude that the aim of this PhD thesis does not consist in the substitution of traditional synthetic fibres with hemp ones because, even if these fibres are characterised by specific properties comparable with the most commonly glass fibres, hemp composite materials are not able to offer mechanical performances comparable with GFRP or CFRP laminates. Then, on the basis of the actual environmental sensitivity, the idea is related to the extension of the application fields of these fibre typologies. One way to extend the limits in using hemp fibres in load bearing application is the hybridisation with high performance carbon fibre in hybrid composite, both in traditional laminate configuration and as core in sandwich structure. The results of these research works, lead to conclude that the hybridisation of traditional CFRP composites with hemp layers is a valid solution for the development of new load-bearing structures, as it allows for the development of laminates with tailorable properties in the out-of-plane direction according to the relative position of the natural and synthetic fibres. Moreover, the substitution of a fraction of traditional fibres with hemp ones, leads to a greener composite material with reduced environmental impact.